MODELING AND SIMULATION OF FLUID CATALYTIC CRACKING UNIT

A

Thesis Submitted

in Fulfillment of the Requirement

for the Award

of

Doctor of Philosophy

By

Gupta Rajkumar Satyapal

DEPARTMENT OF CHEMICAL ENGINEERING
THAPAR INSTITUTE OF ENGINEERING AND TECHNOLOGY
(DEEMED UNIVERSITY)
PATIALA-147 004 (Pb.)
INDIA

Dedicated to my parents

CERTIFICATE

This is to certify that the thesis entitled "**MODELING AND SIMULATION OF FLUID CATALYTIC CRACKING UNIT**", which is being submitted by Mr. Gupta Rajkumar Satyapal in fulfillment of the requirement for the award of the degree Doctor of Philosophy in chemical engineering, to Thapar Institute of Engineering and Technology (Deemed University), Patiala is a record of the candidate's own work carried out by him under our supervision and guidance. The matter embodied in this thesis has not been submitted in part or full to any other University or Institution for the award of any degree.

Vineet Kumar
Professor and Head
Department of Chemical Engineering
Thapar Institute of Engineering and Technology
(Deemed University)
Patiala- 147 004, India

V.K. Srivastava
Professor (Retired)
Department of Chemical Engineering, and
Ex-Dean Industrial Research and Development (IRD)
Indian Institute of Technology, Delhi
New Delhi-110 016, India

ACKNOWLEDGEMENTS

I express my foremost and deep sense of gratitude to my guides Dr. Vineet Kumar, and Dr. V.K, Srivastava for their meticulous guidance, clear thinking, and forbearance. I am extremely fortunate to have such sincere academicians and generous guides who have been a source of inspiration and encouragement to me in completing this research work in its present form. I have a deep sense of admiration for their goodness and for their any time availability during this research work.

I am thankful to Dr. S.C. Saxena, Director, Thapar Institute of Engineering and Technology, Patiala for his moral support during the completion of this research work. I am also thankful to Dr. K.K, Raina, Dean (R&LSP), Thapar Institute of Engineering and Technology, Patiala for his timely encouragement. I very sincerely acknowledge the cooperation from my friends and colleagues in the Department of Chemical Engineering for their help during various stages of this study.

Heartfelt thanks are due to Dr. Shusheel Mittal, Professor and Head, School of Chemistry and Biochemistry, Thapar Institute of engineering and Technology, Patiala who extended all possible help during all stages of this research work. I am also thankful to Dr. D. Gangacharyulu, Assistant Professor, Department of Chemical Engineering, Thapar Institute of Engineering and Technology, Patiala who helped me a lot during this study. Special thanks are due to Dr. Shishir Sinha, Assistant Professor, Department of chemical Engineering, Thapar Institute of Engineering and Technology, Patiala who have helped me a lot during the literature search stage of this study.

My sincere thanks are due to Dr. A. K, Gupta, Professor, Department of Chemical Engineering, Indian Institute of Technology, Delhi for his keen interest and support during this work.

I am thankful to Dr. Vinay Gupta, Mr. Ashok Kumar, and Ms. Parveen Kumari, who extended all possible help.

I am extremely grateful to the celebrated authors whose research works have been freely consulted and referred in my research work.

I wish to express my indebtedness towards my wife, Ms. Nishma Gupta who have always been a source of strength and whose affection and patience enabled me to complete this dissertation. I also owe a sense of apology to my son Dev and daughter Shreya whom I could not give their share of my time during this work.

Everything happens only with the grace of god. I thank the Almighty God for providing me an opportunity, strength and ambience to successfully accomplish this work.

(Raj Kumar Gupta)

ABSTRACT

Fluid catalytic cracking unit (FCCU) plays most important role in the economy of a modern refinery as it is used for value addition to the refinery products. Crude oil, as produced from the ground, contains hydrocarbons ranging from light gases and LPG to residues boiling above 343 ^{0}C (650 ^{0}F). Products of various boiling ranges can be obtained by distillation. Compared to the products demand, crude oil is short of lighter material in the boiling range of the transportation fuel (gasoline and diesel) and long on heavier material. Fluid catalytic cracking (FCC) units convert a portion of this heavy material into lighter products, chiefly gasoline and middle distillates.

Because of the importance of FCCU in refining, considerable effort has been done on the modeling of this unit for better understanding and improved productivity. In last fifty years, the mathematical modeling of FCC unit have matured in many ways but the modeling continues to evolve to improve the closeness of models' predictions with the real process whose hardware is ever-changing to meet the needs of petroleum refining.

The FCC unit comprise of three stages: a riser reactor, a catalyst stripper, and a regenerator (along with other accessories). From modeling point of view, the riser reactor is of prime importance amongst these stages. Detailed modeling of the riser reactor is a challenging task for theoretical investigators not only due to complex hydrodynamics and the fact that there are thousands of unknown hydrocarbons in the FCC feed but also because of the involvement of different types of reactions taking place simultaneously. In the present work a new kinetic model of the riser reactor is developed using the common assumptions made by various researchers on various aspects of the riser modeling.

The traditional and global approach of cracking kinetics is lumping. Mathematical models dealing with riser kinetics can be categorized into two main types. In one category the lumps are made on the basis of boiling range of feed stocks and corresponding products in the reaction system. This kind of model has an increasing trend in the number of lumps of the cracked gas components. The other approach is that in which the lumps are made on the basis of molecular structure

characteristics of hydrocarbon group composition in reaction system. This category of models emphasizes on more detailed description of the feedstock. Theses models do not include chemical data such as type of reaction and reaction stoichiometry. The number of kinetic constants in these models increases very rapidly with the number of lumps. Moreover, the values of kinetic constants depend on the feedstock composition and must be determined for each combination of feedstock and catalyst. All these models assume that FCC feed and products are made of a certain number of lumps, and kinetic parameters for these lumps are estimated empirically considering the conversion of one lump to the other. In both of these categories, however, reaction kinetics being considered is that of 'conversion' of one lump to another and not the 'cracking' of an individual lump.

More recently, models based upon 'single-events' cracking, structure oriented lumping, and reactions in continuous mixture were proposed by various researchers. Nevertheless, the application of these models to catalytic cracking of industrial feedstocks (vacuum gas oil), is not realized because of the analytical complexities and computational limitations.

In the present work, a new approach of kinetic scheme for the FCC riser is introduced which considers cracking of one lump (pseudocomponent) giving two other lumps in one single reaction step. The proposed model falls under the first category in which lumps are formed on the basis of boiling point, but in this approach, each individual lump is considered as a pure component with known physico-chemical properties. Also, the reaction stoichiometry is considered. The proposed model also incorporates two phase flow and catalyst deactivation. Since a new cracking reaction mechanism is introduced, a new semi empirical approach based on normal probability distribution is also developed to estimate the cracking reactions' rate constants.

The pseudocomponents based approach for design and simulation of crude distillation unit is highly successful. To apply this approach to FCC simulation, it is assumed that one mole of a pseudocomponent on cracking gives one mole each of two other pseudocomponents and some amount of coke may also form. The feasibility of a cracking reaction is found by using the stoichiometry of that reaction. The reactions for which the molecular weight of a cracking pseudocomponent is equal to or more than the probable product pseudocomponents are considered feasible. In the present work, a new semi-empirical scheme for the estimation of rate constants is developed.

This scheme makes the kinetic model more versatile. Six tunable parameters have been introduced to adjust more than ten thousand reaction rate constants needed to explain complete reaction mechanism in a typical FCC riser reactor.

Riser reactor is conceptualized as having a number of small volume elements placed one over the other. The conditions at the inlet of the first volume element are known. The material and energy balance equations are solved in the volume elements considering the proposed reaction kinetics, two phase hydrodynamics, and catalyst deactivation. The various products' yields, catalyst activity, and riser temperature are predicted all along the riser height. Plant data reported in the literature is used for the validation of the developed model. A sensitivity analysis of the proposed tuning parameters is done which suggested that the products' yields were insensitive to one tuning parameter out of the proposed six tuning parameters. Also, the value obtained for one of the tuning parameter out of the proposed six tuning parameters was zero. These two tuning parameters were than dropped for the subsequent case studies for the simulation of the riser reactor and FCC unit.

A regenerator model adopted from the literature is integrated with the proposed riser model to simulate the entire FCC unit. The steady state simulation of the FCC unit is then done to study the effect of various operating parameters on the performance of this unit.

The work done in this study is organized into **five chapters**. The introduction of the fluid catalytic cracking (FCC) process/unit is presented in the **first chapter,** a literature review on the *modeling and simulation of FCC unit* follows in the **second chapter**.

Chapter 3 deals with the riser model development. A regenerator model based on the model of Arbel et al. (1995) is also presented. In the last section the riser model and regenerator model are integrated to simulate the FCC unit.

Results of the riser simulation, regenerator simulation, and entire FCC unit's simulation are presented and discussed in **Chapter 4**. The tuning parameters of the riser kinetic model are obtained using the plant data reported in literature. Then the sensitivity analysis is done by tracking the effect of change in products' yields with the change in each tuning parameter's value (keeping other tuning parameters same). The less sensitive tuning parameters were dropped for subsequent simulations. Riser reactor model is validated by comparing with the plant data (reported in literature for different plants) and with an already existing riser reactor model's results.

Regenerator simulation and comparison of regenerator model's results with the plant data are also presented in this chapter. The steady state simulation results of entire FCC unit along with the effect of changing C/O ratio and air flow to the regenerator on the process parameters is also included in this chapter.

Chapter 5 summarizes the conclusions drawn from the study. Also, it is proposed that the proposed kinetic modeling approach for the riser kinetics may be used for the more advanced modeling of the FCC unit. Integration of this detailed kinetic scheme (any number of pseudocomponents) with the other aspects of riser modeling (hydrodynamics, heat and mass transfer, catalyst deactivation etc.) is easier as compared to other detailed kinetic models, as the resulting material and energy balance equations are easier to handle and solve.

CONTENTS

LIST OF FIGURES

Figure No.	Title	Page No.

LIST OF TABLES

NOMENCLATURE

A_r	Cross-sectional area of riser (m^2)
A_{rgn}	Cross-sectional area of regenerator (m^2)
C/O ratio	Catalyst to oil ratio (kg catalyst/kg oil)
C_{cj}	Coke concentration on catalyst coming out of j^{th} volume element (wt %)
$C_{i,j}$	Concentration of i^{th} pseudocomponent in j^{th} volume element ($kmol/m^3$)
C_{rgc}	Coke on regenerated catalyst (kg coke/kg catalyst)
C_{sc}	Coke on spent catalyst (kg coke/kg catalyst)
Cp_{cat}	Specific heat of catalyst (kJ/kg)
Cp_{coke}	Specific heat of coke (kJ/kg)
Cp_i	Specific heat of i^{th} pseudocomponent (kJ/kg)
$Cp_{mix,j}$	Specific heat of the gas and solid mixture in j^{th} volume element (kJ/kg)
Cp_{st}	Specific heat of steam (kJ/kg)
D_{rgn}	Regenerator diameter (m)
ΔE_i	Activation energy term in $k_{max,i}$ expression (kJ/kmol)
F_{air}	Molar flow rate of air to the regenerator (kmol/s)
f_{O2}	Molar flow rate of O_2 in gas (kmol/s)
f_{CO}	Molar flow rate of *CO* in gas (kmol/s)
f_{CO2}	Molar flow rate of CO_2 in gas (kmol/s)
f_{N2}	Molar flow rate of N_2 in gas (kmol/s)
f_{total}	Total gas molar flow rate (kmol/s)
H_{coke}	Heat of combustion of coke (kJ/kg)
$Hcomb_i$	Heat of combustion of i^{th} pseudocomponent (Btu/lb)
$H_{dense\ bed}$	Height of the regenerator dense bed (m)
H_{fCO}	Heat of formation of *CO* (kJ/kmol)
H_{fCO2}	Heat of formation of CO_2 (kJ/kmol)
H_{rgn}	Heat generated in the regenerator (kJ/s)
$(\Delta H_r)_{i,m,n}$	Heat of reaction for the cracking of i^{th} pseudocomponent to produce m^{th} and n^{th} pseudocomponents (kJ/kmol)

$k_{i,m,n}$	Rate constant for the cracking of i^{th} pseudo component to produce m^{th} and n^{th} pseudocomponents [m^3/(kgcat.s)]
$k_{max,i}$	Maximum value of rate constant for the cracking of i^{th} pseudocomponent [m^3/(kgcat.s)]
$k_{0,i}$	Frequency factor in the $k_{max,i}$ expression [m^3/(kgcat.s)]
k_1	Coke combustion rate constant to form *CO* [1/(atm s)]
k_2	Coke combustion rate constant to form CO_2 [1/(atm s)]
k_3	Overall *CO* combustion rate constant [kmol of CO/(kgcat. atm^2 s)]
k_{3c}	Rate constant for the catalytic combustion of *CO* [kmol of CO/(kgcat. atm^2 s)]
k_{3h}	Rate constant for the homogeneous combustion of *CO* [kmol of CO/(m^3 atm^2 s)]
M_{air}	Mass flow rate of air to the regenerator (kg/s)
m_c	Mass of a cluster (kg)
Mcat	Mass flow rate of catalyst (kg/s)
$Mcoke_j$	Mass flow rate of coke at the outlet of j^{th} volume element (kg/s)
Mcokeformedj	Cumulative mass of coke formed in j^{th} volume element (kg/s)
Mst	Mass flow rate of steam (kg/s)
MW_{air}	Molecular weight of air (kg/kmol)
MW_{CO}	Molecular weight of *CO* (kg/kmol)
MW_{CO2}	Molecular weight of CO_2 (kg/kmol)
MW_{coke}	Molecular weight of coke (kg/kmol)
MW_i	Molecular weight of i^{th} pseudocomponent (kg/kmol)
N	Total number of components, including pure components and pseudo components
N_C	Total number of hypothetical volume elements in the riser/total number of hypothetical compartments in the regenerator
p	Riser pressure (atm)
p_{co}	Partial pressure of *CO* in regenerator (atm)
p_{o2}	Partial pressure of O_2 in regenerator (atm)
P_{rgn}	Regenerator pressure (atm)
$P_{i,j}$	Molar flow rate of i^{th} component, PC_i, through j^{th} volume element (kmol/s)
R	Gas constant [kJ/(kmol K)]
R'	Gas constant [atm m^3/(kmol K)]
R_i	Overall rate of formation of i^{th} component (kmol/s)

$r_{i,m,n}$	Rate of reaction of i^{th} pseudocomponent giving m^{th}, and n^{th} pseudocomponents (kmol/s)
r_1	Rate of coke combustion to *CO* [kmol/(m^3 s)]
r_2	Rate of coke combustion to CO_2 [kmol/(m^3 s)]
r_{02}	Net rate of disappearance of O_2 (kmol/s)
r_{CO}	Net rate of formation of *CO* (kmol/s)
r_{CO2}	Net rate of formation of CO_2 (kmol/s)
$T_{air,in}$	Air temperature at the regenerator inlet (K)
T_{in}	Temperature of reaction mixture at the riser inlet (K)
T_j	Temperature of reaction mixture leaving j^{th} volume element (K)
T_{rgn}	Regenerator temperature (K)
$T_{riserout}$	Temperature of the catalyst at the riser outlet (K)
T_{sc}	Temperature of spent catalyst (K)
TDH	Total disengagement height (ft)
$\Delta T_{stripper}$	Drop in the catalyst temperature in the stripper (K)
Δt_j	Residence time of gas phase in j^{th} volume element (s)
$\Delta tCat_j$	Residence time of catalyst in j^{th} volume element (s)
u	Superficial gas velocity (m/s)
u_j	Superficial gas velocity through j^{th} volume element (m/s)
u_c	Cluster velocity (m/s)
$u_{c,j}$	Cluster velocity through j^{th} volume element (m/s)
u_g	Actual gas velocity (m/s)
$u_{g,j}$	Actual gas velocity through j^{th} volume element (m/s)
V_j	Volume of j^{th} compartment in regenerator
VGO	Vacuum gas oil
W	Regenerator catalyst holdup (kg)
$y_{i,j}$	Mass fraction of i^{th} gas phase component in j^{th} volume element
Δz_j	Height of j^{th} volume element in the riser/height of j^{th} compartment in the regenerator (m)

Subscripts

i, m, n	i^{th}, m^{th}, and n^{th} pseudocomponents
j	j^{th} volume element in the riser starting from the bottom

Greek letters

ϕ_j	Catalyst activity coefficient
$\alpha_{i,m,n}$	Mass of coke formed when one kmole of pseudocomponent PC_i cracks to give one kmole each of PC_m and PC_n, (kg coke/kmol PC_i)
β_c	CO/CO_2 ratio at the catalyst surface in the regenerator
β_{c0}	Preexponent constant in β_c expression (2512)
$\delta_{g,j}$	Volume fraction of gas in j^{th} volume element of the riser
ε	Regenerator dense bed viodage
ε_c	Cluster voidage in the riser
ρ_c	Density of cluster phase in the riser (kg/m^3)
ρ_{cat}	Density of catalyst (kg/m^3)
ρ_{coke}	Density of coke (kg/m^3)
$\rho_{g,j}$	Density of gas phase in j^{th} volume element of the riser (kg/m^3)
ρ_{gas}	Gas phase density in the regenerator (kg/m^3)
τ	Tuning parameter

Chapter - 1

INTRODUCTION

Fluid catalytic cracking is the primary conversion unit in many petroleum refineries. Crude oil, as produced from the ground, contains hydrocarbons ranging from light gases and LPG to residues boiling above 343 ^{0}C (650 ^{0}F). Products of various boiling ranges can be produced by distillation. Compared to the products demand, crude oil is short of lighter material in the boiling range of the transportation fuel (gasoline and diesel) and long on heavier material. Fluid catalytic cracking (FCC) units convert a portion of this heavy material into lighter products, chiefly gasoline and middle distillates.

Figure 1.1 is a block flow diagram for a typical high conversion refinery. Crude oil is distilled in an atmospheric distillation unit to produce LPG, naphthas, kerosene, and diesel oil. The residue from the atmospheric distillation unit is fed to the vacuum distillation unit where it is separated into vacuum gas oils and vacuum residue. The heavy vacuum gas oil, which normally constitutes 25-30% of the total crude oil volume, is fed to the fluid catalytic cracking unit (FCCU) where it is converted into lighter products.

The heavy vacuum gas oil (VGO) has a boiling range of 343 ^{0}C (650 ^{0}F) to 565 ^{0}C (1050 ^{0}F). In addition to the VGO a wide range of feedstocks can be processed in FCC units such as hydrotreated gas oils, cracked gas oils, and deasphalted oils. The ability of the FCC to process this wide range of feeds into useful products has led to its use as the "garbage disposal" of the refinery. Feedstock quality can vary considerably from unit-to-unit. Even the units that process "traditional" gas oil feeds can see considerable variation in feed quality. Table 1.1 contains typical properties for different gas oils.

There are approximately 400 catalytic crackers operating worldwide, with a total processing capacity of over 45,000 m^3/day (12 million barrels per day). Several oil companies, such as Exxon, Shell, and TOTAL, have their own designs; however, most of the current operating units have been designed or revamped by three engineering companies: UOP, M.W. Kellogg, and Stone & Webster. Although the mechanical configuration of individual FCC units may be different, their common objectives are to upgrade low-value feedstocks to more valuable products.

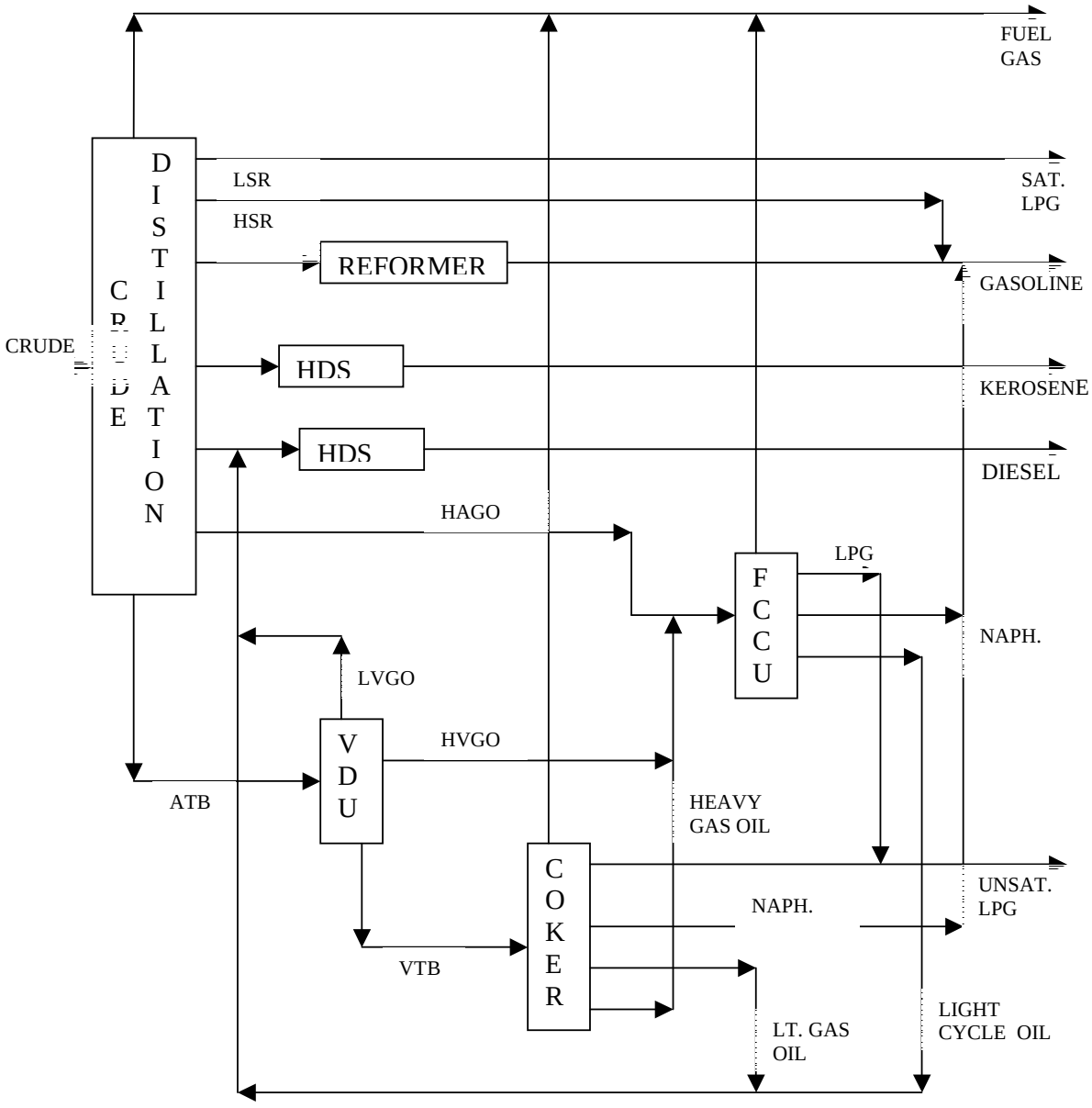

Fig. 1.1: Schematic of a high conversion refinery

Table 1.1: Gas oil properties

Specific Gravity	0.89-0.93
Sulfur, wt%	0.30-2.00
Nitrogen, wt%	0.07-2.00
Conardson Carbon, wt%	0.00-0.20

1.1 FCC Process Description

All modern FCC units consists of two basic components, a riser reactor in which the catalyst is brought in contact with the feed (gas oil), and a regenerator in which the coke deposited on the catalyst during the cracking reactions is burned off for regenerating the catalyst. A schematic of FCC unit is shown in Fig. 1.2. Other auxiliary units such as feed preheat and flue gas systems are also required for control and optimal operation of this unit.

1.1.1 Feed preheat system

The refinery produced gas oil and supplemental feedstocks are generally combined and sent to a surge drum which provides a steady flow of feed to the FCC unit's charge pumps. This drum can also serve as a device to separate any water or vapor that may be present in the feed stocks.

From the surge drum, the feed is normally heated to a temperature of 270-375 ^{0}C (550-700 ^{0}F). This is usually done by heat exchange with intermediate heat removal pumparounds from the main fractionator. While feed preheat system may differ greatly from unit to unit, the feed is normally heated by exchange with the light cycle oil, heavy cycle oil, or bottom pumparounds. This raises the feed temperature to 150-260 ^{0}C (300-500 ^{0}F) which is generally sufficient for most FCCUs. In some cases, however, fired heaters are also used to preheat the feed.

1.1.2 Reactor

Rector-regenerator section is the heart of the FCC unit. Schematic of reactor and regenerator is shown in Fig. 1.2. Almost all reactors presently in use consist of a riser, in which there is short contact time (less than 5 seconds) of catalyst and feed. Virtually all the cracking reactions occur in the riser over this short time period before the catalyst and the products are separated in the reactor. However, some thermal and non-selective catalytic cracking reactions continue to occur in the reactor housing.

From the preheater, the feed enters the riser near the base where it comes in contact with the hot regenerated catalyst coming from the regenerator. The ratio of catalyst to oil is normally kept in the range of 4:1 to 9:1 by weight. The heat carried by the catalyst coming from the regenerator provides the energy to heat and vaporize the feed, and the energy required for the endothermic cracking reactions occurring in the riser. The cracking reactions start instantaneously in the vapor phase as soon as the feed is vaporized. The expanding volume of the vapors that are generated by vaporization and cracking lift the catalyst and carry it up in the riser. Overall these cracking reactions are endothermic and thus, the temperature in the riser decreases as the reaction progresses. Typical riser dimensions are about half a meter to 2 meters in diameter and 20 to 35 meters in length. The ideal riser simulates a plug flow reactor, where the catalyst and the vapor travel along the length of the riser at the same velocity with minimum back-mixing. However, in real cases there is considerable slip and back mixing of catalyst particles.

Efficient contact of feed and catalyst is critical for the desired cracking reactions. Steam is introduced to atomize the feed. The atomization of feed increases the availability of feed at the reactive acid sites of the catalyst. In the presence of a high-activity zeolite catalyst, virtually all of the cracking reactions take place in the riser in two to four seconds time frame. Risers are normally designed for an outlet vapor velocity of 15 to 25 m/s, with an average hydrocarbon residence time of about two second (based on outlet conditions). As a consequence of the cracking reactions, a hydrogen deficient material called coke is deposited on the catalyst that reduces its activity.

At the end of the riser, the product vapors and the catalyst flow through a riser termination device (RTD) which separates the catalyst from the hydrocarbon vapors. Quick separation is essential to avoid the undesirable side reactions. The separated catalyst is then directed to the spent (deactivated) catalyst stripper. Hydrocarbon vapors from the RTD enter the reactor vessel. In modern cracking units, the reactor vessel plays only a minor role in actual cracking reactions. In fact, the reactions occurring in this vessel are generally considered to be undesirable. The primary function of this reactor vessel nowadays is to provide some disengagement space between the RTD and the cyclones.

The product vapors entering the reactor from the RTD get mixed with steam and stripped hydrocarbon vapors and flow through the reactor cyclones. The reactor

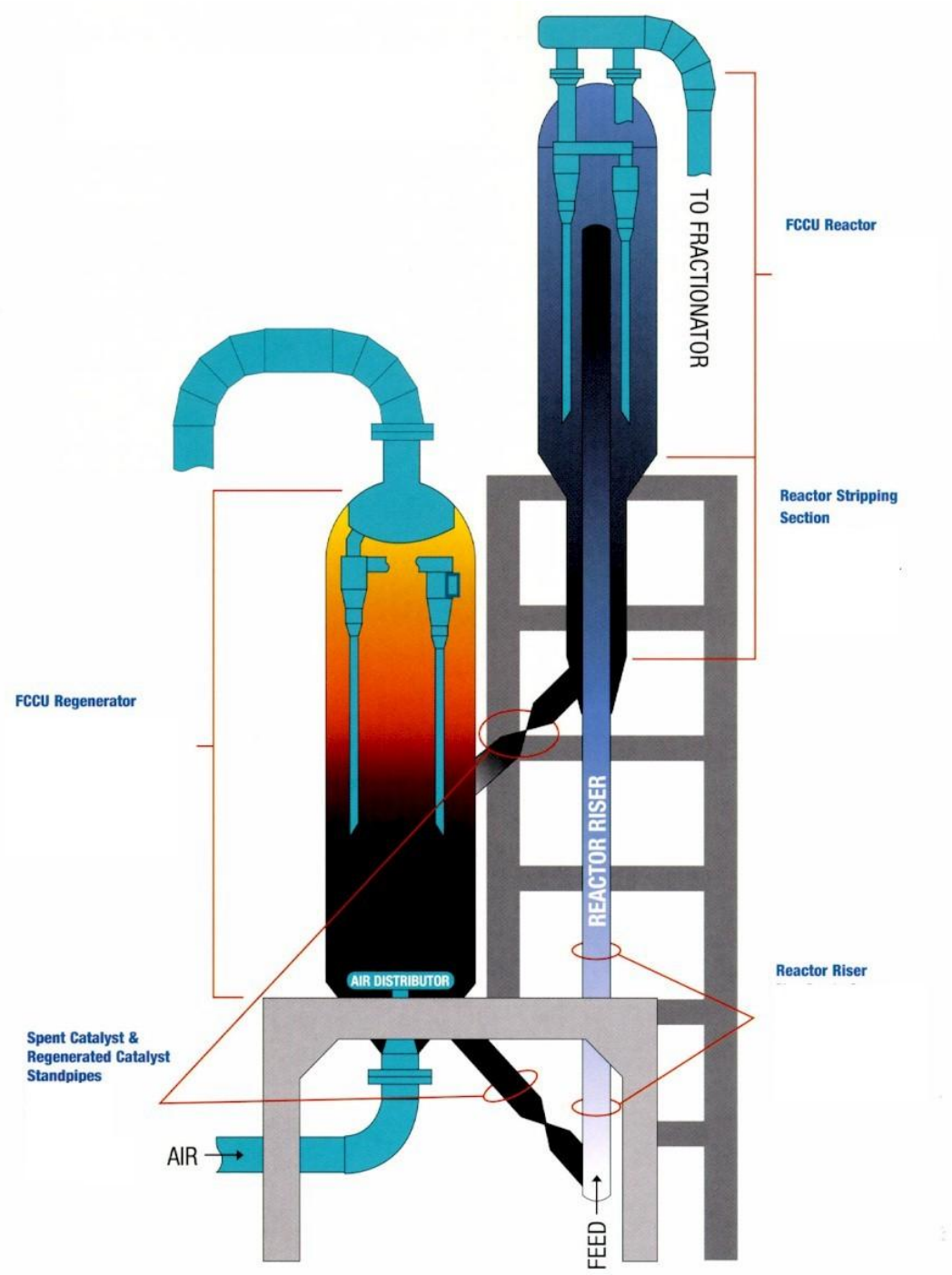

Fig. 1.2: Schematic of FCC unit

cyclones remove the catalyst particles not separated in the RTD. Vapors from the reactor cyclones flow into the main fractionator. Spent catalyst from the RTD and the reactor cyclones flows into the spent catalyst stripper. Here the catalyst is contacted with steam to strip off the vapors adsorbed on the catalyst. Baffles are provided in the stripper to improve the mixing between steam and catalyst.

1.1.3 Regenerator

The spent catalyst from the stripper flows to the regenerator through a spent catalyst standpipe. A slide valve in the spent catalyst standpipe serves to control the level of catalyst bed in the stripper. The regenerator has two main functions: it restores the catalyst activity and supplies heat to crack the feed. The spent catalyst entering the regenerator contains between 0.25 and 0.8 wt% coke, depending on the quality of the feedstock. Components of coke are carbon, hydrogen, and the trace amounts of sulfur and nitrogen.

Air is the source of oxygen for the combustion of coke and is supplied by a large air blower. The air blower provides sufficient air velocity and pressure to maintain the catalyst bed in fluidized state. The air enters the regenerator through an air distributor located near the bottom of the vessel. The catalyst and air are well mixed in a fluid bed (or fast fluid bed) and the carbon (coke) deposited on the catalyst during the cracking reactions is burned off. The heat produced by the combustion of coke raises the temperature of the catalyst which in turn is used for supplying the heat required by the cracking reactions. Flue gases leaving the regenerator pass through the regenerator cyclones where entrained catalyst is removed and returned back to the regenerator. Hot regenerated catalyst from the regenerator enters the riser through the regenerated catalyst standpipe. A slide valve in the spent catalyst standpipe serves to control the quantity of hot catalyst entering the riser and thus, the riser outlet temperature.

In a modern technology jointly licensed by Stone & Webster and IFP a two stage riser regenerator is used. In the first stage only 60-70 % of the coke is burned in an oxygen deficient mode. Regeneration is completed in the second stage which operates with sufficient oxygen for complete combustion.

1.1.4 Flue gas system

The hot flue gas leaving the regenerator contains an appreciable amount of energy. A number of heat recovery schemes are used to recover this energy. In some units, the flue gas is sent to a CO boiler where both the sensible and the heat of combustion are used to generate high-pressure steam. In other units, the flue gas exchanges heat with boiler feed water to produce steam via the use of shell/tube or box heat exchangers.

1.1.5 Catalyst handling

Catalyst particles smaller than 20 microns escape from the reactor and regenerator vessels. The catalyst fines escaping the reactor collect in the fractionator's bottoms product storage tank. The recoverable catalyst fines exiting the regenerator are removed by the electrostatic precipitator. The catalyst losses are related mainly to hydrocarbon vapor and flue gas velocities, the catalyst's physical properties, and attrition.

The activity of the catalyst degrades with time. The loss of activity is attributed to the impurities in the FCC feed, such as nickel, vanadium, and sulfur, and to thermal and hydrothermal deactivation. To maintain the desired activity, fresh catalyst is continually added to the unit. Fresh catalyst is stored in a fresh catalyst hopper and, in most units, is added automatically to the regenerator via a catalyst loader. The circulating catalyst in the FCC unit is called equilibrium catalyst, or E-cat. Periodically, quantities of equilibrium catalyst are withdrawn.

1.2 Modeling of FCCU

Because of the importance of FCCU in refining, considerable effort has been done on the modeling of this unit for better understanding and improved productivity. In last fifty years, the mathematical modeling of FCC unit have matured in many ways but the modeling continues to evolve to improve the closeness of models predictions with the real process whose hardware is ever-changing to meet the needs of petroleum refining. Complexity of the FCC process because of unknown reaction mechanism, complex hydrodynamics, and strong interaction between reactor and regenerator, has made it almost impossible to develop a general model for the integrated process. Therefore, researchers in this field have worked on different

aspects of the process separately for modeling purposes (Gupta et al., 2005). However, maximum attention has been paid on the modeling of riser reactor which is the most important part of the FCCU.

1.3 Aim and Scope of Present Work

In the modeling of riser itself, the kinetic behavior modeling is of prime importance. Most of the models dealing with riser kinetics are based on the extension of simple lumping scheme proposed by Weekman and Nace (1970). In all these models feed and products are assumed to be made up of a few lumps. The kinetic parameters for the conversion of these lumps are estimated empirically. The kinetic parameters thus obtained depend heavily on the nature and composition of the feedstock and may vary considerably from plant to plant. With this in view, the main objective of the present work is to develop a new generic kinetic model of the FCCU riser. This kinetic model considers cracking of one lump (pseudocomponent) giving two other lumps in one single reaction step. The proposed model also incorporates two phase flow and catalyst deactivation. Since a new cracking reaction mechanism is introduced, a new semi empirical approach based on normal probability distribution is also proposed to estimate the cracking reactions' kinetic constants. A regenerator model adopted from the literature is integrated with the proposed riser model to simulate the entire FCC unit and to study the effects of various operating parameters on the performance of this unit.

Chapter - 2

LITERATURE REVIEW

The importance of FCCU in refining has lead to concerted modeling efforts of all the aspects of this unit. In the present chapter the various aspects of the FCCU modeling from the literature are complied in three sections. These sections deal with riser modeling, regenerator modeling, and integrated riser and regenerator modeling respectively. Conclusions drawn from the literature are listed in a separate section at the end of the chapter.

2.1 Modeling of Riser Reactor

Modeling of the Riser reactor of an FCC unit is quite complex because of the presence of all three phases (solid, liquid, and vapor) in the riser, involvement of physical and chemical rate steps, and its strong interaction with the regenerator. Nevertheless, considerable efforts are made by various workers in all the above aspects of riser modeling. Gupta and Subba Rao (2001) have given the summary of main features of some FCC riser models (Table 2.1).

2.1.1 Riser kinetics

Describing the kinetic mechanism for the cracking of petroleum fractions has been, and still is, a challenge for the researchers in the field of modeling of the fluid catalytic cracking. The presence of thousands of unknown components in the feed to the riser and the parallel/series reactions of these components makes the kinetics modeling difficult. The following classification of important chemical reactions occurring during catalytic cracking was listed by Gates et al. (1979):

1. alkanes cracking:

$C_nH_{2n+2} \rightarrow C_mH_{2m} + C_pH_{2p+2}$ with n = m + p

2. alkenes cracking:

$C_nH_{2n} \rightarrow C_mH_{2m} + C_pH_{2p}$ with n = m+ p

3. β-scission of aromatic alkyl chains:

$ArC_nH_{2n}+1 \rightarrow ArC_mH_{2m-1} + C_pH_{2p+2}$ with n = m + p, and Ar is aromatic ring

4. cycloalkanes cracking:

C_nH_{2n} (naphthene) → C_nH_{2n} (olefin)

5. hydrogen transfer:

-cycloalkane + alkenes → aromatic + alkanes

-coke precursor + alkenes → coke + alkanes

6. isomerisation:

-alkene → branched alkene

7. condensation reactions:

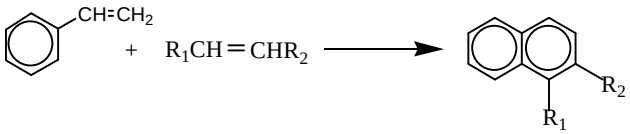

Weekman and Nace (1970) developed a simple kinetic scheme, based on the theory of Wei and Prater (1963), for the kinetic modeling of cracking reactions occurring in the riser reactor. This work can be considered as pioneer in developing the simple kinetic mechanism for FCC modeling purposes. Authors divided the charge stock and products into three components, namely, the original feedstock, the gasoline (boiling range C_5 – 410 ^{0}F), and the remaining C_4's (dry gas and coke), and hence simplified the reaction scheme (Fig. 2.1a). The model predicted the conversion of gas oil (the feedstock) and gasoline yield in isothermal condition in fixed, moving, and fluid bed reactors. The kinetic parameters of the model were evaluated using the experimental data. Since the gas oil and gasoline cracking rates have different activation energies, an optimum reactor temperature was also determined for the system. This simple three lump kinetic scheme was used by several investigators (Lee et al., 1989a; Theologos and Markatos, 1993) for the analysis of many other aspects of FCC modelling. This scheme was further extended to several other kinetic schemes. Among them the four lump model (Yen et al., 1988; Lee et al., 1989a), five lump model (Larocca et al., 1990), six lump model (Coxon and Bischoff, 1987, Takatsuka et al., 1987), ten lump model (Jacob et al., 1976), eleven lump model (Mao et al., 1985; Sa et al., 1985; Zhu et al., 1985), twelve lump model (Oliviera, 1987), thirteen lump model (Sa et al., 1995), and nineteen lump model (Pitault et al., 1994) are widely used.

Table 2.1: Summary of main features of some FCC riser models (Source: Gupta and Subba Rao, 2001)

	Corella and Frances (1991)	Martin et al. (1992)	Flinger et al. (1994)	Ali et al. (1997)	Derouin et al. (1997)	Theologous et al. (1999)
Vaporization	Instantaneous	Instantaneous	Instantaneous	Instantaneous	Instantaneous	Vaporization followed by cracking
Temperature variation	Adiabatic	Isothermal	Isothermal0	Adiabatic	Isothermal	Adiabatic
Molar expansion	Considered	Considered	Not considered	Not considered	Considered	Not considered
Axial catalyst holdup	Slip factor varied from 1.15 to 1.05 along the riser height	Correlation relating slip factor to riser height fitted to plant data	Cluster model approach	Constant	Correlation relating slip factor to riser height fitted to plant data	Single particle dynamics
Mass transfer resistance	Not considered	Not considered		Not considered	Not considered	Not considered
Kinetic model	Five lump	Five lump	Three lump	Four lump	Nineteen lump	Three lump
Deactvation	Non-selective, based on the time-on-stream of catalyst	Non-selective, based on the coke concentration on catalyst	Non-selective, based on the time-on-stream of catalyst	Variation along riser height not considered	Non-selective except relations leading to coke formation. Based on coke concentration on catalyst	Non-selective, based on the time-on-stream of catalyst

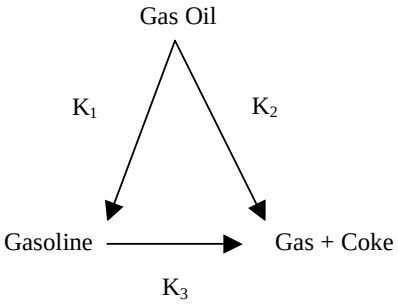

Fig. 2.1(a): Three lump kinetic scheme of Weekman and Nace (1970)

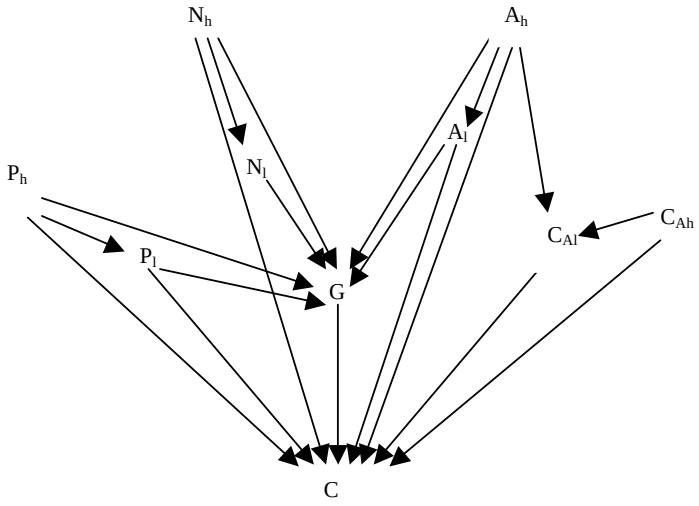

Fig. 2.1(b): Ten lump kinetic scheme of Jacob et al. (1976)

P_l = wt% paraffinic molecules, 430^0- 650^0 F
N_l = wt% naphthenic molecules, 430^0- 650^0 F
C_{Al} = wt% carbon atoms among aromatic rings, 430^0- 650^0 F
A_l = wt% aromatic substituent group, 430^0- 650^0 F
Pl = wt% paraffinic molecules, 430^0- 650^0 F
P_h = wt% paraffinic molecules, 650^0 F^+
N_h = wt% naphthenic molecules, 650^0 F^+
C_{Ah} = wt% carbon atoms among rings, 650^0 F^+
A_h = wt% carbon atoms among rings
G = Gasoline lump (C_5 – 430^0 F)
C = Coke lump (C_1 to C_4 and Coke)
$C_{Al} + P_l + N_l + A_l$ = LFO ($430 – 650^0$ F)
$C_{Ah} + P_h + N_h + A_h$ = HFO (650^0 F +)

The three lump model of Weekman and Nace (1970) was capable of predicting gasoline yield. However, it ignored the important aspect of prediction of coke deposition on the catalyst surface. Lee et al. (1989a) proposed a four lump kinetic model by separating the coke from the three lumps of Weekman and Nace (1970) as a separate lump. The separation of coke as a separate lump was important as the combustion of the coke in the regenerator supplies the heat for the endothermic cracking reactions. Authors also concluded that the C_1- C_4 gas yield increases with the increasing reaction temperature at the expense of the yield of gasoline and coke. The rate constants and activation energies for the reaction scheme were obtained by regression using the experimental data of Wang (1974). This four lump model, because of its simplicity and ease of formulation and solution of kinetic, material and energy equations, was used by Farag et al. (1993), Zheng (1994), Ali and Rohani (1997), Blasetti and de Lasa (1997), and Gupta and Subba Rao (2001) for their studies of various aspects of FCC modeling.

More detailed kinetic schemes were developed by various researchers. Jacob et al. (1976) developed a kinetic model dividing the feed and products into ten lumps reaction scheme (Fig. 2.1b) based on molecular structure of the hydrocarbons. They considered paraffins, naphthenes, aromatic rings and aromatic substituent groups in light and heavy fuel oil fractions. The model differed from the earlier models in the sense that it took into account the feed properties in addition to the boiling range. The model also accounted for the nitrogen poisoning, aromatic adsorption and time dependent catalyst decay. The kinetic constants for various possible reactions of the ten lump model of Gross et al. (1976) are listed in Table 2.2. Rate constants of the model were determined using the experimental data obtained in a fluidized dense bed with a commercial FCC catalyst. This detailed kinetic model was further extended by Oliveira (1987), Coxon and Bischoff (1987), and Theologos et al. (1997) for the kinetics studies of FCC riser reactor. Oliveira (1987) proposed a twelve lump scheme in which the coke lump of ten lump scheme of Jacob et al. (1976) is divided into two gas lumps (gas 1 and gas 2) and a coke lump. A thirteen lump reaction scheme was proposed by Sa et al. (1995), considering coke and cracking gas as two separate lumps and dividing the aromatic part of the vacuum residue into two parts, one of which is in resin and asphaltene fractions, the other in saturate and aromatic fraction. This kinetic

scheme was used by Gao et al. (1999) for their turbulent gas-solid flow and reaction

Table 2.2: Ten-lump model kinetic constants (Source: Arbel et al., 1995)

From		to		Activation energy (Btu/lb-mol)	rate at 1000^0F (1/s)	Heat of reaction (Btu/lb)
HFO	Ph	LFO	Pl	26100	0.196	25
	Nh		Nl		0.196	
	Ah		Al		0.196	
	Ah		Rl		0.489	
	Rh		Rl		0.049	
HFO	Ph	Gasoline	G	9900	0.611	65
	Nh		G		0.939	
	Ah		G	26100	0.685	
HFO	Ph	coke	C	31500	0.099	225
	Nh		C		0.149	
	Ah		C		0.198	
	Rh		C		0.149	
LFO	Pl	gasoline	G	9900	0.282	40
	Nl		G		0.752	
	Al		G	26100	0.196	
LFO	Pl	coke	C	31500	0.099	200
	Nl		C		0.099	
	Al		C		0.050	
	Rl		C		0.010	
Gasoline	G	coke	C	18000	0.048	160

HFO: heavy fuel oil; LFO: light fuel oil; Coke: Coke + C_1- C_4;
A: aromatic substitution group; R: carbons among aromatic rings; P: paraffins;
N: naphtenes; G: gasoline; C: coke; h: heavy; l: light.

model in FCC riser reactor. Pitault et al. (1994) developed a nineteen lump kinetic model, comprising twenty five chemical reactions, based on molecular approach (Table 2.3 shows the lumps considered by the authors). This nineteen lump kinetic model was used by Derouin et al. (1997) in their hydrodynamic model for the prediction of FCC products' yields for an industrial FCC unit. Table 2.4 shows the kinetic constants (of lumped schemes) obtained by various authors.

Another method of kinetic modeling is the 'single-events' method, given by Feng et al. (1993). It permits a mechanistic description of catalytic cracking. It is based on the detailed knowledge of the mechanism of various reactions involving the carbenium ions. Determination of the kinetic constants for these single events requires some key reactions of pure hydrocarbons. Based on the above method, Dewachtere et

al. (1999) developed a kinetic model for catalytic cracking of VGO in terms of elementary steps of chemistry. The lumping was done such that a link with modern analytical techniques is possible. For the network generation, in each lump all likely chemical species are considered and accounted for. Fifty single event rate parameters were determined from an extensive experimental program on catalytic cracking of key components with relevant structures.

Table 2.3: Lumps considered in Nineteen lump model of Pitault et al. (1994)

Feedstock	$C_{25} - C_{42}$; $T_{eb} > 350\ ^0C$ Paraffins Naphthenes with 1, 2, or 3 cycles Naphthenes with more than 3 cycles Aromatic compounds
LCO	$C_{13} - C_{24}$; $T_{eb} = 215 - 350\ ^0C$ Paraffins Olefins Naphthenes Olefinic naphthenes Aromatic compounds
Gasoline	$C_5 - C_{12}$; $T_{eb} = 40 - 215\ ^0C$ Paraffins Olefins Naphthenic hydrocarbons Olefinic naphthenes Aromatic compounds
LPG	$C_3 - C_4$ Paraffins Olefins
Fuel gas	H_2, $C_1 - C_2$
Coke	Conardson carbon

Table 2.4: Values of kinetic constants obtained with commercial FCC catalysts by various authors

Authors	T, K	k_0, s^{-1}	k_1, s^{-1}	K_2, s^{-1}
Weekman (1968)	755	6.3×10^{-3}	5×10^{-3}	5×10^{-4}
Nace et al. (1971)	755	2.8×10^{-3} to 1.1×10^{-2}	2.2×10^{-3} to 9.3×10^{-3}	3.3×10^{-4} to 2.8×10^{-3}
Parakos et al. (1976)	783-811	0.36-0.7	0.27-0.52	0.03-0.52
Corella et al. (1985)	793	0.19	0.12	6.6×10^{-3}
Corella et al. (1986)	773	0.23	0.18	3.2×10^{-2}
Lee et al. (1989a)	755-888	5.63×10^{-3} to 3.15×10^{-3}	4.34×10^{-3} to 2.2×10^{-2}	2×10^{-4} to 6.86×10^{-4}

k_0 = rate constant for the cracking reaction of gas oil
k_1 = kinetic constant for the formation of gasoline from gas oil
k_2 = kinetic constant for the formation of gases from gas oil

Other efforts in the kinetic modeling include, (i) a strategy to estimate kinetic constants of a lumped reaction, by using the data obtained at 480 ^{0}C, 500 ^{0}C and 520 ^{0}C in a micro-activity reactor, that decreases the number of parameters to be estimated simultaneously for the 3 lump, 4 lump and 5 lump kinetic models (Ancheyta et al., 1997) (ii) a study on the effects of metal traps in a FCC catalyst contaminated with high levels of nickel and vanadium (3000 ppm Ni and 4500 ppm V) using pulse reaction technique for testing of FCC catalysts in a down-flow micro activity reactor at different carrier gas flows (120-150 ml/min, at STP) and different temperatures (510-550 ^{0}C) (Farag et al., 1993). The four lump kinetic model was used to describe the gas oil conversion and the yields of gasoline, light gases, and coke in terms of catalyst activity. The data with FCCT (cracking catalyst with in situ metal traps) showed that the selectivity to gasoline as well as the gasoline yield was significantly improved, coke formation was reduced, and the gas formation was increased. (iii) a study of sensitivity analysis of Weekman's riser kinetics (Weekman, 1979) by Pareek et al. (2002) using CATCRACK (Kumar et al., 1995). Authors grouped the 20 rate constants of Weekman's kinetic model in five diffeent categories to demonstrate the advantage of such grouping in fine-tuning the simulator.

More advanced models incorporated kinetics and other physical rate steps using advanced computational techniques. Peixoto and de Medeiros (2001) used the concept of continuous description of catalytic cracking of petroleum fractions. They characterized the petroleum fractions using multi indexed concentration distribution function (CDF) developed by Aris (1989). Authors used the twelve lump scheme, combined with instantaneous adsorption hypothesis of Cerqueira (1996) and deactivation hypothesis of Oliveira (1987) in their model. Bidabehere and Sedran (2001) developed a model to analyze the simultaneous effects of diffusion, adsorption, and reaction at high temperature inside the particles of commercial FCC catalysts. Authors also experimentally established the relative importance of diffusion, adsorption and reaction using two equilibrium catalysts and n-hexadecane as a test reactant in a riser simulator reactor. Pareek et al. (2003) developed a non-isothermal model for the riser reactor which was incorporated in CATCRACK for obtaining the temperature and conversion profiles within the riser reactor. Authors predicted a temperature drop of about 30-40 ^{0}C in the riser.

Order of cracking reactions:

Weekman (1968) and Weekman and Nace (1970) represented kinetics of the gas oil cracking by a second order rate expression. Weekman and Nace (1970) assumed a first order reaction rate for the cracking of gasoline as it represents a narrower boiling fraction with smaller range of cracking rates. Several other researchers have also considered second order kinetics for gas oil and first order kinetics for the gasoline (Lee et al., 1989a; Gianetto et al., 1994; Blasetti and de Lasa, 1997).

Pachovsky and Wojciechowski (1971) represented the cracking kinetics for both gas oil and gasoline by first order rate equations; however they expressed the kinetic constants as a function of conversion. Pitault et al., (1994) also used first order cracking kinetics for all the lumps.

2.1.2 Riser hydrodynamics

The riser reactor of FCC unit can be divided into two zones with different functions. One is the feed-injection zone at the bottom of the riser, where the catalyst particles are accelerated, the evaporation of feed oil takes place, and the cracking

reactions are initiated. Other zone comprises of the middle and upper sections of the riser (Gates et al., 1979; Mauleon and Courelle, 1985).

In the feed-injection zone the hydrocarbons feed sprayed in the form of droplets through the feed nozzles comes in contact with the hot regenerated catalyst. The intimate contact between feed and hot catalyst rapidly vaporizes the feed and the increased amount of vapor raises the velocity and lowers the density of the flowing system (Murphy, 1992). This part of the riser reactor thus consists of three phases i.e., catalyst (solid), hydrocarbon vapors (gas), and hydrocarbon droplets (liquid). The influx of feed oil, atomizing steam and hot regenerated catalyst results in high velocity, temperature and concentration gradients in this zone. In the middle and upper section, hydrocarbon vapors and solid catalyst are present since all the feed droplets vaporize after traveling 2-4 m up from the feed inlet (Gao et al., 2001).

Feed injection zone:

In a typical design of an injector configuration, catalyst flowing at high density comes in contact with a feed introduction system of high penetration. About 5 wt% steam that serves as atomizing media is injected into the feed-injection zone as well. Catalyst particles get coated with feed as they flow through a feedstock spray. Some researchers (Merry, 1971; Chen and Weinstein, 1993) showed that the directed feed jets introduced into a fluidized-bed reactor have a considerable effect on the hydrodynamics of the riser. The jet can form a coherent void, bubble trains, and a surrounding compaction zone. Efforts have been done in feed-injection design to control the flow of hydrocarbons at plug flow conditions for minimizing the temperature gradients in the inlet zone that causes undesirable cracking reactions (McKetta, 1981; Yen et al., 1985; Mauleon and Courelle, 1985).

The overall performance of a riser can be predicted using one-dimensional mass, energy and chemical species balances, however, this approach cannot be applied to the inlet zone because of the its complex nature (Theologos and Markatos, 1993). The authors developed a three dimensional, two phase model for simulating the flow, heat transfer and chemical reaction to study the complex behavior of the inlet zone. The model can predict the effect of feed injection geometry on the catalyst acceleration, heat transfer between the phases, and chemical reactions. Theologos et al. (1997) used the above model and predicted that the feed vaporizes completely at the first 1.5 to 3 m of the reactor height and showed that selectivity of the primary

products improved with increasing the number of feed injection nozzles (Fig. 2.2 & 2.3). This can be attributed to the fact that the increased number of nozzles at the bottom promotes proper contact of the feed oil with the catalyst particles. Design of feed nozzle is also important for the performance of FCCU. Goelzer et al. (1986) compared the conversion and yield pattern achievable in a riser reactor using multi-pipe nozzle with that using spray nozzle.

Mirgain et al. (2000) studied the feed vaporization models to understand the main physical phenomena in a conceptual mixing chamber, for suggesting the improvements in current FCC technology. Authors demonstrated that feedstock droplet undergo homogeneous vaporization in the gas phase and heterogeneous vaporization as they collide with catalyst particles. Homogeneous vaporization cannot completely vaporize the oil droplets of size greater than 10 μm. On the other hand, if the droplets are sprayed on a dilute suspension or on a dense jet of catalyst particles, the droplet-catalyst contact is not proper for heat transfer and vaporization. Thus, the best way to ensure fast vaporization of feed droplets in FCC risers and downers is to spray the droplets onto a jet of catalyst particles with viodage ranging from 70 % to 90%.

Rate of vaporization of feed droplets depends largely on the droplet size. A number of workers have studied this parameter in detail. Elshishini et al. (1992) studied the effect of bubble size in the riser reactor. They predicted that an increase of bubble size leads to a decrease in the rates of heat and mass transfer between the bubble and dense (solid) phase, as a result the temperature of dense phase is remains high and this leads to the lesser yields of the gasoline due to over cracking. Gupta and Subba Rao (2001) in their hydrodynamics model of the riser reactor discussed the effect of feed droplet size on the conversion and yield patterns, catalyst temperature, catalyst holdup, and catalyst activity in the riser reactor. Subsequently they predicted the effect of feed atomization on regenerator temperature and on carbon on spent catalyst in their simulator for the entire FCC unit (Gupta and Subba Rao, 2003). Gao et al. (2001) in their hydrodynamic model studied the effect of changing spray droplet diameter, volumetric concentration and temperature of the feed in the feed injection zone. They predicted complete vaporization of feed within the first 4 m height of the riser reactor.

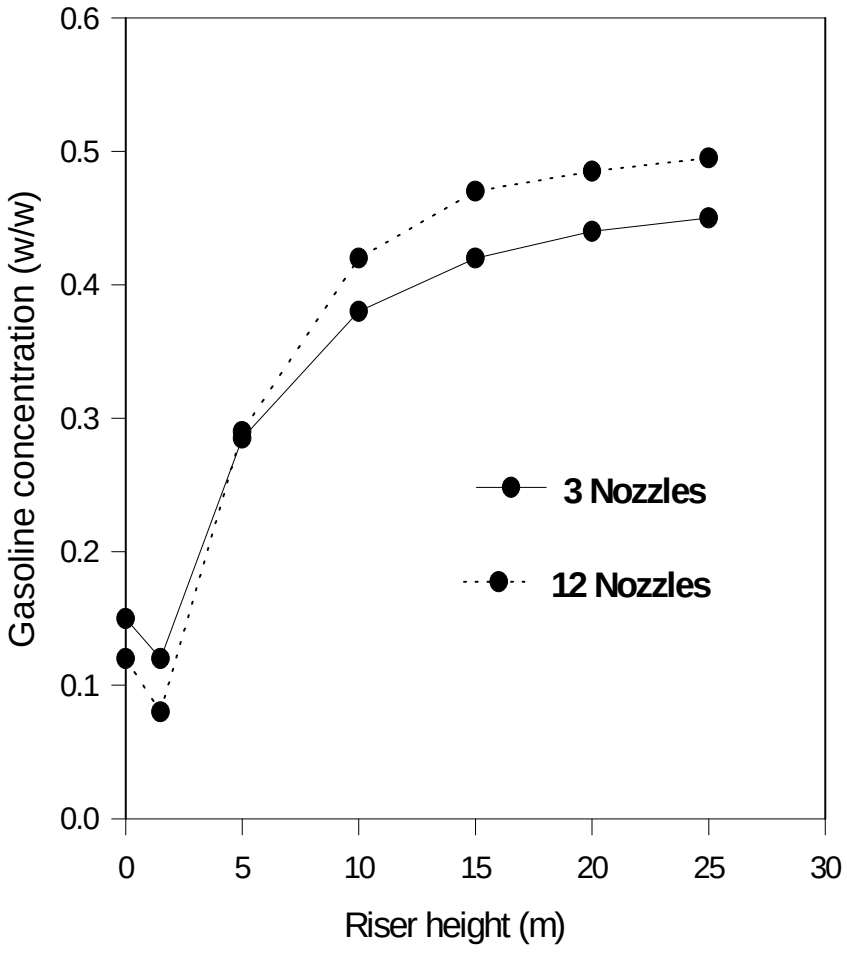

Fig. 2.2: Effect of number of nozzles on gasoline yields (Source: Theologos et al., 1997)

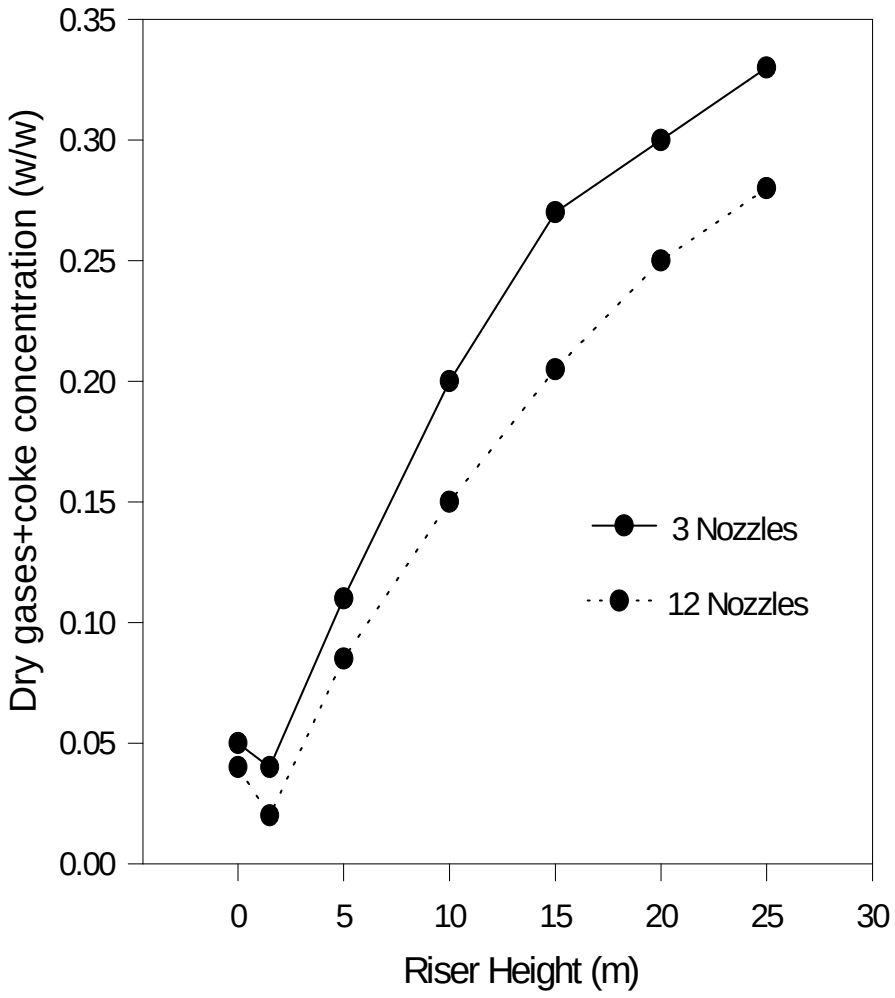

Fig. 2.3: Effect of number of nozzles on dry gases+coke yields (Source: Theologos et al., 1997)

Middle and upper section:

This part of the riser reactor has solid phase (catalyst & coke) and vapor phase (steam, hydrocarbon feed and product vapor). Vapor stream carries with it the catalyst particles in suspension and there is some back mixing of these particles because of slip between the solid and vapor phase. This makes the prediction of solid velocity profile difficult. The slip velocities higher than the terminal settling velocity of a single particle are observed in the riser. This may be attributed to the particle moving in clusters, which are agglomerates of loosely held particles.

At the riser wall the velocity of the solid and vapor stream is nearly zero and the effect of back mixing is also prominent. The velocity is maximum at the center of the riser. Since the flow in the riser is turbulent, the wall effect is confined to a small portion of the riser cross section. In the rest of the cross section the velocity is almost same. Hence the flow can be divided into two regions; one is a turbulent core region in the centre and an annulus region near the wall. A core annulus type of flow pattern in CFBs has been shown to exist in several experimental studies (Capes and Nakamura, 1973; Bader et al., 1988; Tsuo and Gidaspow, 1990; Zhou et al. 1994, 1995, Samuelsberg and Hertager, 1996, Das et al. 2003). A radial non-homogeneous distribution of solid particles has also been reported in several other experimental observations (Weinstein et al., 1986; Hartge et al., 1986).

Model developed by Samuelsberg and Hjertager (1996) predicted core-annulus flow in the riser which was in agreement with the experimental observations of Miller and Gidaspow (1992). Their prediction of maximum velocities in the core, and annulus and solid volume fractions profiles agreed with the experimental observations but the radial profile of solid, and shear viscosity in the core were under-predicted. Model predicted the non-homogeneity of velocities, temperature, and yield profiles in the riser reactor.

Several other hydrodynamics models have been proposed to describe the axial and radial distribution of solids density in CFB risers. Tsuo and Gidaspow (1990), Senior and Brereton (1992), Xu and Yu (1997), Sun and Gidaspow (1999), van der Meer et al. (1999), Ocone et al. (2000), Sundaresan (2000), van der Meer et al. (2000), and Das et al. (2003) have worked in this direction and studied the vertical pneumatic transport of solids referred to as circulating fluid bed (CFB) for solid gas systems and determined the radial gas and particle velocity profiles using

mathematical models. Kimm et al. (1996) proposed a hydrodynamic model describing the flow in laboratory scale down-flow reactor.

Tracer studies on the industrial scale riser reactor were conducted by some researchers (Bernard et al., 1989; Viitanen, 1993) to obtain axial and radial dispersion coefficients which are useful for modeling purposes. The axial velocity profiles of the gas and the catalyst reported by Viitanen (1993) are given in Fig.2.4. Authors attributed the cause of decline in the gas velocity after 16 m height to the inaccuracy of the calculation.

Flinger et al. (1994) proposed a cluster model approach to explain the higher observed slip velocities in the riser. They assumed two phases in the riser – a dispersed cluster phase containing all the catalyst, and a continuous gas phase. Das et al. (2003) compared the results of three dimensional hydrodynamics with one dimensional hydrodynamics and showed that the single dimensional model can predict the high slip velocities when the particle diameter is significantly altered.

Theologos and Markatos (1993) proposed a three dimensional mathematical model considering two phase flow, heat transfer, and reaction in the riser reactor. The authors developed the full set of partial differential equations that describes the conservation of mass, momentum, energy and chemical species for both phases, coupled with empirical correlations concerning interphase friction, interphase heat transfer, and fluid to wall frictional forces. The model can predict pressure drop, catalyst holdup, interphase slip velocity, temperature distribution in both phases, and yield distribution all over the reactor. Theologos et al. (1997) coupled the above mathematical model with a ten lump reaction scheme to predict the yield pattern of the FCC riser reactor. Gao et al. (1999) developed model that predicts three-dimensional, two-phase flow inside the riser-type reactor.

Godfroy et al. (1999) compared ten different hydrodynamic models with a set of experimental data, from different literature sources, that covered a wide range of operating conditions and showed reasonable to poor overall agreement. They described a hydrodynamic model that gave the best overall agreement with the experimental data. Following assumptions were made for the development of model: the slip factor increases with the riser diameter and decreases with the gas velocity, the normalized void fraction profile is a unique function of the radial distance, the centerline void fraction is equal to the average raised to power of 0.4, the velocity at the wall is zero, the radial profile of axial gas velocity and the radial profile of axial

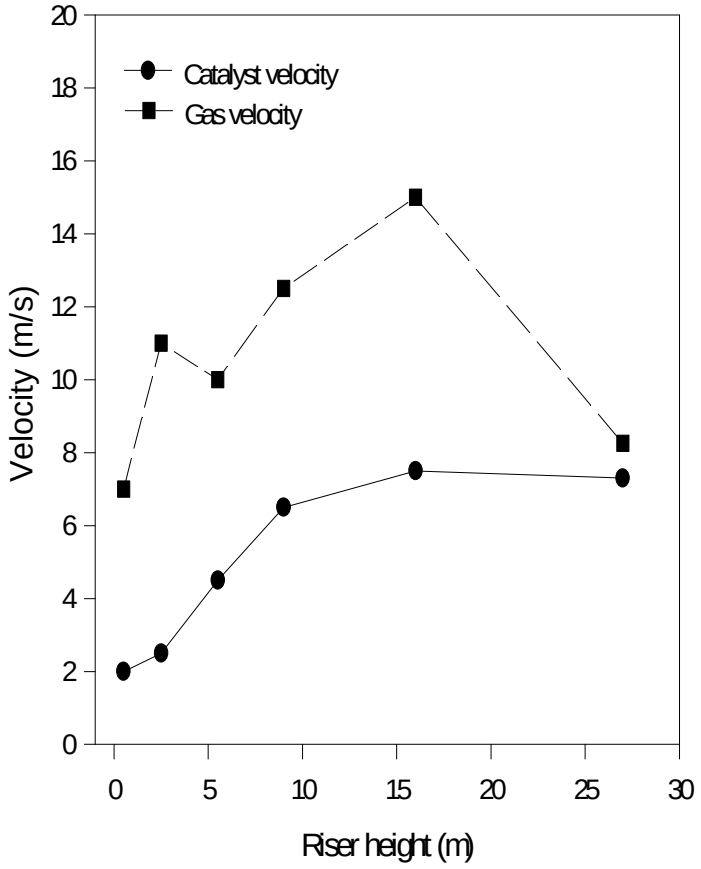

Fig. 2.4: Axial velocity profiles of the gas and solid phases in the riser (Source: Viitanen, 1993)

velocity follows the same power law, and the slip velocity at the center equals the single particle terminal velocity. The solid wall velocities were calculated on the basis of solid flux balance. The model predicted an axial pressure gradient for sand particles quite well but, over-predicted for the FCC particles. However, it correctly predicted the trend and the fractional change in pressure drop. The authors also developed an equation for the prediction of slip factor. A comparison of the slip factors for the FCC powder is given in Table 2.5.

Table 2.5: Slip factors for FCC powder reported by various authors

Gas velocity U_g (m/s)	Powder velocity G_s (kg/m^2.s)	Column diameter	Sphericity			
			ψ^a	ψ^b	ψ^c	ψ^d
11.0	500	0.2	1.16			1.9
7.6	500	0.2	1.45			2.3
5.2	500	0.2	1.74			2.7
11.0	500	0.18	1.9			1.6
7.6	300	0.18		2.3		2.2
5.7	300	0.18		2.3		2.5
8.9	500	0.18		2.0		2.1
10.1	500	0.18		2.3		2.0
5.6	550	0.15			2.5	2.5
7.0	550	0.15			2.2	2.2
9.0	550	0.15			1.9	2.0

[a] Knowlton (1995). [b] van Swaaij et al. (1970). [c] Contractor et al. (1994). [d] Godfroy et al. (1999).

A 3-D, two-phase, turbulent flow model developed by Gao et al, (1999) incorporated detailed kinetics (thirteen lump scheme) and demonstrated that excessive cracking occurred beyond the 10m riser height resulted in the increase of by-products yield at the expense of desirable products. They further developed their model to three-phase flow (Gao et al., 2001) by incorporating the effect of feed vaporization into their two-phase model which explained the synergetic effects of hydrodynamics, heat transfer, and feed vaporization on FCC reactions.

Berry et al. (2004) developed a two dimensional adiabatic model for the FCCU riser combining a predictive riser hydrodynamic model with the four lump

kinetic model of Gianetto et al (1994). Authors predicted the effect of increasing gas velocity on axial and radial suspension density, and on conversion and yield.

Gidaspow and Huilin (1998) experimentally measured the solids pressure inside the CFB riser, this information coupled with hydrodynamic models can be used for predicting the particle and velocity distribution profiles inside the CFBs. van der Meer et al. (1999) studied the dimensionless groups for hydrodynamic scaling of a CFB. Authors demonstrated that at least five dimensionless groups are required for full hydrodynamic scaling of a CFB.

Geometry of the CFB riser has been found to have considerable influence on the hydrodynamics of circulating fluidized beds (Brereton and Stromberg, 1986; Jin et al., 1988; Schnitzlein and Weinstein, 1988). Zhou et al. (1994 and 1995) obtained the detailed solid voidage profiles and solid velocity profiles with the aid of an optical fiber probe in CFB risers of square cross-section. van der Meer et al. (2000) measured solids flow patterns in laboratory scale riser reactor of square cross-section.

2.1.3 Catalyst deactivation

Catalyst used for the cracking loses its activity mainly due to following three reasons: (i) physical changes due to coke deposition and structural changes due to sintering, (ii) Poisoning due to the presence of metals (nickel and vanadium) and non-metal (sulphur, nitrogen, oxygen) in the FCC feed, and (iii) Deposition of coke on the active sites.

Catalyst deactivation due to physical changes and metal deposition is irreversible in nature but this deactivation step is very slow. And the fresh catalyst is added periodically to compensate for this loss. Activity loss due to coke deposition is very fast but is reversible and the catalyst can be regenerated easily by burning off the coke deposited on the catalyst surface.

Most of the popular theories on deactivation are based on the time-on stream concept. Many researchers have used this concept to formulate various empirical functions to be used for accounting the catalyst decay since a long time (Voorhies, 1945; Wojciechowski, 1968, 1974; Nace, 1970; Gross et al., 1974).

Various models for time dependent catalyst decay have been proposed for different lengths of contact time. Models of Weekman (1968) and Nace et al. (1971) used relatively high contact times (1.2 to 40 min), and Models of Paraskos et al. (1976) and Shah et al. (1977) used relatively low contact times (0.1 to 10 s). Froment

and Bischoff (1979) proposed a mechanistic based model considering catalyst decay rate a function of the fraction of active sites and the concentration of the reactants. Corella et al. (1985) studied the catalyst decay for a wide range of contact times (2 to 200 s) considering homogeneous and non homogeneous catalyst surfaces. Authors showed that the order of deactivation kinetics decreases with the contact time, taking values 3, 2, and 1, successively. They further justified the change of order of deactivation with the different contact times by showing the discrepancy in the values of these constants obtained by Weekman (1968) and Nace et al. (1971) for relatively large contact times and Shah et al. (1977) and Parakos et al. (1976) for short contact times. The deactivation equations used by these authors are listed in Table 2.6. Corella et al. (1986) determined the kinetic parameters of cracking and of deactivation for a given feed-catalyst system. Corella and Menendez, (1986) developed a model in which the catalyst surface was assumed to be non-homogeneous with acidic sites of varying strength. Larocca et al. (1990) reported that the catalyst deactivation can be represented by both an exponential decay function and a power decay function with an average exponent of 0.1-0.2.

Corella (2004) discussed the modeling of the kinetics of selective deactivation of the catalysts. A selective deactivation kinetic model uses different activity, deactivation function, and or deactivation order for each reaction in the network. Although they reflect reality better than the nonselective models, they may not be useful because of the complexity and handling difficulties.

Although the time-on stream theory is widely accepted there is no specific function that can be used for the deactivation. Different empirical equations were employed by various researchers to fit their experimental data. However, there are two functions that fit the experimental data quite well: power function and exponential function. The exponential function is more widely used. Kraemer et al. (1991) used the data from two different experimental reactors and showed that exponential decay function or power law function could equally represent the data; however, the power law assumes the unrealistic limits of infinite catalyst activity at zero time-on-stream and requires two parameters to describe deactivation. They further concluded that the simple first order decay function is an effective equation for describing the catalyst activity decay for short reaction times (less than 20 seconds).

Table 2.6: Empirical equations used for the catalyst deactivation by various authors

Author	Kinetic equation of activity		ψ	d
	differential	integrated		
Weekman (1968)	$-da/dt = \alpha a$	$a = e^{-\alpha t}$	α	1
Weekman and Nace 1970)	$-da/dt = \beta A^{-1/\beta}\alpha^{(\beta+1/\beta)}$	$a = A^{-\beta}$	$\beta A^{-1/\beta}$	$(\beta+1)/\beta$ (if$d\neq1$)
Wojciechowski (1968)	$-da/dt = Aa^{g}$	$a = [1+(g-1)At]^{-1/(g-1)}$	A	g (if $g\neq1$)
Corella et al. (1985)	$-d(k_0a)/dt = \psi k_0^{(1-d)}(k_0a)^{d}$	integrated for d=1 d=2 d=3	ψ	1 2 3

a = average activity of catalyst
t = time
ψ = average deactivation function
d = order of deactivation
k_0 = cracking kinetic constant, average value for all the reactants present in the gas oil

Den Hollander et al. (2001) determined the performance of a coked (0.56wt% coke on catalyst) and fully regenerated FCC by cracking a hydrowax feedstock in a micro-riser equipment. Authors predicted that the activity of coked catalyst was lower but was still significant, and the selectivity was similar to the regenerated catalyst. They performed a kinetic analysis, using a five lump reaction scheme, and demonstrated that the activity of coked catalyst is constant; it is not further affected by additional coke deposition.

Structure of coke:

The coke deposited on the catalyst surface does not have a specific molecular structure. The commonly used formula for coke is CH_n, where n is normally taken from 0.4 to 2.0 (de Lasa and Grace, 1979; Errazu et al., 1979).

2.2 Modeling of Regenerator

Regenerator modeling includes three main aspects, viz., hydrodynamics, combustion reaction kinetics, and temperature (heat removal) control. The fluidized catalyst bed in the regenerator is not a single homogeneous phase, and does not obey a single flow pattern which makes the hydrodynamics challenging, the combustion kinetics poses difficulty because of the unknown composition of the coke deposited

on the catalyst surface and also because of the variable CO/CO_2 ratio under different operating conditions.

The phenomena of multiplicity of steady states (bifurcation behavior) are observed in the FCC units (Iscol, 1970; Edward and Kim, 1988; Elnashaie and Elshishini 1990). The combustion process in the regenerator is the main reason for this multiplicity since the reactions in the riser are endothermic and kinetics is monotonic it can not be the source of bifurcation behavior. The three steady states known to exist in the units are high temperature steady state, low temperature steady state and middle unstable steady state (temperature between low and high). Temperature control in the regenerator is therefore crucial because of the bifurcation behavior.

2.2.1 Regenerator kinetics

The reactions taking place in the regenerator are the coke combustion reactions. This coke is the byproduct of the cracking reactions taking place in the riser and gets deposited on the catalyst surface during the course of cracking. Carbon and hydrogen are the major constituents of the coke that reacts with oxygen, present in hot air entering from the bottom of the regenerator. Krishna and Parkin (1985) reported the stoichiometry of the regeneration reactions based on the open literature data and pilot-plant studies conducted at Gulf Research and Development Co., Pittsburgh as:

$$CH_{x(s)} + \left[\frac{\beta+2}{2(\beta+1)} + \frac{x}{4}\right] O_{2(g)} \rightarrow \frac{\beta}{\beta+1} CO_{(g)} + \frac{1}{\beta+1} CO_{2(g)} + \frac{x}{2} H_2O_{(g)} \qquad (2.1)$$

and

$$2CO_{(g)} + O_{2(g)} \rightarrow 2CO_{2(g)} \qquad (2.2)$$

where, $CH_{x(s)}$ is hydrocarbon deposit on the catalyst, β is intrinsic CO/CO_2 ratio at the catalyst site and is given by the following equation:

$$\beta = k_{B0} e^{(-E_B/RT)} \qquad (2.3)$$

The value of x reported by Lee et al. (1989b) to be a number between 0.4 and 2.0. The exact value can be determined from the flue gas analysis. Authors determined this value from the flue gas data collected from the Kaohsiung Oil Refinery which came out to be 1.64.

The rate of the carbon combustion is first order with respect to the carbon-on-catalyst and oxygen partial pressure (Krishna and Parkin, 1985; Lee et al., 1989b). The oxidation of CO takes place by two ways with different first order rate constants, one is homogeneous oxidation in the gas phase and the other is catalytic oxidation (Krishna and Parkin, 1985; Lee et al., 1989b; Arbel et al., 1995). The rate of CO oxidation is expressed as being first order with respect to the partial pressure of CO and half order with respect to the partial pressure of O_2 for both homogeneous and catalytic oxidation reactions (Krishna and Parkin, 1985). The overall rate expression for the CO oxidation can be obtained by adding the rates of homogeneous and heterogeneous oxidation reactions.

Morley and de Lasa (1987) showed that the intrinsic kinetic constant for coke burning at the reaction site is equal to the global kinetic constant. Coke burning was calculated from the observed oxygen concentration and CO_2 to CO product ratio assuming the coke combustion and the CO post combustion reactions to be additive.

2.2.2 Regenerator hydrodynamics

The spent catalyst from the separator enters into the regenerator unit where it is fluidized by the hot air blowing from the bottom of the regenerator. This fluidized catalyst bed is not a single homogeneous phase, and is always very difficult to model due to unclear flow pattern.

Based on fluidization characteristics of the particles, Geldart (1973) classified the particles into C, A, B, and D types. FCC catalyst particle are Geldart A type particles. With the increase in gas velocity through a bed of particles in the upward direction, various fluidization regimes like packed bed regime, particulate bed regime, bubbling bed regime, slugging bed regime, turbulent bed regime, fast fluidization regime, and dilute transport are encountered. For modeling purposes, early researchers divided the fluidized bed into two beds of different densities namely the dense bed and dilute bed. The bottom part of the regenerator consisted of the dense bed wherein most of the catalyst particles were present and the upper part contained dilute bed where mostly gas and fewer catalyst particles were present. Later some more detailed models like grid effect model, two region model, and bubbling bed model were developed by various workers.

The grid effect model (Behie and Kehoe, 1973; Errazu et al., 1979) was developed for a shallow bed with diameter larger than height. In this model it is

assumed that the air columns in the bed are similar in shape and have identical heights and do not intermix with each other. Because of this assumption the simulation of a real process in which this type of grid is not formed leads to serious errors.

A further improvement of the grid effect model came in the form of two-region model (de Lasa and Grace, 1979; de Lasa et al., 1981). In this model the authors suggested that the dense phase could be further subdivided into two phases the bubble phase, and emulsion phase. It is assumed that the bubbles in the bubble phase are of same size and do not contain any catalyst particles, and the emulsion phase is a mixture of air and catalyst particles and is kept at the minimum fluidization condition.

The effect on the catalyst because of the rising air bubbles was not considered in the two-region model. This effect was, however, already introduced by Kunii and Levenspiel (1969) in their bubbling bed model. They assumed the catalyst underneath a bubble will be carried up by the bubble until it reaches the emulsion phase and mixes with it. They used the term "cloud-and-wake" to describe the situation where particles are being carried over. This bubbling bed model also assumes plug flow for both bubble phase and emulsion phase whereas the grid-effect and two-region models assume the emulsion phase in mixed flow. Hence, in the bubbling bed model the oxygen concentration is a function of position in the bed.

de Lasa et al. (1981) compared the following five different fluidized bed models for the regenerator using experimental data from the industrial regenerator: (i) a grid model where the bubble mass transfer coefficients were estimated with Davidson and Harrison (1963) correlation (ii) a grid model where bubble mass transfer coefficients are predicted by means of Kunii and Levenspiel (1969) equation (iii) a pure bubble model with mass transfer coefficient estimated with Davidson and Harrison (1963) correlation (iv) a pure bubble model where mass transfer coefficient predicted by means of Kunii and Levenspiel (1969) equation (v) a CSTR model. The authors showed that the CSTR model was useful for the evaluation of the overall coke conversion and is simpler than the other models which become complex on the consideration of the freeboard region (FBR) effect.

Krishna and Parkin (1985) in their three-region model for the regenerator considered the transfer line carrying the spent catalyst from the stripper to the regenerator as the first region, dense bed of the regenerator as second region and dilute phase above the dense bed as the third region. A plug flow model for the

transfer line was developed by the authors to account for carbon burning and CO oxidation in the transfer line. Their simulation results showed that less than 4% carbon is removed from the catalyst in the transfer line. The model is capable of predicting temperature and gas composition profiles taking into account carbon burning and CO oxidation reactions and catalyst entrainment effects.

Lee et al. (1989b) studied three different models (grid-effect model, two-region model, bubbling-bed model) for a fluidized-bed catalyst regenerator. They compared the results with actual operating data for selecting a suitable model for simulation. The authors concluded that the bubbling-bed model of the fluidized-bed regenerator, with the two thermally uniform stages for heat balance, was able to describe the actual regenerator with least error.

2.3 FCC Unit's Control Models

Proper control of the unit allows the refiners to handle changing feed-stocks and market needs. Dynamic models of varying degree of rigor have been proposed by many researchers. The phenomena of multiplicity of steady states make the control of the unit difficult.

Elshishini et al. (1992) studied the effect of bubble size in reactor and regenerator for all the three steady states. Elnashaie and Elshishini (1993) developed an unsteady state model of industrial FCC units by extending the earlier steady state models of Elnashaie and El-Hennawi (1979) and Elnashaie and Elshishini (1990). They investigated the dynamic behavior of the system for open-loop and closed-loop feed-back control systems.

Avidan and Shinnar (1990) discussed the effects of cracking reactions' chemistry, kinetics, and thermodynamics on the riser design. They also discussed the various designs of reactor and regenerator and their controllability. McFarlane et al. (1993) developed a type IV FCC unit model which includes almost all major equipment (feed and preheat system, cracking riser, regenerator, air blowers, and catalyst transport system) and operating constraints. Although, the model provides major dynamics effects of the unit however, it lacks in detailed description of the reactor kinetics and does not predict feed conversion. Elnashaie and Elshishini (1993) extended their steady-state model to an unsteady-state model for investigating the dynamic responses of the FCC unit in open-loop and closed-loop feedback-controlled

modes. Zheng, (1994) developed a dynamic model of FCC unit which included the dynamics effects of startup and shutdown. Arbel et al. (1995) developed a dynamic model of FCC units which includes more detailed kinetics of the cracking reactions (ten lump scheme) and includes a complete description of CO to CO_2 combustion kinetics incorporating the effect of catalytic combustion promoters in the regenerator. Ali and Rohani, (1997) developed a simple dynamic model of FCC unit. The model does not contain any partial differential equation and is easy to solve, and hence can be used particularly for control studies. Han et al. (2000) developed a detailed dynamic simulator of FCC unit including many auxiliary units (pre-hater, catalyst cooler, blower). They included detailed hydrodynamics of cracking reactor and catalyst regenerator. Their riser model incorporated ten lump cracking reactions scheme and regenerator model incorporated two-regime (dense bed and freeboard) and two-phase (emulsion and bubble) behavior of typical fluidized beds.

Optimal operation, through proper control, of FCC unit makes a refinery highly profitable. Krishna and Parkin (1985) developed a steady state model for the regenerator and coupled it with a riser reactor model for the monitoring and optimization of commercial FCC units. Khandalekar and Riggs (1995) applied nonlinear process model based control (PMBC) to Model IV industrial problem. They modeled the riser as a plug flow reactor for simplified optimization analysis and applied nonlinear model based control for reactor temperature, regenerator temperature and the flue gas oxygen concentration. They used feed temperature, catalyst circulation rate and regenerator air flow rate as manipulated variables. The dynamic microscopic oxygen and energy balances in the regenerator and the steady state energy balance for the reactor were used as nonlinear models for control. Ellis et al. (1998) modeled a type IV FCC unit using ten lump reaction scheme for the reactor. Authors used the steady state optimization models of the regenerator and riser reactor, a simplified reactor yield model, and models of the various process constraints. They also compared the relative performance of constraint control, off-line optimization, and online optimization for different feed characteristics and product pricing structures.

2.4 Concluding Remarks

The following conclusions may be drawn from the above discussion on the available literature

- Kinetic modeling of the riser reactor is based either on the lumping scheme or on the 'single events approach'. The kinetic constants evaluated using the lumping scheme are empirical in nature and are too much feed and plant specific. The 'single-events' method is difficult to use because of its analytical complexity and computational limitations.
- Feed atomization by using properly designed nozzles improves the yield of valuable products.
- Choice of the model for the regenerator hydrodynamics largely depends on the hardware of the regenerator being investigated.
- Regenerator kinetics is quite matured because of the known combustion reactions taking place in the regenerator. However, the CO/CO_2 ratio varies from unit to unit.
- Catalyst deactivation can be modeled either in the form of exponential or hyperbolic function of time-on-stream or as a function of coke content on the catalyst.
- Tremendous developments in computer software and hardware have paved the way for advanced control studies on FCC units using neural networks, and CFD.

Although, kinetic models incorporating a fairly large number of lumps have already been developed, still for the advanced modeling of the FFC unit a kinetic scheme with four to five lumps is preferred to avoid complexities in determination of rate constants, formulation of rate equations and their solution. This complexity limits the applicability of these detailed kinetic models incorporating larger number of lumps. In the present work a kinetic scheme for the riser reactor based on pseudo components approach is developed. This kinetic scheme incorporates fairly large number of pseudo components leading to several thousands of parallel reactions, yet the model equations can be solved easily. The proposed kinetic model for the riser reactor can be coupled easily with the other complex aspects of the FCC unit for developing more advanced model of the unit.

Chapter - 3

MODEL DEVELOPMENT

A typical FCC unit mainly consists of three components, a riser reactor, a catalyst stripper and a regenerator. For the modeling of FCCU, these three components need to be considered separately. The first section of this chapter deals with the riser model development. Stripper modeling is discussed in the second section. In the third section a regenerator model based on the model of Arbel et al. (1995) is developed. In the last section the riser model and regenerator model are integrated to simulate the entire FCC unit.

3.1 Riser Model

For the modeling of the riser reactor, a novel kinetics scheme is developed in the present work. This new kinetic scheme is coupled with the well known material and energy balance equations, and riser hydrodynamics proposed by Pugsley and Berruti (1996) and Gupta and Subba Rao (2001).

The following commonly used assumptions are made for the development of the riser model:

- At the riser inlet, hydrocarbon feed comes into contact with the hot catalyst coming from the regenerator and instantly vaporizes (taking away latent heat and sensible heat from the hot catalyst). The vapor thus formed move upwards in thermal equilibrium with the catalyst (Corella and Frances,1991; Martin et al., 1992; Fligner et al., 1994; Ali et al., 1997; Derouin et al., 1997).
- There is no loss of heat from the riser and the temperature of the reaction mixture (hydrocarbon vapors and catalyst) falls only because of the endothermicity of the cracking reactions (Corella and Frances,1991; Ali et al., 1997; Theologos et al., 1999, Gupta and Subba Rao, 2001).
- The endothermicity of the cracking reactions is calculated by finding the difference in the heat of combustion of each pseudocomponent involved in the reaction, thus heat effects of all other reactions such as hydrogen-shift, polymerization, condensation, etc., are assumed to be included in the overall heat of reaction.

- Gas phase velocity variation on account of gas phase temperature and molar expansion due to cracking is considered. Ideal gas law is assumed to hold (Gupta and Subba Rao, 2001).
- Catalyst holdup is estimated by a local force balance. Catalyst particles are assumed to move as clusters to account for the observed high slip velocities (Gupta and Subba Rao, 2001).
- Heat and mass transfer resistances are assumed as negligible (Corella and Frances, 1991; Martin et al., 1992; Ali et al., 1997; Derouin et al., 1997; Theologos et al., 1999).

3.1.1 Riser kinetics

The traditional and global approach of cracking kinetics is lumping. Mathematical models dealing with riser kinetics can be categorized into two main types. In one category the lumps are made on the basis of boiling range of feed stocks and corresponding products in the reaction system. This kind of models has an increasing trend in the number of lumps of the cracked gas components. The other approach is that in which the lumps are made on the basis of molecular structure characteristics of hydrocarbon group composition in reaction system. This category of models emphasize on more detailed description of the feedstock (Wang et al., 2005). In both of these categories, however, reaction kinetics being considered is that of 'conversion' of one lump to another and not the 'cracking' of an individual lump. Theses models do not include chemical data such as type of reaction and reaction stoichiometry. Moreover, the values of kinetic constants depend on the feedstock composition and must be determined for each combination of feedstock and catalyst.

More recently, models based upon 'single-events' cracking, structure oriented lumping, and reactions in continuous mixture were proposed by various researchers. Nevertheless, the application of these models to catalytic cracking of industrial feedstocks (vacuum gas oil), is not realized because of the analytical complexities and computational limitations.

In the two main categories of models, it is assumed that when one kilogram of an individual lump cracks the same amount of another lump is formed with a fixed reaction rate, and all rate constants are determined empirically. All these models contradict the basic theme of cracking reaction that when one mole of a reactant

cracks down it should give at least two moles of products. With this in view, in the present work, a new approach of kinetic scheme is being proposed. The proposed model falls under the first category in which lumps are formed on the basis of boiling point, but in this approach, each individual lump is considered as a pure component with known physico-chemical properties. Also, the reaction stoichiometry is considered. No separate coke lump is considered and it is assumed that when one mole of a lump cracks down it gives one mole each of two other lumps and the balance material gives the coke.

The riser is modeled as a vertical tube comprising of a number of equal sized compartments (or volume elements) of circular cross section (Fig. 3.1). Volume elements are designated by symbol j (j = 1, 2, …, N_C) and numbering of the volume elements is done from bottom (inlet) to top (outlet). Each volume element is assumed to contain two phases (i) solid phase (catalyst and coke) and (ii) gas phase (vapors of feed and product hydrocarbon, and steam). In a volume element, each phase is assumed to be well mixed so that heat and mass transfer resistances can be ignored. Model equations are written for both the phases in each j^{th} volume element for all pseudocomponents PC_i (i=1,2,….,N). Cracking reactions' rate constants in each volume element are evaluated at the local temperature of the j^{th} volume element and are subsequently used for calculating the change in molar concentration of each component and the heats of reactions. This approach of finite volume method (FVM) is widely used in computational fluid dynamics (CFD) such as one developed for membrane separation process by Kumar and Upadhyay (2000). It is assumed that known amount of reactants enter the j^{th} volume element, cracking reactions take place in the element for a period equal to the residence time of the hydrocarbons entering the element. The concentration of the reacting mixture at the outlet of j^{th} volume element serve in defining the reactant feed for the $(j+1)^{th}$ volume element. To start computation from volume element number one, i.e., the inlet of the riser reactor, the known process parameters at the inlet of the riser are used.

In the present work, the number of lumps being considered is N (=50), but these lumps are treated as hypothetical components (henceforth called pseudocomponents, and abbreviated as *PC*) with all physical, thermodynamic, and critical properties known, as if they are pure components (a brief description of generating these pseudocomponents is given in Appendix–I). The pseudocomponent based approach for design and simulation of crude distillation unit is highly

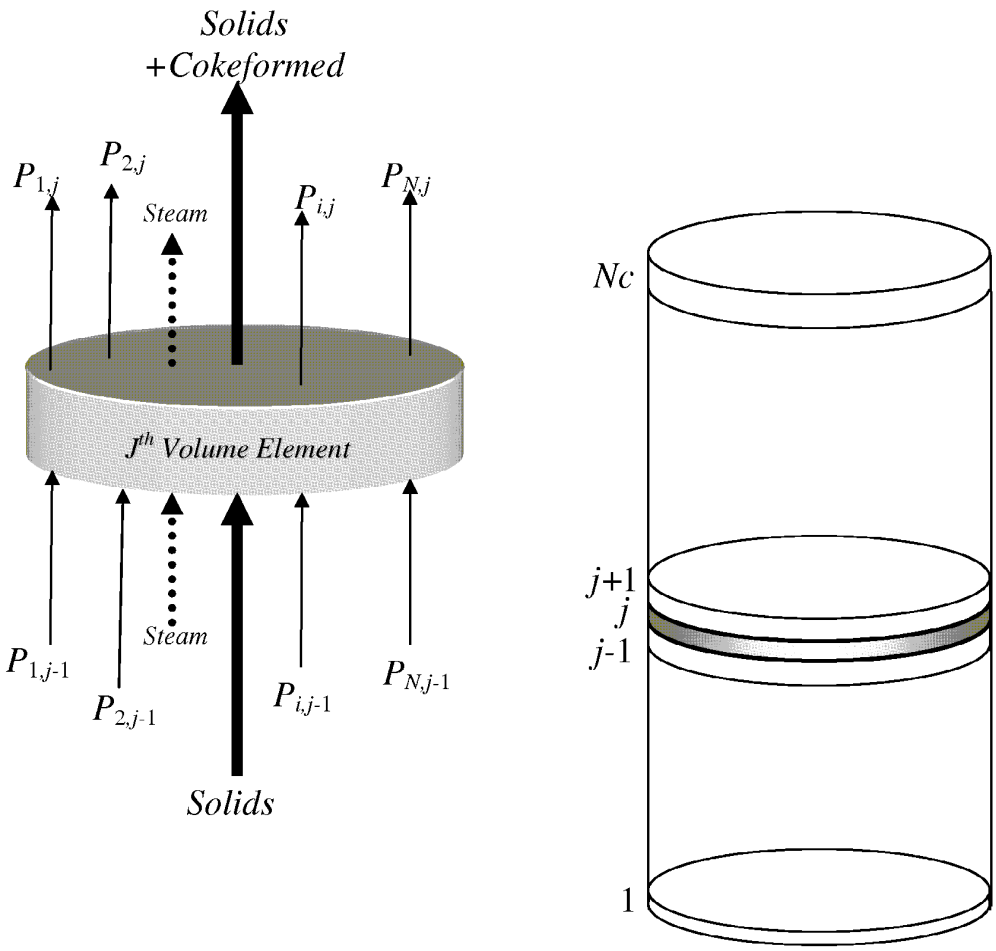

Fig. 3.1: A typical volume element in the riser reactor

successful. To apply this approach to FCC simulation, it is assumed that when one mole of a pseudocomponent is cracked, it gives one mole each of two other pseudocomponents and some amount of coke may also form. A schematic diagram of the reaction mechanism is given in Fig. 3.2. There are total *N* blocks in each column of the diagram and each block in a column represents one pseudocomponent (blocks in a row represent same pseudocomponent).

Pseudocomponents are numbered in increasing order of normal boiling point, which also ensures increasing order of molecular weight. According to the proposed scheme, there are several possible ways through which one particular pseudocomponent (say i^{th} pseudocomponent, PC_i) can crack down to give a pair of pseudocomponents PC_m, and PC_n along with some amount of coke as cracking byproduct according to the following reaction,

$$PC_i \xrightarrow{k_{i,m,n}} PC_m + PC_n + \alpha_{i,m,n} \qquad (\Delta H_r)_{i,m,n} \tag{3.1}$$

Where *i*, *m*, and *n* are pseudocomponents' numbers, $\alpha_{i,m,n}$ is the amount of coke formed in kilograms when one kmole of i^{th} pseudocomponent cracks to produce one kmole each of m^{th} and n^{th} pseudocomponents. The value of $\alpha_{i,m,n}$ can be calculated by taking difference in molar masses of reactant and product hydrocarbons as follows,

$$\alpha_{i,m,n} = MW_i - (MW_m + MW_n). \tag{3.2}$$

In equation (3.1) *m*, and *n* can vary from 1 to *N*, thus, there are ${}^{N}C_2$ possible ways through which cracking reaction for one pseudocomponent PC_i can be written. Only two of such possible reactions are shown by solid line in Fig. 3.2. The dashed line represents the same reaction, as the values of *m* and *n* in equation (3.1) are interchangeable. Thus the total number of reactions that could be written for the complete set of reaction becomes $N \times {}^{N}C_2$ (for N=50, total number of reactions become 61,250). However, all of these reactions are not feasible. The feasibility of a reaction is found using the stoichiometry of the cracking reaction (equation 3.1). Only those reactions are considered feasible for which the value of $\alpha_{i,m,n}$ calculated by the equation (3.2) is either zero or positive. Obviously, for all *i* (*i* = 1 to N), *m* and *n* each can vary from 1 to *i* only. This natural constraint greatly reduces the number of feasible cracking reactions but still the number is too large (more than ten thousand in the present case with N=50).

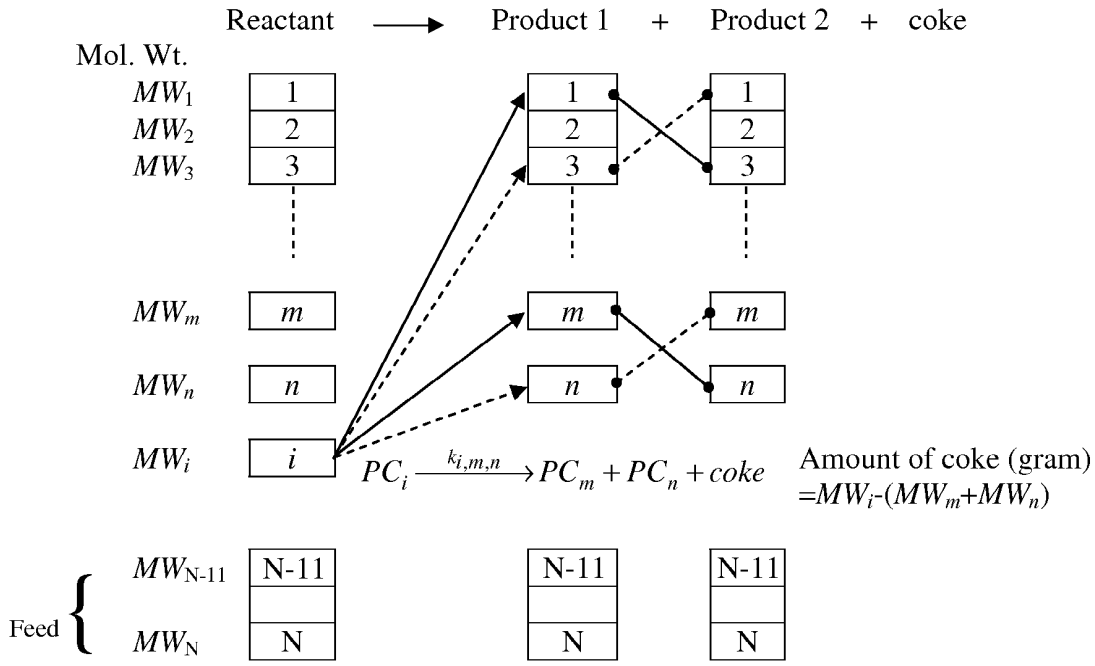

Fig. 3.2: Schematic diagram of reaction mechanism

To handle such a large number of reactions in riser (tubular) reactor special considerations for estimation of reaction rate constants and a technique for solving material and energy balance equations are required. In the present work, a new semi-empirical scheme for the estimation of rate constants is developed. This scheme makes the kinetic model more versatile. Six tunable parameters have been introduced to adjust more than ten thousand reaction rate constants ($k_{i,m,n}$) needed to explain complete reaction mechanism in a typical FCC riser reactor. Development of this correlation is discussed in detail in the following paragraphs.

The reaction rate constant, k, is normally determined by an Arrhenius equation in terms of frequency factor, k_0, and energy of activation ΔE. However, this equation lacks theoretical validation and the parameters k_0 and ΔE are nothing more than empirical constants (Fogler, 1992). This indicates that the reaction rate constant k is a parameter that needs to be determined empirically, using experimental data. In the present case, however, all data available in literature relevant to calculate the rate constants are for lumped reaction mechanism which is in fact rate constants for conversion of one lump to other and not for cracking of one lump giving two other lumps. Due to lack of experimental data, a purely hypothetical correlation for predicting Arrhenius type rate constant is being used.

Hypothetical scheme:

It is well observed fact that most physical, thermodynamic, or transport properties of hydrocarbons of a particular group have similar behavior, and properties of these hydrocarbons can be well correlated empirically (Daubert, 1998). In the present case, we are dealing with pseudocomponents, which are mixtures of large numbers of hydrocarbons of almost equal boiling point but widely different properties. However, the average characteristic of these mixtures of hydrocarbons with almost equal boiling point is characterized by Watson characterization factor K_W (as discussed in Appendix-I). Therefore it can safely be assumed that the cracking behavior of all pseudocomponents should follow a similar trend, as all the pseudocomponents are generated with exactly the same value of K_W. In fact, pseudocomponents are neither paraffin, olefin, nor aromatic. The Watson characterization factor is an indicator of an average characteristic in terms of paraffinicity, as well as aromaticity of the hydrocarbon mixtures (pseudocomponents).

These pseudocomponents are treated just as a pure component with specific characteristics, represented by K_W, which helps in determining all its physico-chemical properties.

In absence of experimental data, the rate constant of a particular reaction may be correlated with the probability of reaction to take place. A higher probability of the reaction will correspond to higher cracking rate and hence a higher rate constant. According to the proposed reaction scheme (equation 3.1) a pseudocomponent PC_i, cracks to give two other pseudocomponents PC_m, and PC_n and some amount of coke ($\alpha_{i,m,n}$) may also form. For the cracking of one specific PC_i (i.e., for one fixed value of i between 1 to N) there are a large number of parallel 'feasible' reactions taking place through which two components PC_m and PC_n are formed such that m and n can lie between 1 to i only (Fig. 3.2). However, the rate constants of all these feasible reactions (with different values of i, m, and n) must be different from one another. There are only three possible ways through which variation in the magnitude of cracking rate constant of i^{th} pseudocomponent with changing molecular weight of PC_m and PC_n can occur, (i) the rate constant of a cracking reaction is maximum when molecular weights of PC_m and PC_n are almost equal (Fig. 3.3(a)), (ii) the rate constant is maximum when molecular weights of PC_m and PC_n are widely apart (Fig. 3.3(b)), and (iii) the rate constant is almost constant for all values of m and n. These three possibilities can be expressed in terms of probability distribution as, (i) probability of cracking of a pseudocomponent molecule from its middle is maximum, (ii) cracking of molecule from its sides is more probable than from the middle, and (iii) cracking of molecule from anywhere is equally probable. First of all we consider the first case, i.e., when cracking from middle of the molecule has highest probability. Pitault et al. (1994) has also supported this assumption. Here it should be noted that 'middle of the molecule' means the molecular weight of PC_m and PC_n are equal, since there is no differentiation between ring-chain and straight chain molecules of pseudocomponents. Thus in this first case, cracking of pseudocomponents from the middle has highest probability, therefore, the numerical value of the rate constant should also be highest when molecular weights of the two product pseudocomponents are equal. It implies that for the cracking of i^{th} pseudocomponent (PC_i) giving two other pseudocomponents PC_m and PC_n, the rate constant is maximum ($k_{max,i}$) when molecular weight of m^{th} and n^{th} components are equal. In the present scheme,

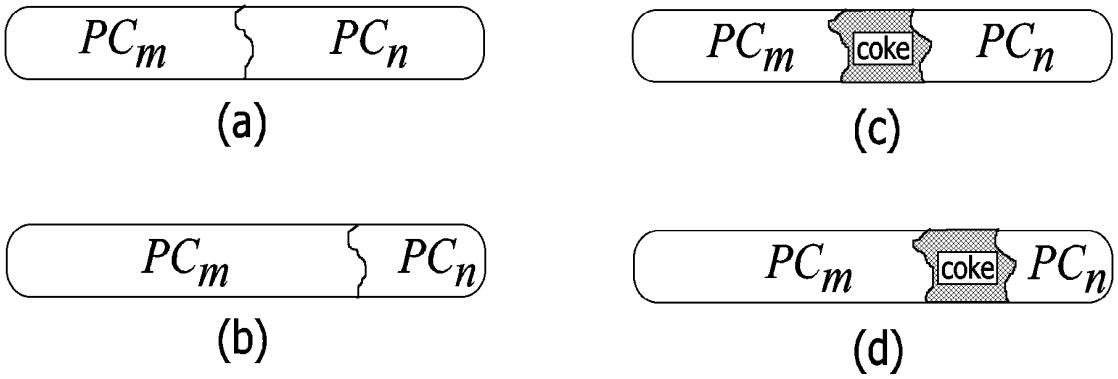

Fig. 3.3: Schematic representation of cracking of a pseudocomponent
(a) cracking from middle of the molecule (without coke formation), (b) cracking from side of the molecule (without coke formation), (c) cracking from middle of the molecule (along with coke formation), (d) cracking from side of the molecule (along with coke formation)

however, this is possible only when $m = n$ since there are no two pseudocomponents having equal molecular weights. For cases when $m \neq n$ (Fig. 3.3(b)), a function *f(x)* is defined to predict $k_{i,m,n}$ so that the function value approaches $k_{\max,i}$ when x (=MW_m – MW_n) tends to zero, and *f(x)* is less than $k_{\max,i}$ for all $|x| > 0$. This function could be any even function with a maxima at $k_{\max,i}$. However, in the present case, due to lack of experimental data, and using probabilistic approach, it is assumed that the probability of cracking of a pseudocomponent may follow a normal distribution. The normal distribution function in standard form is given by;

$$f(x) = \frac{1}{\sigma\sqrt{2\pi}} e^{\frac{-x^2}{2\sigma^2}} . \tag{3.3}$$

At $x = 0$, this function has maximum value which corresponds to the rate constant of the most probable cracking reaction, $k_{\max,i}$. Therefore

$$f(0) = \frac{1}{\sigma\sqrt{2\pi}} = k_{\max,i} \tag{3.4}$$

$$\text{Hence } 2\sigma^2 = \frac{1}{\pi\,(k_{\max,i})^2} \tag{3.5}$$

Substituting equation (3.4) and (3.5) in (3.3) we get the normal distribution function

$$f(x) = k_{\max,i}\, e^{-x^2\pi(k_{\max,i})^2} \tag{3.6}$$

Another parameter in equation (3.1) is the amount of coke formed during cracking reaction. At this juncture, the point to think about is whether the cracking reaction's rate increases, decreases, or remains unchanged when coke formation increases? The formation of coke can be depicted as in Fig. 3.3(c) and 3.3(d), and the mass of coke formed (in kg) when one kmole of reactant (PC_i) cracks can be given by

$$\alpha_{i,m,n} = MW_i - (MW_m + MW_n) \tag{3.7}$$

It appears from Tables 3.1 and 3.2 that the rate constant for the conversion of a lump to coke is significantly lower than the rate constants for the conversion of same lump to other hydrocarbon lumps. It indicates that the formation of coke is not favored during the cracking reaction. From this fact an inference can be drawn that the probability (or the rate constant) of a cracking reaction decreases with increasing coke formation (or $\alpha_{i,m,n}$). Since we are considering cracking of pseudocomponents, which themselves are mixtures of large number of actual compounds, it seems that the

Table 3.1: Kinetic data for the cracking reactions reported by Arbel et al. (1995)

Cracking reaction	Activation energy (kJ/mol)	Freequency factor (hr^{-1})	Rate at 538^0C (hr^{-1})	Molecular weight of cracking lump
HFO to LFO	60.7086	1.422×10^7	1760.4	380
HFO to gasoline	23.0274	1.026×10^5	3380.4	380
HFO to coke	73.269	3.704×10^7	712.8	380
LFO to gasoline	23.0274	8.215×10^4	2707.2	255
LFO to coke	73.269	1.852×10^7	356.4	255
Gasoline to coke	41.868	8.555×10^4	172.8	120

HFO: Heavy fuel oil; LFO: Light fuel oil

Table 3.2: Kinetic data for the cracking reactions reported by Lee et al. (1989a)

Cracking reaction	Activation energy (kJ/mol)	Freequency factor (hr^{-1})	Rate at 548^0C (hr^{-1})	Molecular weight of cracking lump
Gas oil to gasoline	68.2495	7.978×10^5	39.364	380
Gas oil to gas	89.2164	4.549×10^6	9.749	380
Gas oil to coke	64.5750	3.765×10^4	6.012	380
Gasoline to gas	52.7184	3.255×10^3	2.470	120
Gasoline to coke	115.4580	7.957×10^1	1.364	120

decrease in rate constant with increasing coke formation should be a continuous function (say, $g(\alpha)$) where α is the amount of coke formation ($\alpha_{i,m,n}$). Thus the general correlation for the rate constant can be expressed as the product of these two functions as:

$$k_{i,m,n} = f(x)\, g(\alpha) \tag{3.8}$$

In this work, we hypothesize that the function $g(\alpha)$ is an exponential decay function of the form

$$g(\alpha_{i,m,n}) = \frac{e^{-\alpha_{i,m,n}} - e^{-MW_i}}{1 - e^{-MW_i}} \tag{3.9}$$

such that,

$g(\alpha_{i,m,n}) = 1$ *at* $\alpha_{i,m,n} = 0$ (i.e., no coke formation)

and

$g(\alpha_{i,m,n}) = 0$ *at* $\alpha_{i,m,n} = MW_i$ (i.e., all hydrocarbon mass is converted to coke)

Combining equations (3.6), (3.8) and (3.9), we get

$$k_{i,m,n} = k_{\max,i}\, e^{-\pi (MW_m - MW_n)^2 (k_{\max,i})^2} \frac{e^{-(MW_i - (MW_m + MW_n))} - e^{-MW_i}}{1 - e^{-MW_i}} \tag{3.10}$$

A schematic three dimensional surface of $k_{i,m,n}$ as functions of coke formation ($\alpha_{i,m,n}$) and x (the difference between MW_m and MW_n**)** for the cracking of a typical pseudocomponent is shown in Fig. 3.4. It can be observed that at different values of coke formation, the grid-line parallel to the x-axis follows the normal distribution function of different curvature, and the function has a maxima at x=0.

Up to this point we have considered only hypothetical correlations, without any experimental verification. The equation (3.10) is quite rigid to accommodate experimental data as the surface shown in Fig. 3.4 can change only by changing $k_{max,i}$. Therefore, at this stage, we introduced two tunable parameters τ_1 and τ_2 which can be used to adjust the span (variance) of the normal distribution function and the curvature of the decay function, respectively, such that

$$k_{i,m,n} = \left[k_{\max,i} \cdot e^{-\tau_1 \left[(MW_m - MW_n) \cdot k_{\max,i} \right]^2} \right] \times \left[\frac{e^{-(MW_i - (MW_m + MW_n))/\tau_2} - e^{-MW_i}}{1.0 - e^{-MW_i}} \right] \tag{3.11}$$

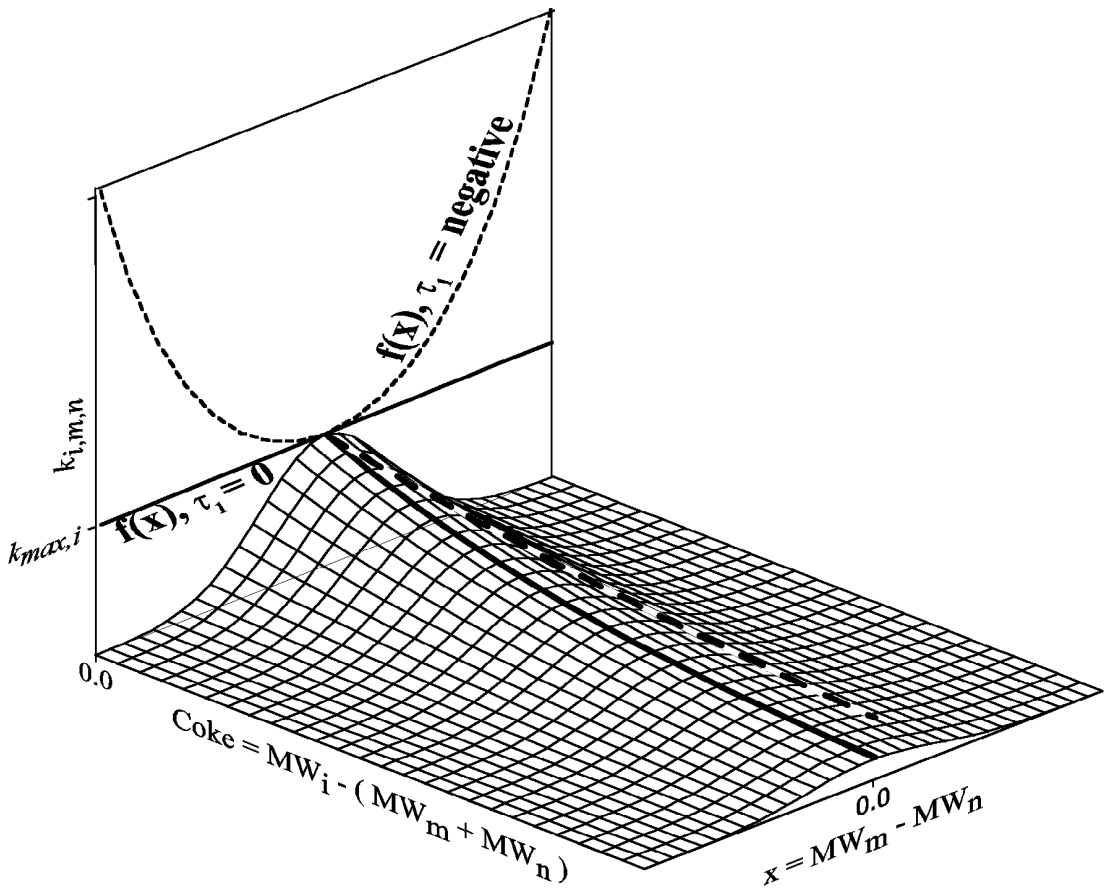

Fig. 3.4: Schematic representation of the probability distribution function *f(x)* (on the vertical plane) and the reaction rate constant $k_{i,m,n}$ as a function of coke formation and the difference in molecular weights of the products

By increasing τ_2, decay of exponential function *g(α)* is reduced. The thick solid line on the grid surface (Fig. 3.4) is elevated vertically upward to thick dashed line when τ_2 is increased. Hence by increasing τ_2 reaction rate constant can be increased even with higher coke formation. On the other hand, by decreasing value of τ_1 the function *f(x)* (hence the entire surface of Fig. 3.4) can be made flatter. If the value of τ_1 is reduced to zero, the intersection of the surface with $k_{i,m,n}$–x plane becomes a straight line. By further decreasing the value of τ_1 the surface becomes concave upward. In Fig. 3.4, the intersection of such surface with $k_{i,m,n}$–x plane is shown by a thin dashed line. Thus if τ_1 is positive, the cracking behavior of pseudocomponents is as explained for case (i), whereas, negative value of τ_1 leads to case(ii), i.e., the rate constant is highest when molecular weights of PC_m and PC_n are widely apart. For the third case, when rate constant is independent of molecular weights MW_m and MW_n, τ_1 is zero. Thus by introducing these two tuning parameters, τ_1 and τ_2, equation (3.11) can be used to predict rate constants for all possible schemes.

With change in temperature, it is expected that there should not be any change in the probability distribution for the cracking of a particular pseudocomponent. i.e., shape of the normal distribution curve remains unchanged at all temperatures. At the same time, reaction rate constant $k_{i,m,n}$ has to follow the Arrhenius equation. This is possible only if $k_{max,i}$ follows the equation

$$k_{\max,i} = k_{0,i}\, e^{\frac{-\Delta E_i}{RT}} \tag{3.12}$$

Where the energy of activation (ΔE_i) and frequency factor ($k_{0,i}$) are the characteristics of i^{th} pseudocomponent (PC_i), therefore numerical values of these parameters should be different for different pseudocomponents. In other words, ΔE_i and $k_{0,i}$ should be a function of some characteristic property of i^{th} pseudocomponent. One such property could be the molecular weight (MW_i). To predict such a relation, data of Tables 1 and 2 can be used. Although, these tables represent data for conversion reaction (not a cracking reaction), an assumption can be made from the data. Overall, it appears that parameters ΔE_i and $k_{0,i}$ has an increasing trend with increasing molecular weight of reactant lump. These trends may have the following relationship with molecular weight of cracking lump.

$$k_{0,i} = \tau_3\, MW_i^{\tau 4} \tag{3.13}$$

$$\Delta E_i = \tau_5 MW_i^{\tau 6} \quad (3.14)$$

Therefore, the parameter $k_{max,i}$ used in equation (3.11) can be expressed in terms of the frequency factor ($k_{0,i}$) and the energy of activation (ΔE_i) with four more tunable parameters τ_3, τ_4, τ_5, and τ_6. After considering three different cases and the sensitivity analysis, it was observed that the tuning parameter τ_1 and τ_4 are insignificant; therefore these can be eliminated from the list of tunable parameters. This indicates that the rate constant is independent of molecular weight of product pseudo components and the frequency factor is independent of the molecular weight of the cracking pseudocomponent.

Rate of cracking reactions:

The theoretical kinetic scheme developed in the present work assumes that all the cracking reactions are of first order. This is in agreement with the reported cracking rate of gas lump and gasoline lump. Many researchers have reported the cracking of heavier fractions of feed such as gas oil lump to be of second order due to deeper cracking action. In the present case, feed is broken into a large number of narrow boiling lumps (pseudocomponents), therefore, first order cracking can be assumed safely even for heavier lumps (i.e., high molecular weight pseudocomponents).

Thus for first order reactions, the rate of disappearance of i^{th} pseudocomponent due to cracking in j^{th} volume element through one reaction as indicated in equation (3.1) is given by

$$r_{i,m,n} = \phi_j \cdot k_{i,m,n} \cdot C_{i,j} \cdot (Mcat \cdot \Delta tCat_j) \quad (3.15)$$

Where, the concentration of i^{th} pseudocomponent at the inlet of j^{th} volume element is given by

$$C_{i,j} = \frac{P_{i,j}}{u_{g,j} A_r \delta_{g,j}} \quad (3.16)$$

$P_{i,j}$ in equation (3.16) is kmol of i^{th} component entering per second into the j^{th} volume element. A_r, $u_{g,j}$ and $\delta_{g,j}$ respectively are area of cross-section of the riser, local gas velocity, and gas phase volume fraction in the j^{th} volume element. $\Delta tCat_j$ is the residence time of catalyst in the j^{th} volume element, hence $Mcat \cdot \Delta tCat_j$ in equation (3.15) is the mass of catalyst present in j^{th} volume element.

3.1.2 Catalyst deactivation

Non-selective deactivation of catalyst, because of coke deposition, is assumed. The activity coefficient, ϕ_j (equation 3.15), depends on the coke concentration on the catalyst. Pitault et al. (1995) proposed following correlation for the estimation of activity coefficient

$$\phi_j = \frac{B+1}{B+\exp\left(A \cdot C_{cj}\right)}. \tag{3.17}$$

The values for deactivation constants A and B reported by the authors are 4.29 and 10.4 respectively; the same are used in this work. C_{cj} is the concentration of coke on catalyst coming out of j^{th} volume element (wt%).

3.1.3 Material balance

Calculation of material balances with several thousand parallel reactions is practically impossible by analytical solution of ordinary differential equations (ODE) representing the rate equations. Using higher order numerical techniques, such as Runge-Kutta method, is also not feasible for solving these ODEs due to excessive computational load. Therefore, a finite volume method (FVM) based approach was used for computing material balances. As discussed earlier, in this FVM approach it is assumed that the riser reactor is made up of a large number of volume elements of circular cross-section and of very small height, placed one over the other.

Both the gas phase and solid phases pass through each volume element in the upward direction, with different velocities. Since the height of a typical j^{th} volume element Δz_j is very small, therefore the residence-time for the gas phase, Δt_j, and the residence-time of the solid phase, $\Delta tCat_j$, is also very small. Applying concepts of finite volume approach, it is assumed that all reactions take place for Δt_j time at a constant rate determined by the prevailing temperature, pressure, and concentration at the inlet of j^{th} volume element. After time Δt_j the temperature and concentration of the stream (which is now outgoing stream from j^{th} element) are determined by the following material balance equations.

Material balance over j^{th} volume element for the gas phase:

Rate of mass in from the $(j\text{-}1)^{th}$ element – rate of mass out from j^{th} element

= rate of mass converted to coke in j^{th} element

(3.18)

or

$$\sum_{i=1}^{N} P_{i,j-1} MW_i - \sum_{i=1}^{N} P_{i,j} MW_i = \left(\sum_{i=1}^{N} \sum_{m=1}^{i} \sum_{n=1}^{m} r_{i,m,n} \alpha_{i,m,n} \right)_{for\ all\ feasible\ reactions} \quad (3.19)$$

Similarly,

Material balance over j^{th} volume element for solid phase:

Rate of mass out from j^{th} element – rate of mass in from the $(j\text{-}1)^{th}$ element

= rate of mass accumulated in j^{th} element

= rate of mass of coke formed (3.20)

or

$$\left(Mcat + Mcoke_j\right) - \left(Mcat + Mcoke_{j-1}\right) = \left(\sum_{i=1}^{N} \sum_{m=1}^{i} \sum_{n=1}^{m} r_{i,m,n} \alpha_{i,m,n} \right)_{for\ all\ feasible\ reactions} \quad (3.21)$$

Where, $Mcoke_j$ is the mass flow rate of coke at the outlet of j^{th} volume element (i.e., cumulative mass of coke formed up to j^{th} volume element).

In equations (3.19) and (3.21) summation for i is done from 1 to N. However, summation for m is done from 1 to i only because no product species can have molecular weight greater than the reactant species, whereas summation over n is done from 1 to m only as the products PC_m and PC_n are interchangeable.

3.1.4 Heat balance

It is assumed that the hydrocarbon feed, after coming into contact with hot catalyst from the regenerator, instantaneously vaporizes at the inlet of the first volume element of the riser [It takes about 0.1 s to fully vaporize the feed in modern units. This time represents about 3% of the mixture residence time in the riser. Therefore it is justifiable to assume instantaneous vaporization of the feed (Ali at al., 1997).]. Afterwards, the feed is assumed to be in thermal equilibrium with the catalyst all along the riser height. At the entrance (the first volume element of the riser reactor) the equilibrium temperature, T_{in}, is calculated by taking into account the specific heat of catalyst, steam and feed and the latent heat of vaporization of the feed.

As the pseudocomponents are chemically stable hypothetical components and according to the proposed reaction mechanism one pseudocomponent produces two

other chemically stable pseudocomponents, this indicates that the proposed reaction mechanism includes all possible reactions taking place during cracking (such as hydrogen-transfer, condensation, isomerisation, etc.) that leads to the formation of chemically stable products in the form of pseudocomponents. Therefore, the overall heat of reaction $(\Delta H_r)_{i,m,n}$, of equation (3.1) can be estimated by finding the difference between the heat of combustion of all products and the heat of combustion of the reactant.

Heat of combustion of pseudocomponents, *Hcomb* (BTU/lb), is estimated by the following equations in terms of the API gravity of the hydrocarbon.

$$Hcomb_i = 57.6\,API_i + 17700 \qquad for\ API_i \le 25 \tag{3.22}$$

$$Hcomb_i = -0.1727\,API_i^2 + 24.875\,API_i + 839.7\ln(API_i) + 15923.175$$

$$for\ 25 \le API_i \le 50 \tag{3.23}$$

$$Hcomb_i = 24\,API_i + 18820 \qquad for\ API_i \ge 50 \tag{3.24}$$

Equations (3.22) through (3.24) were obtained by curve fitting of graphical data proposed by Maxwell (1968). Curve fitting was done in such a way that there is no discontinuity in the heats of combustion values predicted by these three equations.

Thus for the cracking of i^{th} pseudocomponent, giving m^{th} and n^{th} pseudocomponents heat of reaction (kJ/kmole) becomes

$$(\Delta H_r)_{i,m,n} = \alpha_{i,m,n} \cdot H_{coke} + (MW_m Hcomb_m + MW_n Hcomb_n - MW_i Hcomb_i) \times 2.326 \tag{3.25}$$

The multiplying factor 2.326 is for converting heat of combustion from BTU/lb to kJ/kg, and H_{coke} is the heat of combustion of coke (kJ/kg). Thus the energy balance equation for the j^{th} volume element can be written as:

$$\left(Mcat \cdot Cp_{cat} + Mcoke_{j-1} \cdot Cp_{coke} + \sum_{i=1}^{N} P_{i,j-1} MW_i \cdot Cp_i \right)\left(T_{j-1} - T_j\right) = \left(\sum_i \sum_m \sum_n r_{i,m,n} \cdot \Delta Hr_{i,m,n} \right)_{for\ all\ \ feasible\ reactions} \tag{3.26}$$

Rearranging the above energy balance equation, we get

$$T_j = T_{j-1} - \frac{\left(\sum_i \sum_m \sum_n r_{i,m,n} \cdot Hr_{i,m,n}\right)_{for\ all\ feasible\ reactions}}{\left(Mcat \cdot Cp_{cat} + Mcoke_{j-1} \cdot Cp_{coke} + \sum_{i=1}^{N} P_{i,j-1} MW_i \cdot Cp_i\right)} \quad (3.27)$$

The temperature (T_j) thus calculated was used for the estimation of kinetic parameters and other temperature dependent properties of the pseudo components in the next (j^{th}) volume element.

3.1.5 Riser hydrodynamics

In the proposed riser model two phase flow viz. cluster phase and gas phase are considered. Cluster phase includes the loosely held particles of catalyst and the coke. The cluster phase and gas phase hold up vary along the riser height. Solid particles spend more time in the riser than hydrocarbon vapor due to slip between the two phases. For the calculation of solid and gas phase hold up along the riser height a model proposed by Gupta and Subba Rao (2001), based on force balance on clusters, is used. A similar model was also proposed by Pugsley and Berruti (1996).

For calculating the catalyst and gas velocities following analysis was proposed by Gupta and Subba Rao (2001).

Force balance on clusters fluidized by gas:

Net force on a cluster = Drag force on cluster – gravitational force on cluster

$$m_c \frac{du_c}{dt} = C_d A_c \left(\frac{1}{2} \rho_g \left(u_g - u_c\right)^2\right) - m_c g \quad (3.28)$$

Where, m_c, C_d, u_c, A_c, ρ_g, u_g, and g are mass of cluster (kg), drag coefficient, cluster velocity (m/s), projected area of cluster (m^2), gas phase density (kg/m^3), gas phase velocity (m/s), and gravitational acceleration (m/s^2), respectively.

The cluster volume and surface area calculations are based on equivalent spherical diameter. Thus mass and projected area of the cluster can be written as

$$m_c = \frac{\pi}{6} d_c^{\,3} \rho_c \quad (3.29)$$

$$A_c = \frac{\pi}{4} d_c^{\,2} \quad (3.30)$$

In the above equations d_c is cluster diameter, 6.0×10^{-3} m (Flinger et al., 1994), and ρ_c is cluster density. Since the flow in the riser is in turbulent region, therefore the drag coefficient is taken as 0.44.

On substitution of m_c and A_c, equation (3.28) can be written as

$$\frac{du_c}{dt} = \frac{3}{4}\left(\frac{C_d}{d_c}\right)\left(\frac{\rho_g}{\rho_c}\right)\left(u_g - u_c\right)^2 - g \tag{3.31}$$

Cluster velocity in a volume element is the volumetric flow rate of the clusters divided by the fractional cross sectional area available for clusters in that volume element.

Therefore

$$u_c = \frac{Mcat}{\rho_c A \delta_c} \tag{3.32}$$

Where A is cross sectional area of the riser and δ_c is cluster holdup fraction.

In the present work the velocity of solid phase moving in clusters is corrected for the amount of coke deposited on the catalyst particles, this gives the velocity of the cluster phase

$$u_{c,j} = \left(\frac{Mcat + Mcoke_{j-1}}{A_r \rho_s \delta_{c,j}}\right) \tag{3.33}$$

The residence time of the gas phase can be represented as the ratio of distance and velocity as

$$dt = \frac{dz}{u_g} \tag{3.34}$$

On the other hand, if u is the superficial gas velocity, then the actual gas phase velocity (u_g) is given by

$$u_g = \frac{u}{1-\delta_c} \tag{3.35}$$

Therefore in j^{th} volume element superficial gas velocity u_j is given by

$$u_j = \left(\frac{M_{st} + \sum_{i=1}^{N} P_{i,j} MW_i}{A_r \rho_{g,j}}\right) \tag{3.36}$$

Substituting equations (3.32), (3.34) and (3.35) in equation (3.31) and rearranging

$$\frac{-d\delta_c}{dz} = \frac{A_r \rho_c}{uMcat}\,\delta_c{}^2(1-\delta_c)\left(\frac{3}{4}\left(\frac{C_d}{d_c}\right)\left(\frac{\rho_g}{\rho_c}\right)\times\left(\frac{u}{1-\delta_c}-\frac{Mcat}{A_r\rho_c\delta_c}\right)^2 - g\right) \quad (3.37)$$

The density of clusters can be approximated by the following expression

$$\rho_c = \rho_{cat}(1-\varepsilon_c)+\rho_g\varepsilon_c \cong \rho_{cat}(1-\varepsilon_c) \quad (3.38)$$

The clusters are agglomerates of loosely held particles (Fligner et al., 1994). Cluster voidage ε_c may be assumed to be 0.5, in line with the two-phase theory of fluidization.

Equation (3.37) was treated as difference equation by replacing $\frac{d\delta_c}{dz}$ with $\frac{\Delta\delta_c}{\Delta z}$ to find out the value of cluster holdup fraction $\delta_{c,j}$ in j^{th} compartment with initial condition $\delta_{c,1} = 0.5$, clusters form a bed at minimum fluidization condition at the bottom (Gupta and Subba Rao, 2001).

The ideal gas law is assumed to compute gas phase density

$$\rho_{g,j} = \left(\frac{p\sum_{i=1}^{N} y_{i,j}MW_i}{R^{'}T_j}\right) \quad (3.39)$$

And, solid phase density can be calculated as,

$$\rho_{s,j} = \frac{Mcat + (Mcoke_{j-1} + Mcokeformed_{j-1})}{Mcat/\rho_{cat} + \dfrac{Mcoke_{j-1} + Mcokeformed_{j-1}}{\rho_{coke}}} \quad (3.40)$$

Residence time of catalyst in volume element j is

$$\Delta tCat_j = \frac{(\Delta z)_j}{u_{c,j}} \quad (3.41)$$

3.1.6 Model solution

A computer program for the model simulation is developed in 'C'. Model simulation is done on a P-IV (1.0 GHz) computer, which took less than 5 minutes for giving the simulation results. Although we can take variable height of volume elements, however, in the present work the height of each volume element of the riser was kept 10 mm. Further decrease in the height of the volume element had no appreciable effect on the results.

The sequence of calculations is listed below and the flow diagram for the same is given in Fig. 3.5. The model results are presented in results and discussions chapter.

Sequence of calculations:

1. Read in the input data.
2. Generate the TBP data from the given SD/ASTM distillation data as the case may be.
3. Calculate the conditions at the inlet of the riser reactor (T_0, $PC_{i,0}$'s, $C_{Pi,0}$'s, $\rho_{g,0}$, $\Delta\delta_{c,0}$, $u_{c,0}$, $u_{g,0}$, Φ_0) using the appropriate correlations and set j=1 for calculations in the first volume element. As the conditions at the exit of $j\text{-}1^{th}$ volume element are same as the conditions at the inlet of the j^{th} volume element, therefore for the conditions at the inlet of the first volume element subscript '0' is used.
4. Assume the initial values of the tuning parameters (τ_1, τ_2, τ_3, τ_4, τ_5, τ_6).
5. Calculate the values of $k_{max,i}$'s for the cracking of each pseudocomponent, and $k_{i,m,n}$'s for the feasible cracking reactions of a pseudocomponent. Use the values of $k_{i,m,n}$'s for the calculation of net change in the moles of a pseudocomponent in a volume element from the rate equation.
6. Calculate the heat consumed in the j^{th} volume element (ΔH_j) from equation (3.25) summing over the rates for all the feasible reactions.
7. Calculate the moles of each pseudocomponent, at the exit of j^{th} volume element, from the material balance equation.
8. Recalculate the values of $\rho_{g,j}$, $\Delta\delta_{c,j}$, $u_{c,j}$, $u_{g,j,}$ from the riser hydrodynamics, and the value of deactivation function (Φ_j).
9. Calculate the temperature of the reaction mixture at the exit of j^{th} volume element (T_j), from the energy balance equation.
10. Recalculate the values of specific heat of each pseudocomponent ($C_{Pi,j}$s) at T_j.
11. Calculate conversion and yields at the exit of j^{th} volume element.
12. Go to the next volume element (with j=j+1).
13. Repeat steps 5 to 11 till the sum of incremental height equals the height of the riser.
14. Calculate conversion and yields at the exit of the riser.
15. Compare the results with the plant data.

16. If sum of the errors in product yields, and error in temperature is greater than 5%, adjust the values of the tuning parameters and repeat steps 5 to 15.

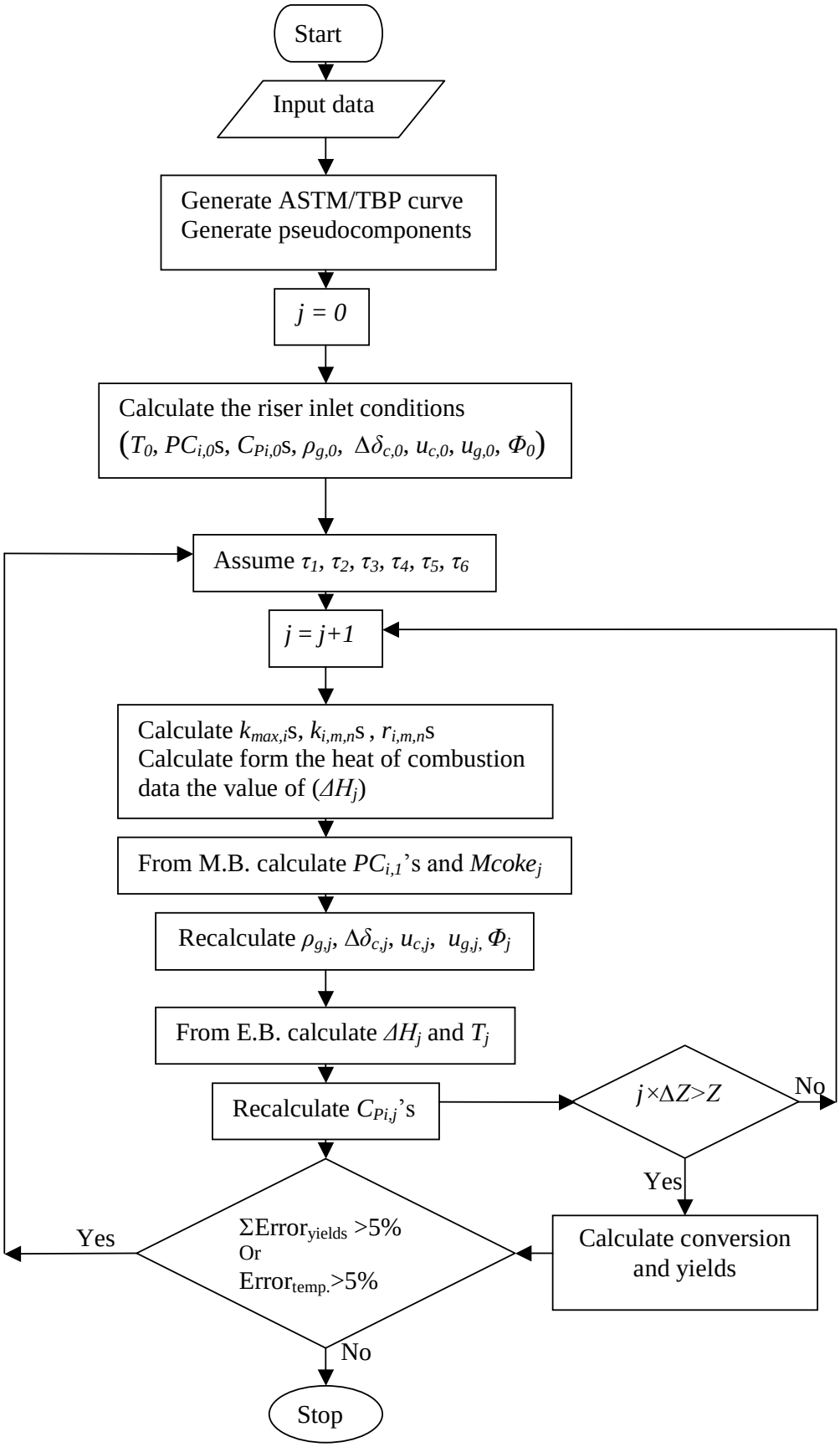

Fig. 3.5: Computational flow diagram for riser reactor model

3.2 Catalyst Stripper Model

It is important to strip the hydrocarbons, present in the interstitial gas and entrained and adsorbed on the catalyst surface, before the spent catalyst is sent for regeneration. Stripping is generally done in a dense, moving fluidized bed by adding steam which flows counter-current to the down flowing catalyst emulsion. Ideally, catalyst and steam are evenly distributed for efficient contacting with minimum back mixing. Baffles are normally installed in the stripper to promote better distribution and contacting of gas and solid.

There is not much information about the operating and design data of the stripper in the open literature. Recently, Mckeen and Pugsley (2003) have modeled a cold flow, laboratory scale FCC stripper using computational fluid dynamics (CFD). The authors simulated their model using the two-fluid CFD code MFIX (www. mfix.org) for operating conditions of gas superficial velocities between 0.1 and 0.33 m/s and solid circulation fluxes ranging between 28 to 90 kg/m^{2}s. However, CFD modeling is out of the scope of the present work, therefore, we have assumed that the stripper performance is ideal for the present work i.e., both the mixing and stripping efficiencies approaching 100%. In a few studies that incorporated stripper modeling, the temperature drop across the stripper is assumed 10 ^{0}C by Dave and Saraf (2002) and 13.88 ^{0}C (25 ^{0}F) by Arbel et al. (1995). We have also assumed a temperature drop of 10 ^{0}C across the stripper. So, the temperature of the spent catalyst entering the regenerator can be calculated as,

$$T_{SC} = T_{riserout} - \Delta T_{stripper} \tag{3.42}$$

3.3 Regenerator Model

After steam stripping, the spent catalyst from the riser reactor enters the regenerator. The catalyst present in the regenerator is fluidized with the hot air entering through an air distributor at the bottom. The oxygen present in the air reacts with the carbon deposited on the catalyst surface to give *CO* and CO_2. Carbon monoxide further reacts with oxygen to give CO_2. The regenerated hot catalyst flows to the riser.

This section includes regenerator kinetics, material and energy balance equations, and regenerator hydrodynamics. At the end the model solution is included.

Most of the modern regenerators operate in the turbulent fluidization regime with a dense region at the bottom containing most of the catalyst inventory and a dilute region at the top (Gupta and Subba Rao, 2003). The dense bed of the regenerator is modeled on the lines of the model of Arbel et al. (1995). The following commonly used assumptions are made for the development of the model:

- The regenerator is modeled as a bed of solids having two regions, a dense bed region and a dilute region. Most of the combustion reactions occur in the dense bed region. Since in the dilute region the catalyst inventory is very low it is assumed that the dilute region has no effect on the regenerator performance (Ali and Rohani, 1997).
- It is assumed that the coke only consists of carbon (Ali et al., 1997).
- The heat liberated by the combustion reactions is assumed to increase the temperature of the catalyst and the flue gas and the regeneration is adiabatic (Gupta and Subba Rao, 2003).
- The solid phase is assumed to be well mixed. The gas phase is assumed to flow through the equal sized well mixed compartments in series (Arbel et al, 1995).
- The solid phase and the gas phase are assumed to be in thermal equilibrium. It is also assumed that the resistance to mass transfer of the gaseous components is negligible (Krishna and Parkin, 1985).
- It is assumed that the entrained catalyst is completely recovered and sent back to the regenerator dense bed (Krishna and Parkin, 1985).

The cluster phase is assumed to be well mixed. Hence, the value of the coke on regenerated catalyst (C_{rgc}) is considered to be uniform everywhere in the regenerator dense bed. The gas phase is conceptualized as 50 equal sized well mixed compartments in series, which approximate to plug flow. An initial guess is provided for the values of C_{rgc} and regenerator temperature (T_{rgn}). The inlet conditions (for the first compartment) for the gas phase are known. For the other compartments the inlet conditions are considered same as the outlet conditions from the compartment below. Both catalytic and homogeneous oxidation of *CO* is considered.

3.3.1 Regenerator kinetics

The following combustion reactions are considered to be taking place in the regenerator:

$$C + \frac{1}{2}O_2 \xrightarrow{k_1} CO \tag{3.43}$$

$$C + O_2 \xrightarrow{k_2} CO_2 \tag{3.44}$$

$$CO + \frac{1}{2}O_2 \xrightarrow{k_{3c}} CO_2 \tag{3.45}$$

$$CO + \frac{1}{2}O_2 \xrightarrow{k_{3h}} CO_2 \tag{3.46}$$

The coke combustion in reactions (3.43) and (3.44) are proportional to C_{rgc} and partial pressure of O_2 in the regenerator (P_{O2}). The CO combustion reactions (3.45) and (3.46) are proportional to P_{O2} and partial pressure of CO in the regenerator (P_{CO}). The rate expressions for these reactions are,

$$r_1 = (1-\varepsilon)\cdot\rho_{cat}\, k_1 \frac{C_{rgc}}{MW_{Coke}} P_{O2} \tag{3.47}$$

$$r_2 = (1-\varepsilon)\cdot\rho_{cat}\, k_2 \frac{C_{rgc}}{MW_{Coke}} P_{O2} \tag{3.48}$$

$$r_3 = k_3 P_{O2} P_{CO} \tag{3.49}$$

Where,

$$k_3 = x_{pt}(1-\varepsilon)\rho_{cat} k_{3c} + \varepsilon\, k_{3h} \tag{3.50}$$

x_{pt} is a relative catalytic CO combustion rate.

The initial ratio of CO/CO_2 at the catalyst surface given by Weisz (1966) is

$$\left(\frac{CO}{CO_2}\right)_{surface} = \frac{k_1}{k_2} = \beta_c = \beta_{c0} e^{\frac{E_\beta}{RT}} \tag{3.51}$$

If k_c is overall coke combustion rate then

$$k_c = k_1 + k_2 \quad (3.52)$$

Where,

$$k_1 = \frac{\beta_c k_c}{\beta_c + 1} \quad (3.53)$$

and

$$k_2 = \frac{k_c}{\beta_c + 1} \quad (3.54)$$

From the above equations, the overall rate of the reaction of O_2, CO, and CO_2 in j^{th} compartment can be written as

$$r_{O_2} = (1-\varepsilon)\rho_{cat}\left(\frac{k_1}{2} + k_2\right)\frac{C_{rgc}}{MW_{Coke}}\frac{f_{O_2,j-1}}{f_{total}}P_{rgn}V_j + \frac{k_3}{2}\frac{f_{O_2}}{f_{total}}\frac{f_{CO}}{f_{total}}P_{rgn}^2 V_j \quad (3.55)$$

$$r_{CO} = (1-\varepsilon)\rho_{cat}k_1\frac{C_{rgc}}{MW_{Coke}}\frac{f_{O_2,j-1}}{f_{total}}P_{rgn}V_j - k_3\frac{f_{O_2}}{f_{total}}\frac{f_{CO}}{f_{total}}P_{rgn}^2 V_j \quad (3.56)$$

$$r_{CO_2} = (1-\varepsilon)\rho_{cat}k_2\frac{C_{rgc}}{MW_{Coke}}\frac{f_{O_2,j-1}}{f_{total}}P_{rgn}V_j + k_3\frac{f_{O_2}}{f_{total}}\frac{f_{CO}}{f_{total}}P_{rgn}^2 V_j \quad (3.57)$$

3.3.2 Material balance

Due to the combustion reactions occurring in the dense bed region, the molar flow rates of the gas phase components CO_2, CO, O_2, and N_2 change along the height of the regenerator dense bed.

The material balance for each component of the gas phase over j^{th} compartment can be written as,

O_2 balance:

Moles of O_2 coming out of the j^{th} compartment

= moles of O_2 coming out of the $(j\text{-}1)^{th}$ compartment

- Moles of O_2 consumed in the j^{th} compartment

(3.58)

or

$$f_{O_2,j} = f_{O_2,j-1} - r_{O_2,j} \quad (3.59)$$

CO balance:

Moles of CO coming out of the j^{th} compartment

= moles of CO coming out of the $(j\text{-}1)^{th}$ compartment

+ net moles of CO produced in the j^{th} compartment (3.60)

or

$$f_{CO,j} = f_{CO,j-1} + r_{CO,j} \quad (3.61)$$

CO_2 balance:

Moles of CO_2 coming out of the j^{th} compartment

= moles of CO_2 coming out of the $(j\text{-}1)^{th}$ compartment

+ net moles of CO_2 produced in the j^{th} compartment (3.62)

or

$$f_{CO_2,j} = f_{CO_2,j-1} + r_{CO_2,j} \quad (3.63)$$

Also, there is no change in the moles of Nitrogen (N_2) during the regeneration process (N_2 being inert).

$$f_{N_2,in} = f_{N_2,out} \quad (3.64)$$

Also,

$$f_{N_2,in} = 0.79F_{air};\ f_{O_2,in} = 0.21F_{air};\ f_{CO,in} = 0;\ f_{CO_2,in} = 0 \quad (3.65)$$

Carbon/Coke balance:

The mass balance for the carbon over the regenerator dense bed can be written as,

Number of moles of coke consumed = number of moles of CO + CO_2 formed (3.66)

$$\frac{M_{Cat}}{MW_{Coke}}\left(C_{sc} - C_{rgc}\right) = f_{CO,out} + f_{CO_2,out} \quad (3.67)$$

3.3.3 Energy balance

Heat generated in the regenerator = heat of formation of CO + heat of formation of CO_2 (3.68)

or

$$H_{rgn} = f_{CO,out}H_{f_{co}} + f_{CO_2,out}H_{f_{CO_2}} \quad (3.69)$$

Heat of formation, in kJ/kmol, of *CO* and CO_2 reported by Gupta and Subba Rao (2003) is given by the following equations:

$$H_{f_{CO}} = -111120.3 + 11.54T_{rgn} - 0.334\times10^{-3}T_{rgn}^{\ 2} - \frac{7.82\times10^{5}}{T_{rgn}} \quad (3.70)$$

$$H_{f_{CO_2}} = -401490.7 + 48.24T_{rgn} - 2.0\times10^{-3}T_{rgn}^{\ 2} - \frac{0.334\times10^{5}}{T_{rgn}} \quad (3.71)$$

Also,

Heat generated in the regenerator = gain in sensible heat of the catalyst

+ gain in sensible heat of the gas phase components (3.72)

or

$$H_{rgn} = Mcat\,Cp_{cat}\left(T_{rgn} - T_{sc}\right) + \left(T_{rgn} - T_{air,in}\right)\left(F_{air}MW_{air} + f_{CO}MW_{CO} + f_{CO_2}MW_{CO_2}\right) \quad (3.73)$$

3.3.4 Regenerator hydrodynamics

Two phases, solid phase and gas phase, are considered in the dense bed of the regenerator. The dense bed properties are calculated based on the molar air flow rate into the regenerator. The ideal gas law is assumed to hold. The density of the gas phase is given by

$$\rho_{gas} = \frac{P_{rgn}}{\frac{R'}{MW_{air}}T_{rgn}} \quad (3.74)$$

where, P_{rgn} is the regenerator pressure. Superficial gas phase velocity is given by

$$u = \frac{M_{air}}{\rho_{gas}A_{rgn}} \quad (3.75)$$

where M_{air} is the mass flow-rate of air. Dense bed void fraction is calculated from the correlation proposed by King (1989)

$$\varepsilon = \frac{u+1}{u+2} \quad (3.76)$$

Several other investigators (Arbel et al., 1995; Dave and Saraf, 2003; Gupta and Subba Rao, 2003) have also used this correlation for the prediction of dense bed void fraction of the regenerator.

Dense bed height is calculated using equation (3.77), and TDH calculations are done using the correlations reported by Ewell and Gadmer (1978)

$$H_{densebed} = W/(A_{rgn}\rho_{cat}(1-\varepsilon)) \quad (3.77)$$

$$TDH = TDH_{20} + 0.1(3.2808D_{rgn} - 20) \quad (3.78)$$

$$Log_{10}(TDH_{20}) = Log_{10}(20.5) + 0.07(3.2808u - 3) \quad (3.79)$$

The volume of a compartment *j* in the regenerator dense bed is given by

$$V_j = A_{rgn}\Delta z_j \quad (3.80)$$

Where,

$$\Delta z_j = \frac{H_{densebed}}{N_C} \quad (3.81)$$

3.3.5 Model solution

A computer program for the model simulation was developed in 'C'. The sequence of calculations is listed below and a flow diagram for the same is given in Fig. 3.6. The model results are presented in results and discussions chapter.

Sequence of calculations:

1. Read in the input data.
2. Determine the process conditions at the inlet of the regenerator.
3. Guess an initial value for T_{rgn}.
4. Guess an initial value for C_{rgc}.
5. Calculate the values of k_1, k_2, k_3, r_{O2}, r_{CO}, r_{CO2}.
6. From the M.B. equations calculate the moles/mol fraction of the gas phase components at the exit of the compartment. These values will serve as inlet values for the next compartment.
7. Go to the next compartment.
8. Repeat steps 5 to 7 till the end of the regenerator dense bed.
9. Calculate the net moles of *CO* and CO_2 formed.
10. From the coke balance equation, calculate C_{rgcnew}.
11. Check for the convergence criterion of C_{rgc}.
12. Repeat steps 4 to 11 till the convergence of C_{rgc} is achieved.
13. From the energy balance equation, calculate T_{rgnnew}.
14. Check for the convergence criterion of T_{rgn}.
15. Repeat steps 3 to 14 till the convergence of T_{rgn} is achieved.

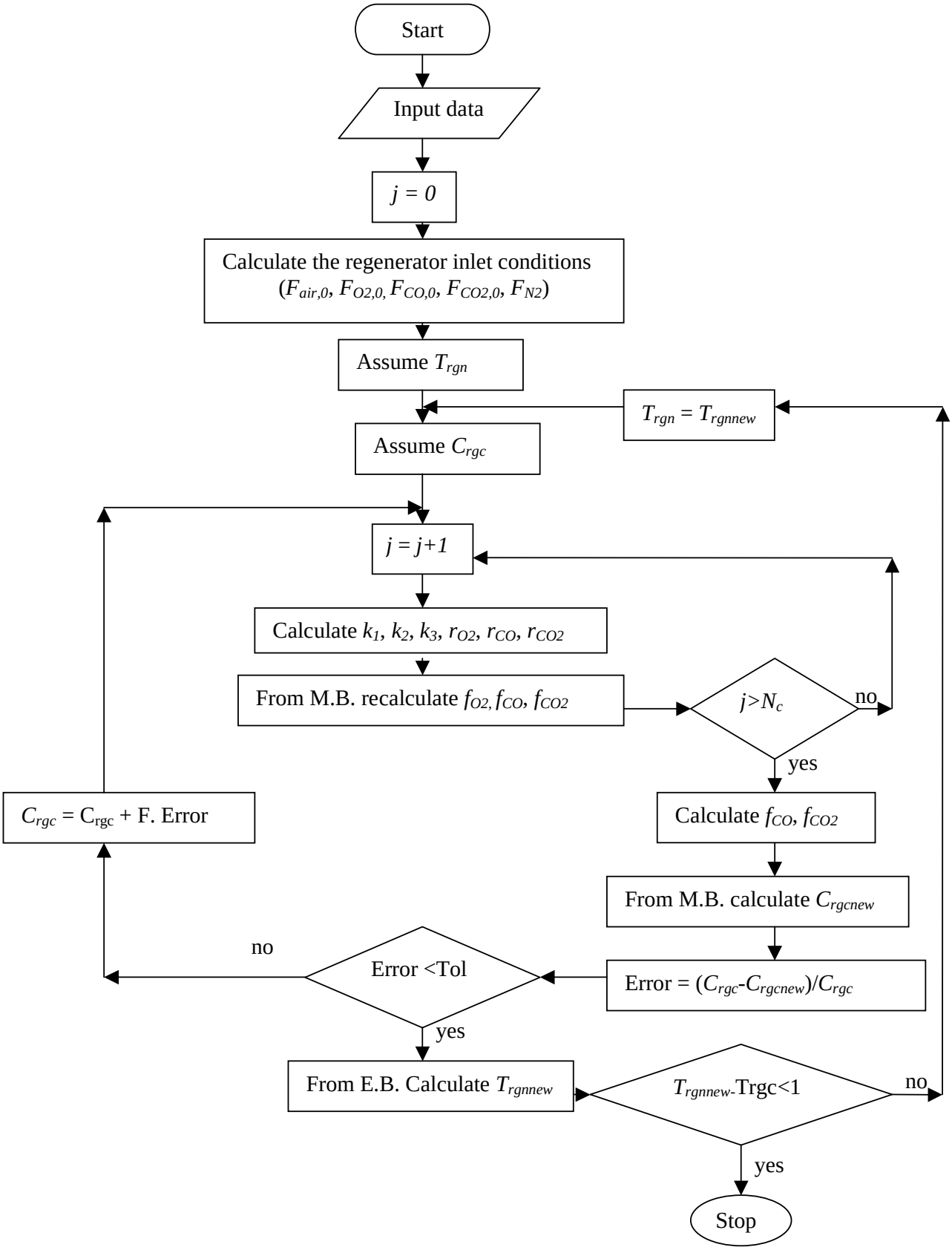

Fig. 3.6: Computational flow diagram for regenerator model

3.4 FCC Unit's Model

Riser and regenerator models were integrated to develop the simulator for the FCC unit. The solution procedure adopted for this simulation is iterative. An initial guess is made for the values of regenerator temperature (T_{rgn}) and coke on regenerated catalyst (C_{rgc}). The assumed value of the T_{rgn} was used to calculate the temperature at the inlet of the riser. The assumed value of C_{rgc} is used to calculate the activity at the inlet of the riser.

From the riser model the values of the riser outlet temperature and coke on spent catalyst are obtained. These values are provided as input to the regenerator program which in turn gives the new values of T_{rgn} and C_{rgc} . A final value of the C_{rgc} equal to 0.001 is assumed. Now the amount of air to the regenerator is adjusted to bring the C_{rgc} value in the regenerator near this value. This is repeated till the new value of T_{rgn} is in tolerable deviation from its old value.

3.4.1 Model solution

A computer program for the model simulation was developed in C. The Sequence of calculations is listed below and a flow diagram for the same is given in Fig. 3.7. The simulation results are presented in results and discussions chapter.

Sequence of calculations:

1. Read in the input data.
2. Assume an initial value for the regenerator temperature (T_{rgn}).
3. Set the value for the coke on regenerated catalyst (C_{rgc}).
4. Run riser reactor's program. Adjust the tuning parameters values for getting the desired amount of coke formed on the catalyst and other products' yields.
5. Run the regenerator's program. Adjust the amount of air input to the regenerator to bring the value of C_{rgcnew} close to the set value of C_{rgc}.
6. Calculate the new value for the regenerator temperature (T_{rgnnew}).
7. Check the convergence criterion for regenerator temperature (T_{rgn}).
8. Repeat steps 4 to 7 till the convergence for T_{rgn} is achieved.

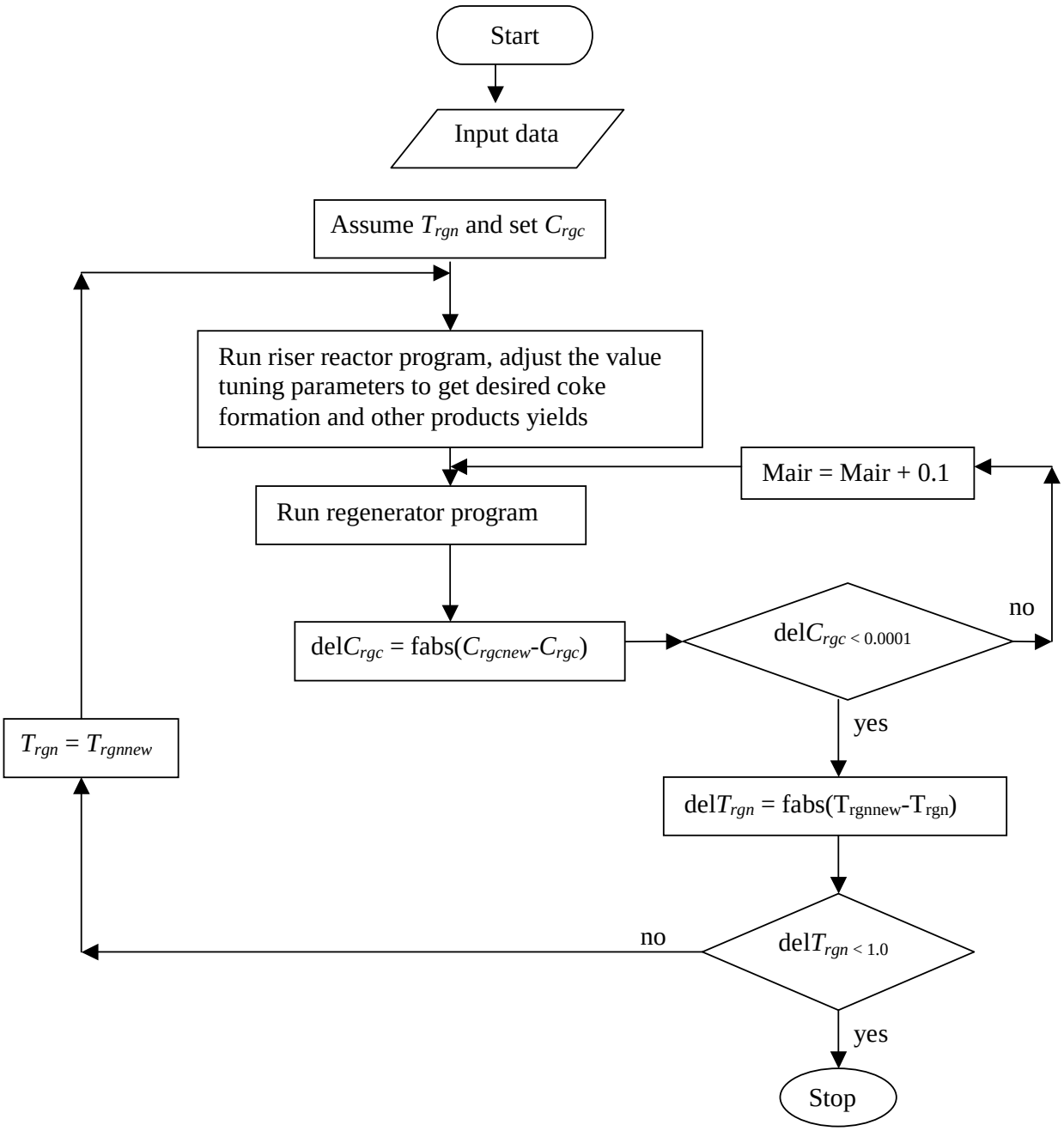

Fig. 3.7: Computational flow diagram for the FCC unit's model

Chapter - 4

RESULTS AND DISCUSSIONS

As discussed in previous chapter, the material balance equations were combined with reaction kinetics and the hydrodynamic model equations to obtain the moles of each pseudo component coming out of any volume element *j* (=1 to *Nc*) of the riser reactor. Thus, the model could predict the yield pattern along the riser height. Model validation is done as three case studies by using industrial data reported in the literature. Results of the proposed model can be tuned by adjusting six tunable parameters as discussed earlier. Numerical values of these tuning parameters were obtained separately for each case study. Stripper and regenerator models were then coupled with the riser model to simulate FCCU. Results of the simulator are being discussed in the following paragraphs. Effects of parameters such as catalyst to oil ratio (C/O ratio) on the riser performance, and C/O ratio and air flow rate on the FCC unit's performance are also included in the discussion.

4.1 Riser Simulation

For all the case studies of riser simulation, boiling point characteristics of feed (simulated distillation, SD) reported by Pekediz et al. (1997) were used (Table A1-1). Various other parameters common to all cases are given in Table 4.1 and plant data used in the three cases are presented in Table 4.2.

Table 4.1: Parameters used for the simulation of riser reactor

Parameter	Value	Source
Heat of combustion of coke	-32950 kJ/kg	Austin (1984)
Molecular weight of coke	12 kg/kmol	Arbel et al. (1995)
Volume fraction of clusters at inlet	0.5	Gupta and Subba Rao (2001)
Specific heat of catalyst	1.15 kJ/kg K	Ali et al. (1997)
Specific heat of steam	2.15 kJ/kg K	Blasetti et al. (1997)
Mass flow rate of steam	1.33 kg/s	Blasetti et el. (1997)
Feed temperature at the riser inlet	494 K	Ali et al. (1997)
Latent heat of feed vaporization	96 kJ/kg	Gupta and Subba Rao (2001)
Catalyst Particle density	1200 kg/m^3	Gupta and Subba Rao (2001)
Catalyst particle diameter	75 μm	Gupta and Subba Rao (2001)
Specific gravity of feed	0.9292 g/cm^3	Pekediz et al. (1997)
Cluster diameter	6 mm	Fligner et al. (1994)

Table 4.2: Plant Data used for simulation of riser reactor

	Ali et al. (1997)	Derouin et al. (1997)	Theologous and Markatos* (1993)
	(Case study – 1)	*(Case study – 2)*	*(Case study – 3)*
Riser height	33 m	(32 m)	50 m
Riser diameter	0.8 m	1.0 m	1.24 m
Riser pressure	2.9 atm	3.15 atm	(2.9 atm)
Catalyst Temperature	960 K	(960) K	1025 K
Feed rate	20 kg/s	85 kg/s	17.5 kg/s
Feed temperature	496 K	650 K	568 K
C/O ratio	7.2	5.53	8.0

*Literature data

Data given in the parentheses are those used in the present work in place of data either not reported or reported in ranges.

4.1.1 Case study 1

Industrial FCC plant data reported by Ali et al. (1997), presented in Table 4.2 was used in this case study. In this case five industrial data at the riser outlet – gasoline yield, gas yield, unconverted hydrocarbon, coke yield, and riser outlet temperature – are available to tune the simulator.

Model tuning was done by adjusting six tunable parameters in such a way that the sum of errors (i.e., sum of absolute value of deviation in the predicted and actual values of product yield and temperature at riser outlet in case of Ali et al., 1997 and at different riser heights in cases of Theologos and Markatos, 1993 and Derouin et al., 1997) is minimum. Since riser reactor model is highly nonlinear and very sensitive to the tuning parameters, techniques like "multivariate Newton-Raphson" or "method of steepest descent" cannot be used. Therefore, six tuning parameters (τ_1, τ_2, τ_3, τ_4, τ_5, and τ_6) were determined by line-search technique followed by golden-section method. In this technique, initial guesses of all six tuning parameters are required just like those required in Newton-Raphson or steepest descent methods. To estimate the optimal value of these parameters, in the present iterative method, one parameter was varied at a time (keeping other five constant). For the sake of clarity, let us take the example of varying τ_1 keeping τ_2, τ_3, τ_4, τ_5, and τ_6 unchanged. Starting with the initial value, a line-search for τ_1 was made, i.e., τ_1 was changed (increased or decreased) in constant small steps till the sum of errors continues to decrease. When the sum of error ceases to decrease by further step change in τ_1, it means the minimum value of sum of errors (that could be achieved by keeping other five parameters fixed at their

present value) is lying between the last and last-but-two value of τ_1 obtained during line-search. These two values of τ_1 were then used for further fine-tuning of its value by determining the minima of sum of errors using the method of golden-section (Mathews, 1998). The method of golden-section is used to find minima almost in the same way as method of bisection is used for finding zero (or root) of a nonlinear equation. After finding this new value of τ_1, the same procedure of line search and golden-section was adopted for finding a new value of other tuning parameter, say τ_2, keeping new value of τ_1, and old initial value of τ_3, τ_4, τ_5, and τ_6 unchanged.

The above procedure of line-search and golden-section was repeated several times for all tunable parameters in a cyclic way, i.e., after determining new value of all parameters (starting from τ_1 and ending at τ_6) in one round, other round of iteration was started once again from τ_1 with all previous values of tunable parameters replaced by new values. This cyclic process of iteration continued till the reduction in sum of errors in one round became insignificant.

Since the system of equations under consideration is highly nonlinear, there was always a chance of divergence of the iterations instead of convergence. Therefore, on-line graphical observations of reported and predicted data were made almost after every iteration. In case of divergence, step size of line search was reduced.

The simulator results, yield pattern and temperature profile, are compared with the industrial data at the riser outlet in Fig. 4.1 and 4.2, respectively. The values of six tuning parameters obtained are τ_1=0.0, τ_2=17.0, τ_3=0.009, τ_4=0.01, τ_5=1540, τ_6=0.43. Fig. 4.2 indicates, as the hydrocarbons and catalyst mixture travel upwards the temperature inside the FCC riser reactor decreases because of the endothermic cracking reactions. The catalyst temperature at the inlet of the riser (960 K) falls sharply to 880 K because sensible heat of catalyst coming from the regenerator is utilized in providing heat for raising the sensible heat of the feed, for vaporizing the feed, and for further heating of the vaporized feed. Afterwards, within first 10 m height inside the riser reactor the temperature drops from 880 K to 790 K. As most of the cracking takes place within first 10 m of the riser height. The temperature at the outlet of the riser is 775^0 K (Fig. 4.2). The decrease in reaction mixture's temperature and catalyst activity along the riser height cause a decline in the reaction rate hence the temperature gradient falls appreciably with the increasing riser height.

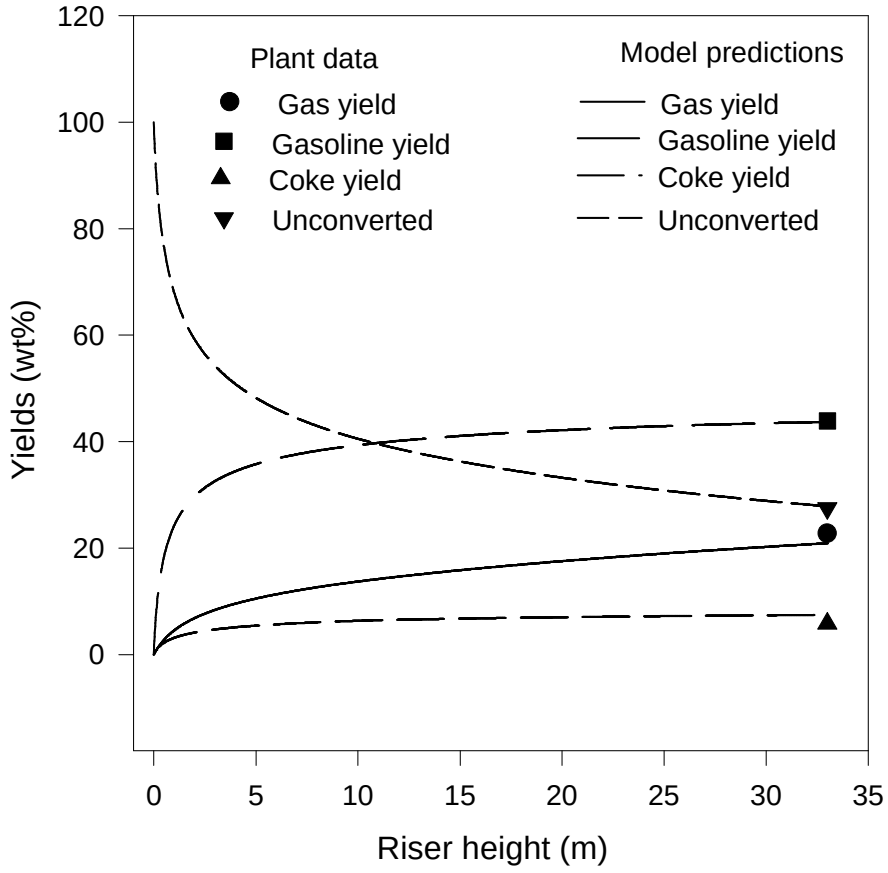

Fig. 4.1: Case study 1, comparison with the data reported by Ali et al. (1997)

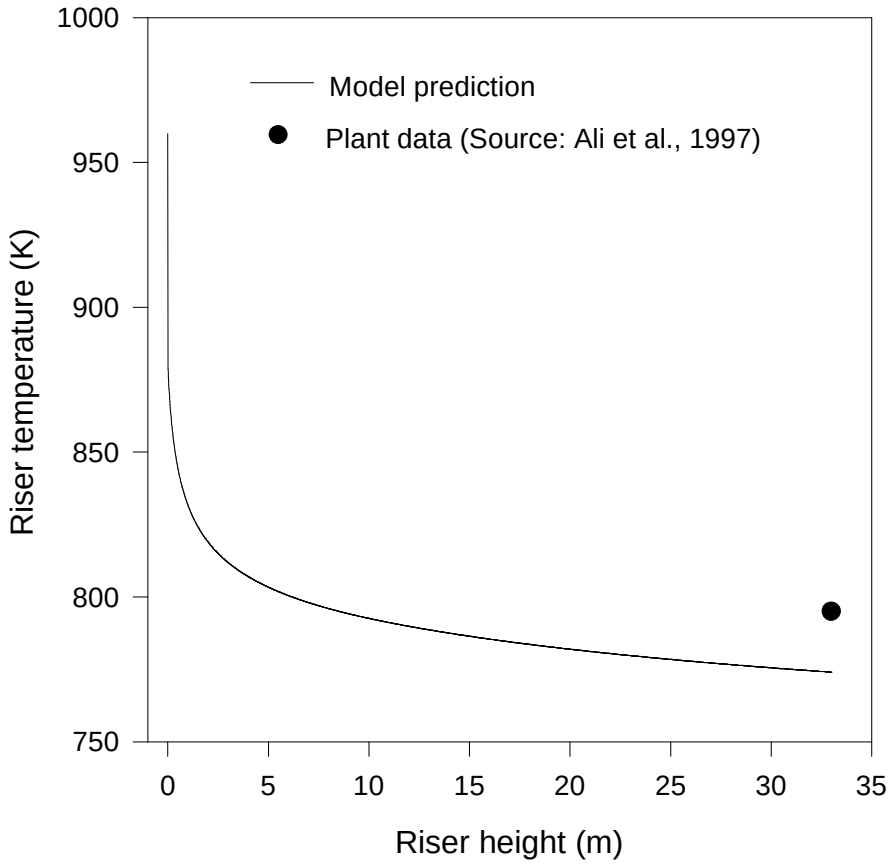

Fig. 4.2: Axial temperature profile along the riser height

Sensitivity analysis:

Sensitivity analysis of these tuning parameters is presented in Fig. 4.3 to Fig. 4.5. Sensitivity analysis is the process of varying the tuning parameters over a wide range about the mean value and recording the relative change in predicted gas, gasoline, and coke yields (Fig. 4.3, 4.4, and 4.5). The sensitivity of one tuning parameter relative to other is also demonstrated in these figures. Such analysis is useful in cases when the experimental data are few in number and statistical analysis can not be applied to predict confidence interval. A detailed discussion about the sensitivity analysis is given by Saltelli et al., (2000). Fig. 4.3 to 4.5 show that in the proposed model, gas yield, and coke yield, are strong functions of τ_2, τ_5 and τ_6, and gasoline yield is very sensitive to τ_5 and τ_6 and moderately sensitive to τ_2, and τ_3 whereas, $\tau 4$ is almost insensitive parameter. It is evident from these figures that τ_4 has virtually no effect on any product yield. This indicates that the frequency factor ($k_{0,i}$) is independent of molecular weight. Also, the value of tuning parameter τ_1 is zero. Therefore only four tuning parameters may be used to tune the model, with $\tau_1 = 0$, and $\tau_4 = 0$. Hence for all the subsequent simulations only four tuning parameters are used.

As is evident from Fig. 4.3 to 4.5, the product yields are very sensitive to the tuning parameters' values. Therefore, only small step intervals were used to change these tuning parameters while iterating for convergence of the program. Also, the tolerance of the line-search was kept of the order of 0.01% of the tuning parameter's value to avoid the program becoming unstable.

Case study 1 with four tuning parameters:

The results for case study 1 using the four tuning parameters are presented in Fig. 4.6 to Fig. 4.9. The values of the four tuning parameters are τ_2=17.0, τ_3=0.009, τ_5=1540, and τ_6=0.43. The product yields profiles given in Fig 4.1 and Fig. 4.6 matches very closely. Also, the temperature profiles obtained in Fig. 4.2 and 4.7 are similar.

The activity of the catalyst also decreases rapidly as byproduct (coke) of the cracking reactions gets deposited on the catalyst surface (Fig.4.8). Figure 4.9 shows an initial decline in the gas velocity which can be attributed to the combined effect of the initial sharp rate of decrease in the mass of the hydrocarbons (hydrocarbons converting to coke) and the sharp rate of increase in the available area for gas flow .

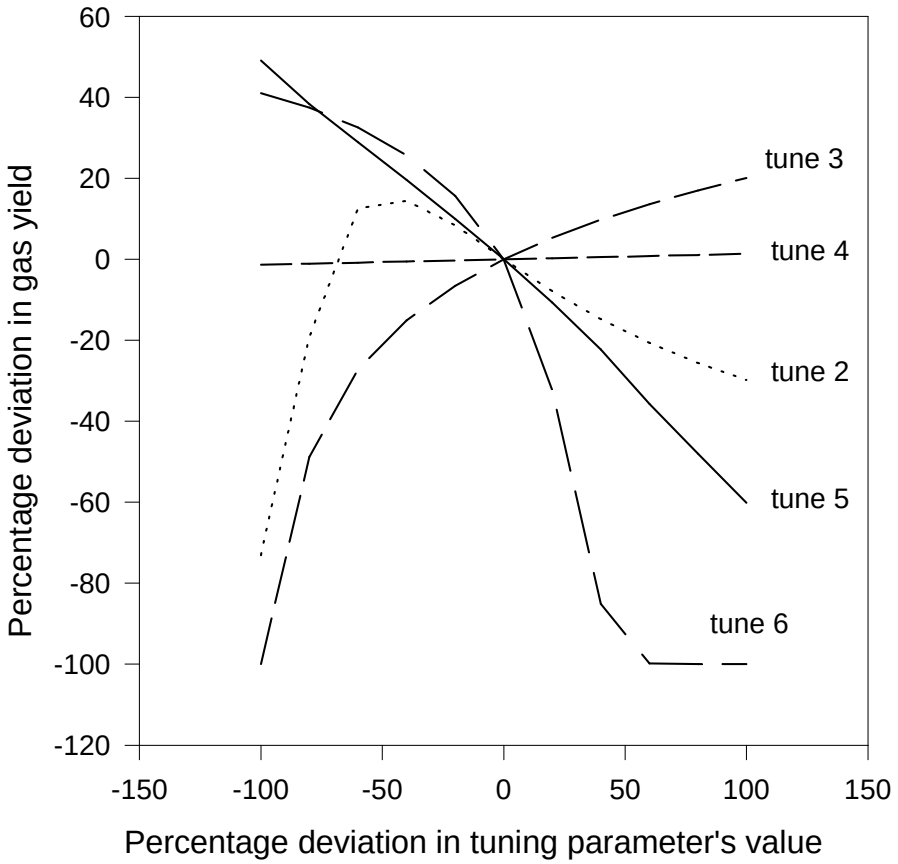

Fig. 4.3: Sensitivity analysis for gas yields

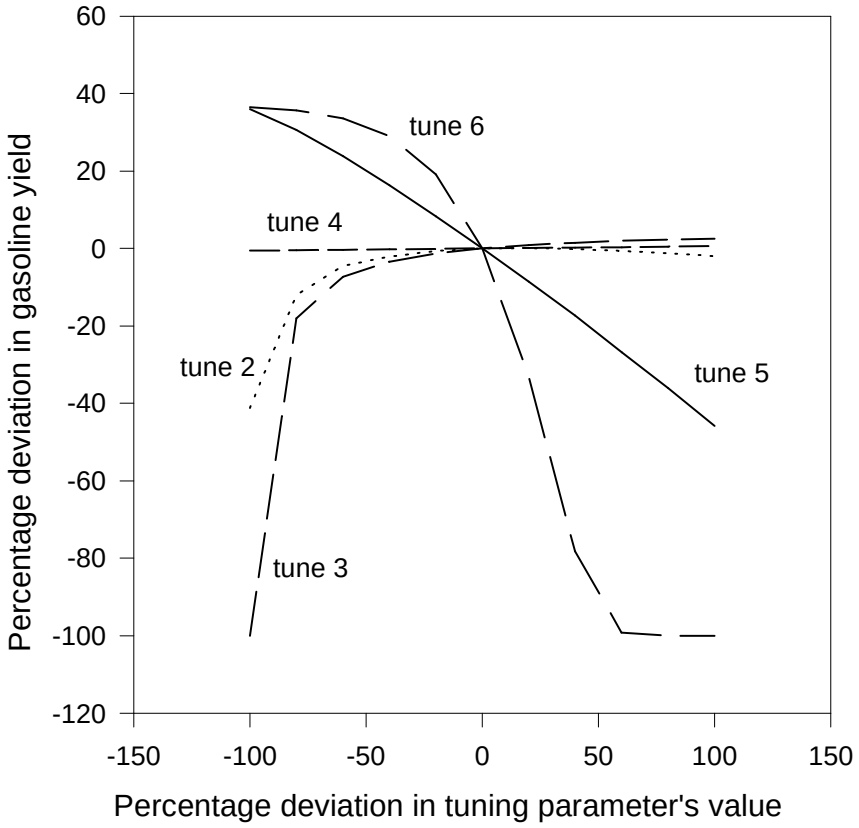

Fig. 4.4: Sensitivity analysis for gasoline yields

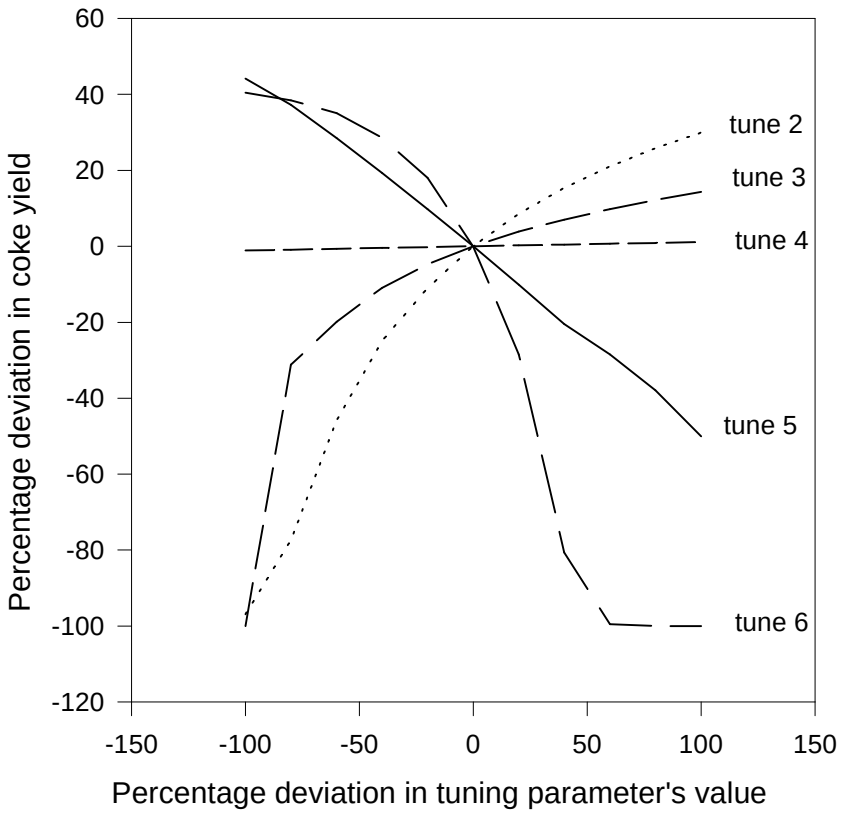

Fig. 4.5: Sensitivity analysis for coke yields

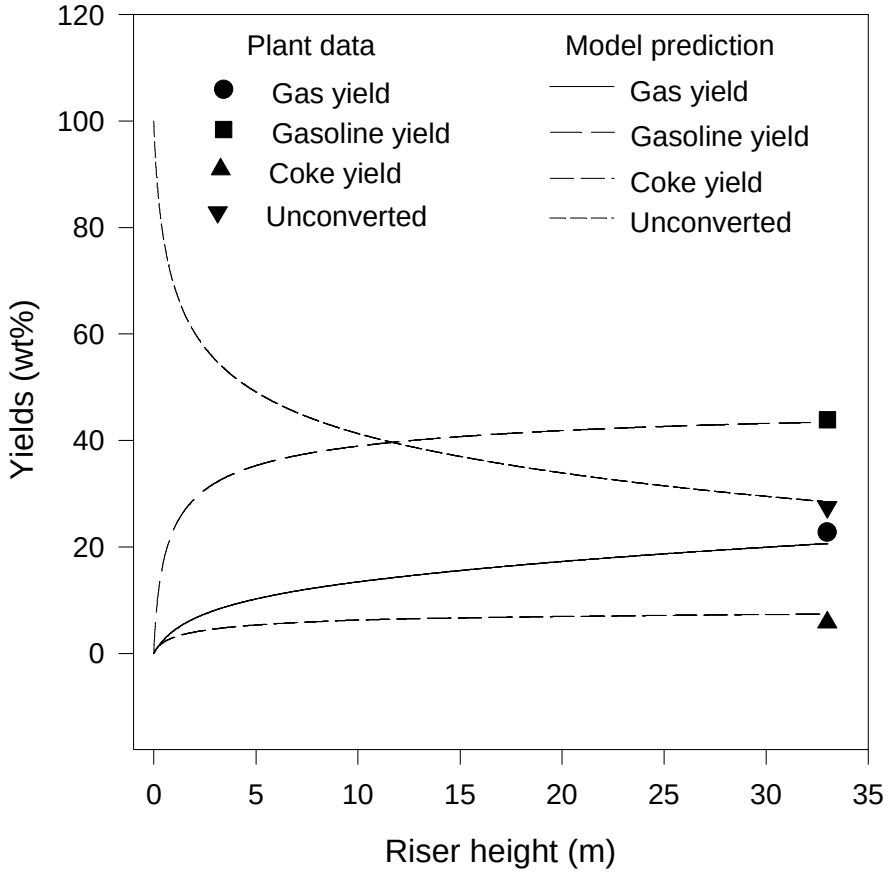

Fig. 4.6: Case study 1, comparison with the data reported by Ali et al. (1997) with four tuning parameters

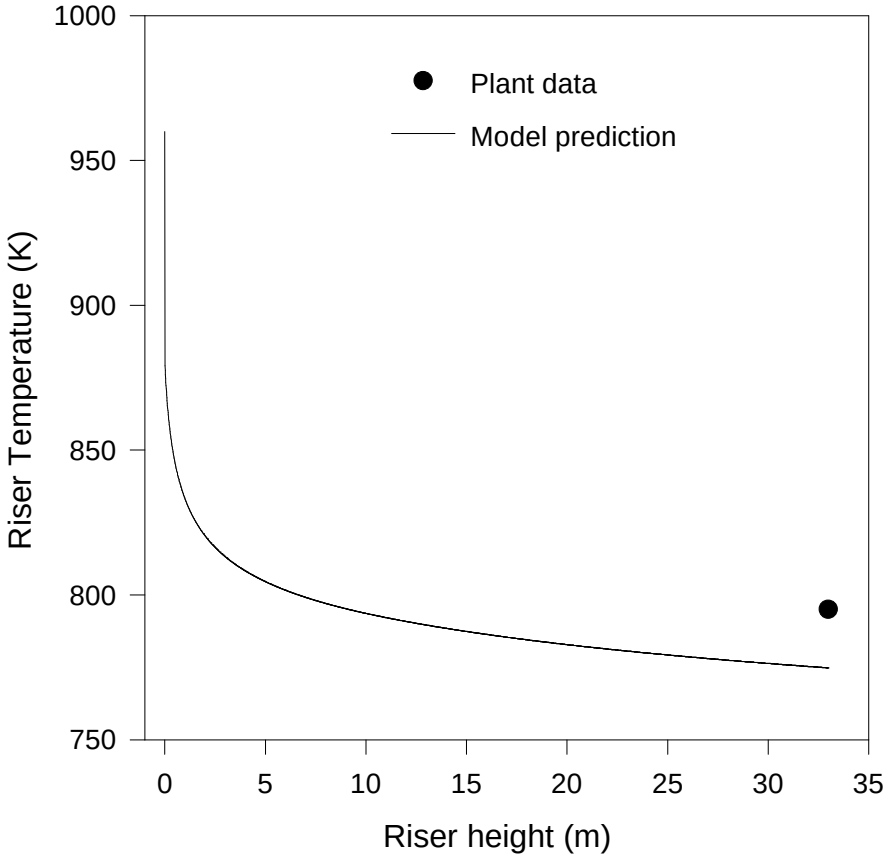

Fig. 4.7: Axial temperature profile along the riser height with four tuning parameters

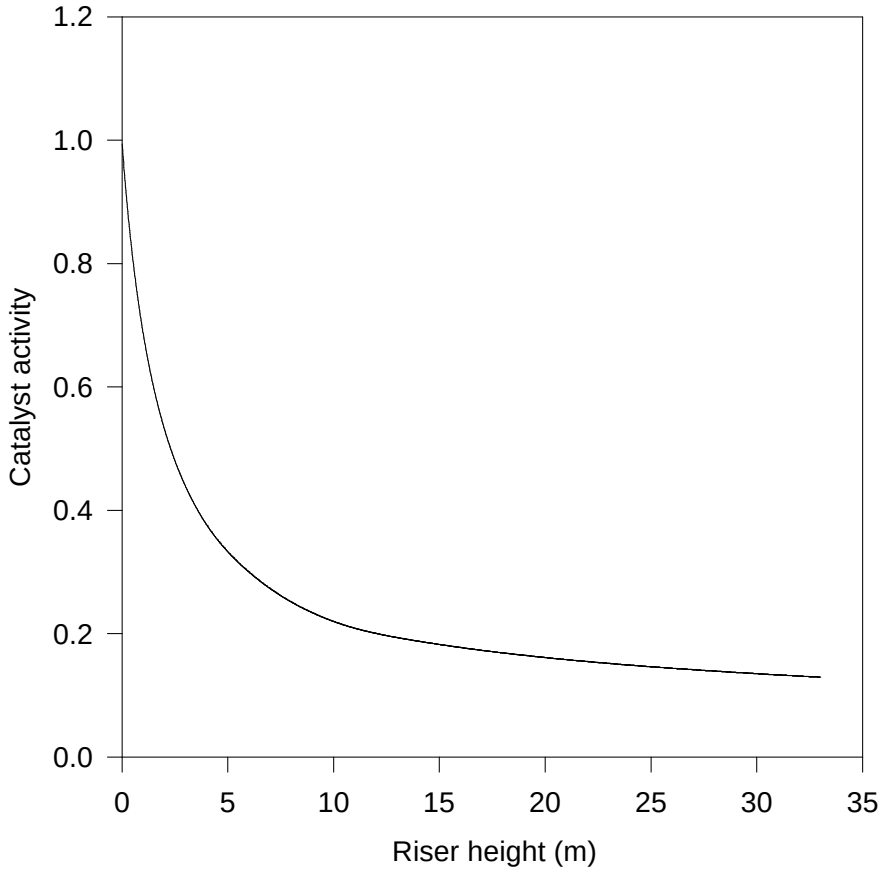

Fig. 4.8: Predicted catalyst activity along the riser height

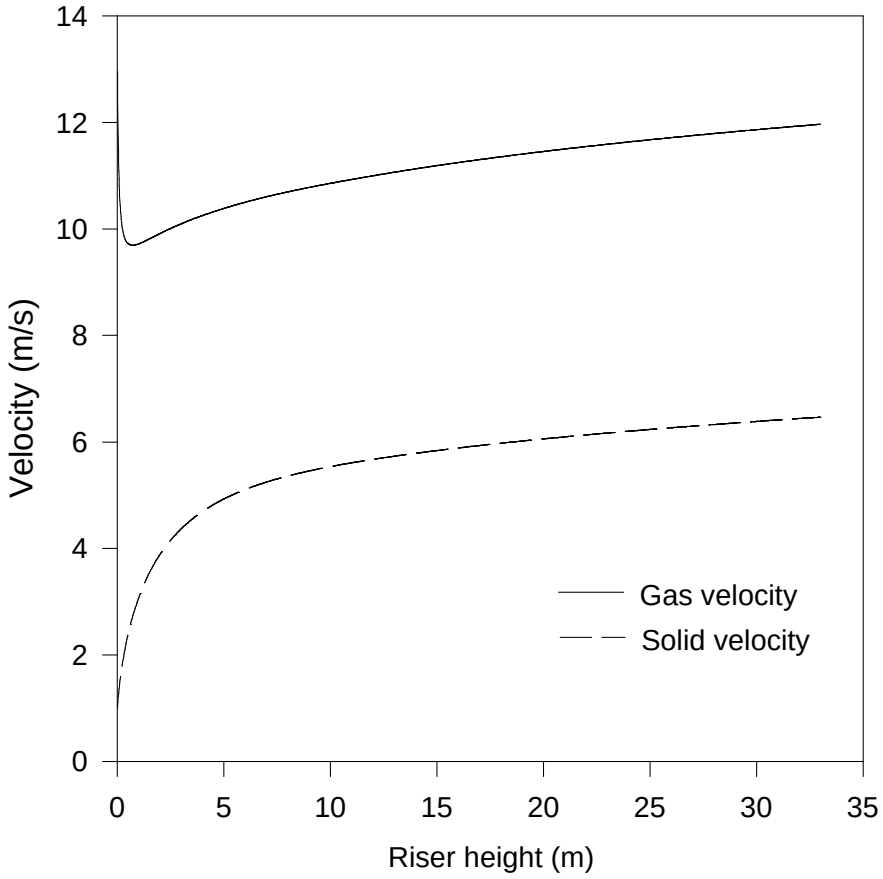

Fig. 4.9: Predicted catalyst and gas velocity profiles along the riser height

Also, high values of slip factor (ratio of gas velocity to cluster velocity) are predicted in riser entry zone which gradually decreases along with riser height and finally reaches 1.8 (Fig. 4.9). Catalyst volume fraction falls from about 0.5 to 0.1 in first few meters of riser height (Fig. 4.10). This sharp decline can be attributed to the fact that the most of the cracking takes place within first few meters of the riser height which causes a considerable increase in the volume of the gas thereby sharply increasing the gas holdup fraction in this region. Furthermore, it is clear from Fig. 4.10 that the effect of initial catalyst volume fraction ($\delta_{c,1}$) has negligible effect on the catalyst volume fraction along the riser height, as the lines for a dense bed at the riser bottom ($\delta_{c,1} = 0.5$) and for a relatively lean bed ($\delta_{c,1} = 0.3$) coincide.

Since plant data for the product yields were available at the riser outlet only, few more comparisons were made in subsequent case studies. Even without changing the values of tuning parameters the results of the simulation were encouraging. However, for better comparison, the tuning parameters were adjusted further in both the following case studies.

4.1.2 Case study 2

In this case FCC plant data (Table 4.2) reported by Derouin et al. (1997) was used to compare the simulator predictions. The authors have reported the product data for gasoline yield and conversion at different positions along the riser height (Fig. 4.11). The results of simulation with τ_2 =17.0, τ_3 = 0.035, τ_5 = 1540, and τ_6 = 0.43, are presented in Fig. 4.11. Model prediction for the gasoline along the riser height matches satisfactorily with the plant data.

4.1.3 Case study 3

The objective of this case study is to compare the results from the present work with other model based on rigorous transport equations. Riser operating conditions given in Table 4.2 (Theologos and Markatos, 1993) were used for the simulation. A comparison of the gasoline yield from the model presented in this work, with the gasoline yield from 3-D, two-phase-flow, heat transfer and reaction model of Theologos and Markatos (1993) is made. Only two tuning parameters τ_3 and τ_5 were changed appreciably.

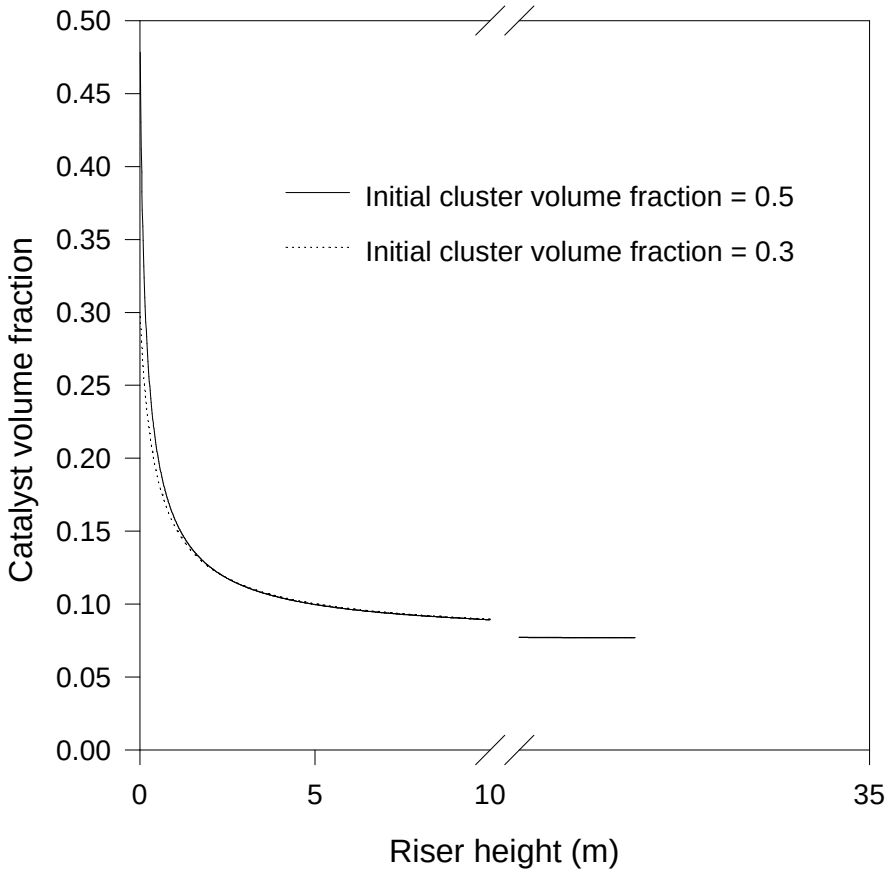

Fig. 4.10: Predicted catalyst volume fraction along the riser height

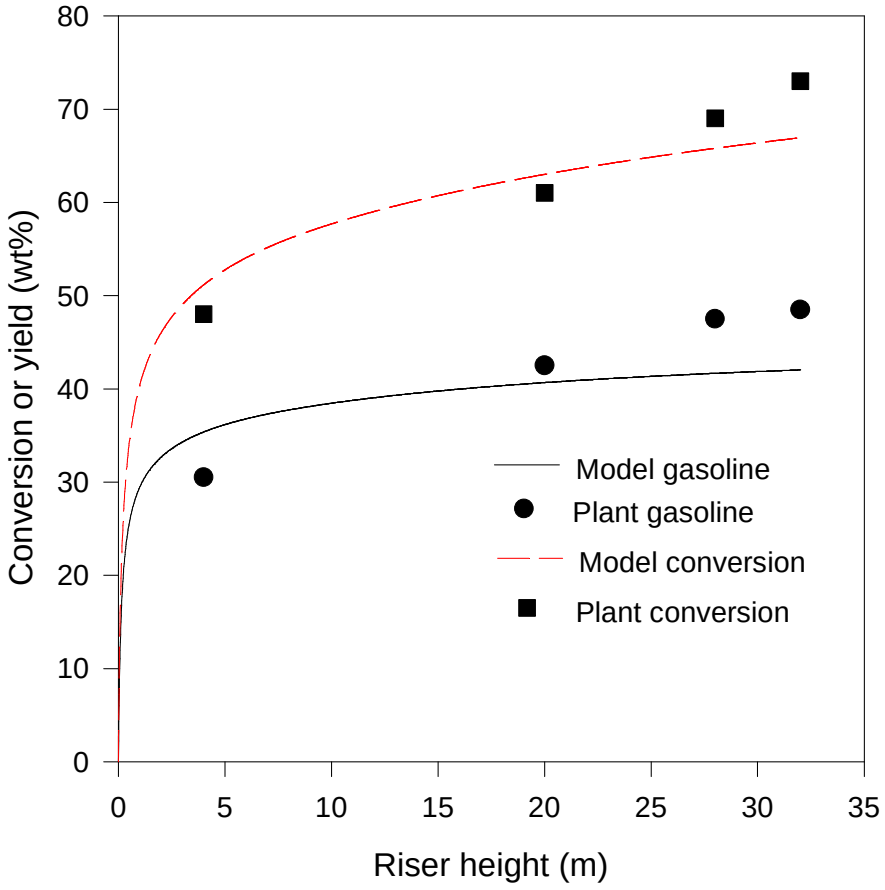

Fig. 4.11: Case study 2, comparison with the plant data reported by Derouin et al. (1997)

The final values of the tuning parameters were τ_2 =13.0, τ_3 =0.0008, τ_5 =1540, and τ_6 =0.4. Comparison of results predicted by present approach and those reported by Theologos and Markatos (1993) is given in Fig. 4.12.

4.1.4 Effect of C/O ratio

Effects of changing catalyst to oil ratio (C/O ratio) on gasoline and coke yields and riser temperature as predicted by the simulator are discussed. Riser dimensions and operating parameters were taken as those of case study-1 (Ali et al., 1997) for this simulation.

The gasoline yield increases with the increasing C/O ratio however, the rate of increase in the gasoline yield decreases at higher values of C/O ratio (Fig. 4.13). This can be attributed to the fact that at substantially high catalyst concentration cracking of pseudo components in the gasoline range (known as secondary cracking reactions) also increases which causes a decrease in the rate of increase of gasoline yield with C/O ratio. On the other hand, the increasing C/O ratio leads to increase in catalyst concentration, and hence increase in rate of both primary and secondary cracking. This increases overall number of moles cracked on the catalyst surface and hence increases amount of coke deposited on the catalyst. The riser temperature increases with the increasing C/O ratio as more heat is brought in by the hot regenerated catalyst (Fig.4.14).

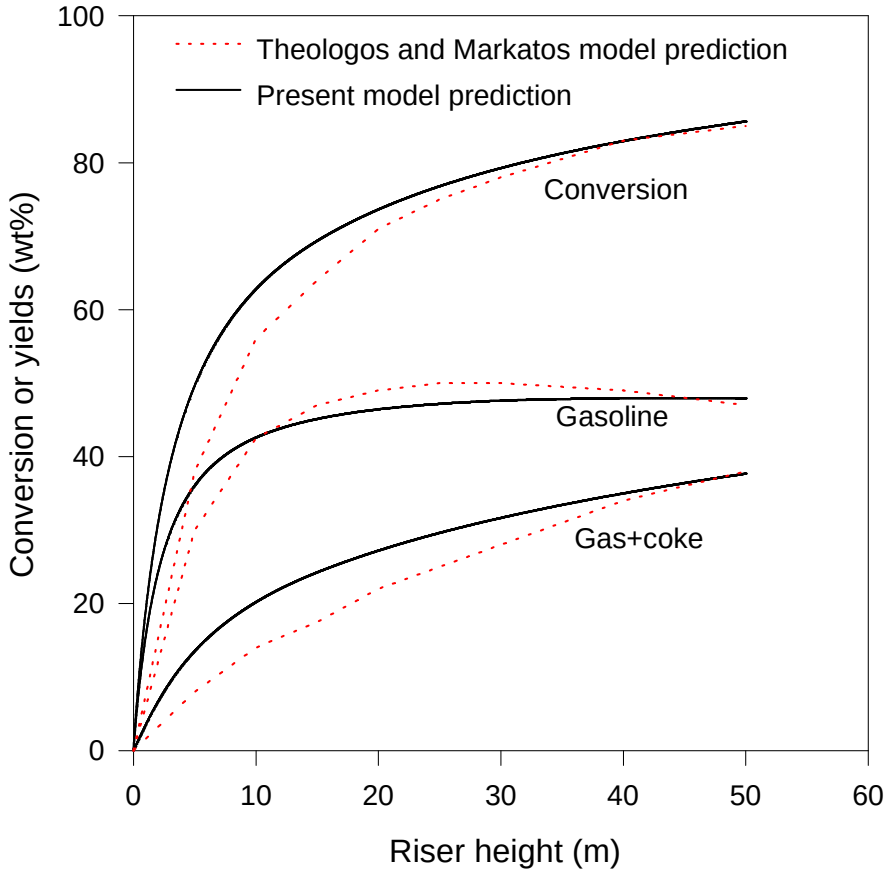

Fig. 4.12: Case study 3, comparison with the simulator data reported by Theologos and Markatos (1993)

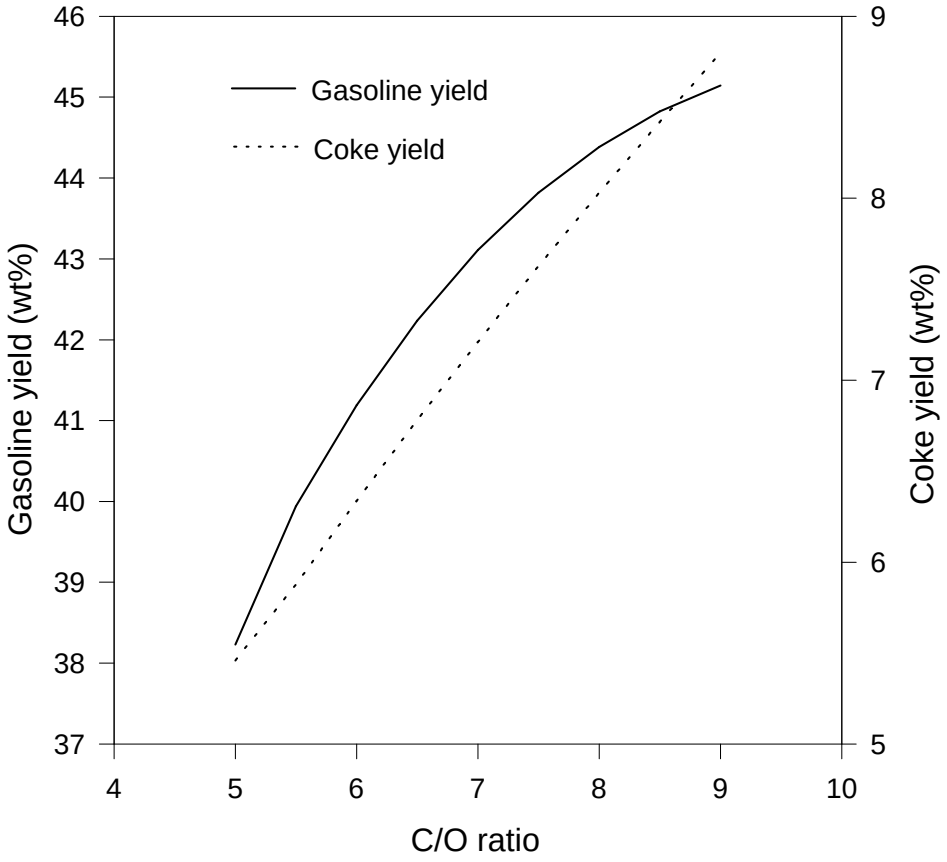

Fig. 4.13: Effect of C/O ratio on the gasoline and coke yields

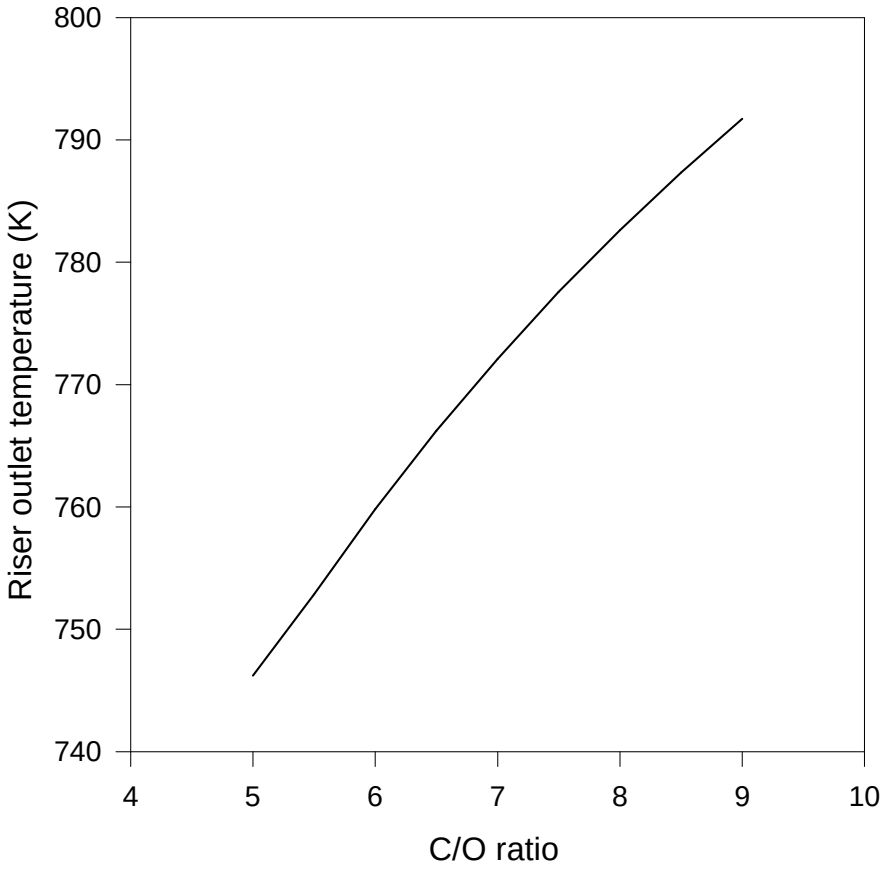

Fig. 4.14: Effect of C/O ratio on the riser outlet temperature

4.2 Regenerator Simulation

Regenerator is simulated using the plant data given in Table 4.3 reported by Ali et al. (1997). The values of other parameters used in the simulation are listed in Table 4.4. Details of the simulation technique are already discussed in Section 3.3. The results of the simulation are shown in Table 4.5.

Table 4.3: Industrial data for the regenerator reported by Ali et al. (1997)

Regenerator diameter (m)	5.8
Regenerator height (m)	11
Catalyst flow rate (kg/s)	144
Air flow rate (kg/s)	16
Catalyst hold up (kg)	70000
Pressure (atm)	2.9
Catalyst (spent) inlet temp. (K)	795
Coke on spent catalyst (kg coke/kg catalyst)	0.0081
Air inlet temperature (K)	378

Table 4.4: Parameters used for the simulation of regenerator

MWcoke, Molecular weight of coke (kg/kmol)	12.0 (Arbel et al., 1995)
β_{c0}, Preexponent constant in β_c expression	9.53×10^{-4} (Arbel et al., 1995)
k_{c0}, Preexponent constant in k_c, [1/(atm s]]	1.069×10^{8} (Arbel et al., 1995)
K_{3c0}, Preexponent constant in k_{3c} [kmol CO/(kg catalyst atm^2 s)]	116.68 (Arbel et al., 1995)
K_{3h0}, Preexponent constant in k_{3h} [kmol CO/(m^3 atm^2 s)]	5.064×10^{14} (Arbel et al., 1995)
E_β, Activation energy for CO_2/CO ratio at the surface [E/R, ^{0}K]	5585.0 (Arbel et al., 1995)
E_c, Activation energy for coke combustion [E/R, ^{0}K]	18889 (Arbel et al., 1995)
E_{3c}, Activation energy for catalytic CO combustion [E/R, K]	13889 (Arbel et al., 1995)
E_{3h}, Activation energy for homogeneous CO combustion [E/R, ^{0}K]	35556 (Arbel et al., 1995)
x_{pt}, relative catalytic CO combustion rate	0.5 (Gupta and Subba Rao, 2003)

Table 4.5: Comparison of the regenerator model predictions with the plant data reported by Ali et al. (1997)

	Model prediction	Plant data
Regenerator temperature (K)	975.8	960
Coke on regenerated catalyst (kg coke/kg catalyst)	0.0037	-
CO (mol%)	5.24	-
CO_2 (mol%)	17.83	17.7

4.3 FCC Unit's Simulation

At a given steady state all the heat generated in the regenerator will be consumed in the riser reactor and the coke generated in the riser reactor will be consumed in the regenerator. For simulating the FCC unit a steady state base case with exact heat balance and coke balance between the riser reactor and regenerator was established. The coke on the regenerated catalyst (C_{rgc}) was assumed to be 0.001 kg/kg of catalyst (Gupta and Subba Rao, 2003). All simulations of the FCC unit were done using this value of the coke on regenerated catalyst so that the desired level of temperature in the regenerator can be obtained.

The steady state base case was established using the data reported by Ali et al. (1997). The value of the coke on regenerated catalyst (0.1% by wt.) was achieved by adjusting the mass flow rate of the air at 20.2 kg/s. For the first iteration of FCC unit's simulation the coke on regenerated catalyst is assumed as 0.1% by weight and regenerator temperature is assumed at 1020 K. The output from the riser program, the coke yield at the riser outlet (calculated as kg coke/kg catalyst) along with the stripper temperature, was given as input to the regenerator program which in turn gave the new value of the regenerator temperature for the 0.1% by weight of coke on the regenerated catalyst (this value of coke on regenerated catalyst was achieved by adjusting the air flow rate to the regenerator). The new value of the regenerator temperature was used as input to the riser program for the next iteration. A difference of 1 K in the previous and new value of the regenerator temperature was used as the convergence criterion for the simulation.

The steady state simulation results are presented in graphical form. The products' yields and conversion at steady state is shown in Fig. 4.15 along with the plant data. The steady state riser temperature profile is shown in Fig. 4.16. Riser outlet temperature is 808 K as against plant data of 795 K. The gasoline, gas, and coke yields continue to increase with the increase in C/O ratio (Fig.4.17 and 4.18). The increase in coke yield with increasing C/O ratio increases the delta coke (coke on spent catalyst-coke on regenerated catalyst), which for a fixed value of coke on regenerated catalyst (0.1% by wt) increases the regenerator temperature (Fig. 4.19). The increased regenerator temperature increases the temperature at the riser inlet which in turn increases the products' yields by promoting the cracking reactions' rates.

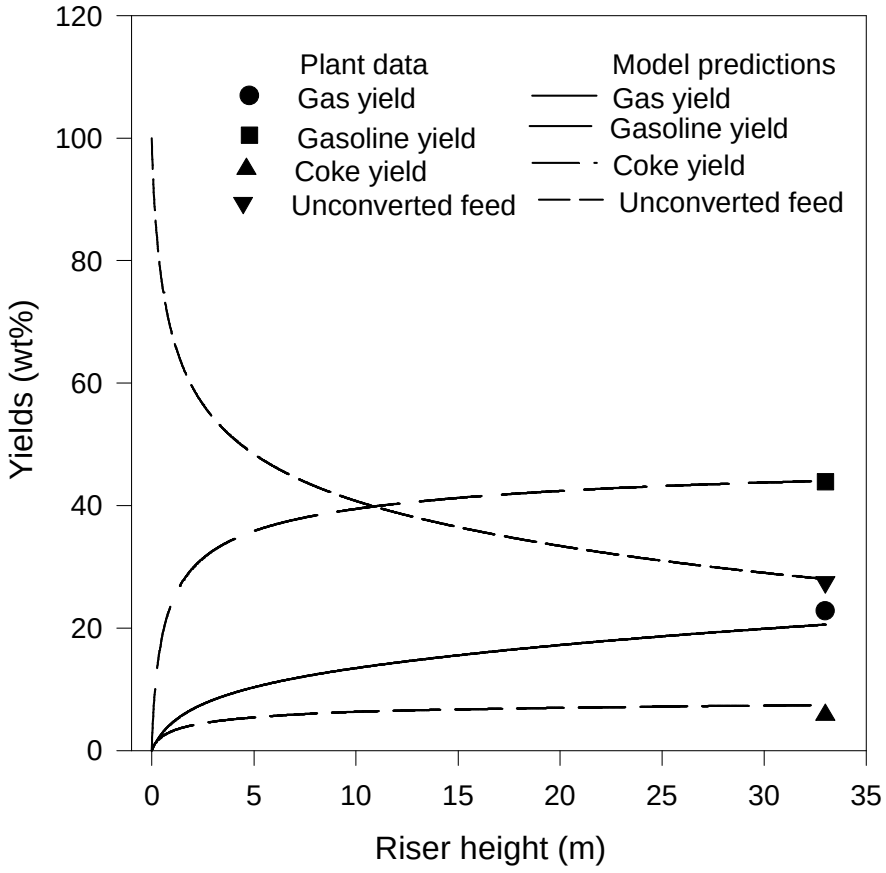

Fig. 4.15: Steady state yield profiles in the riser reactor, comparison with plant data reported by Ali et al. (1997)

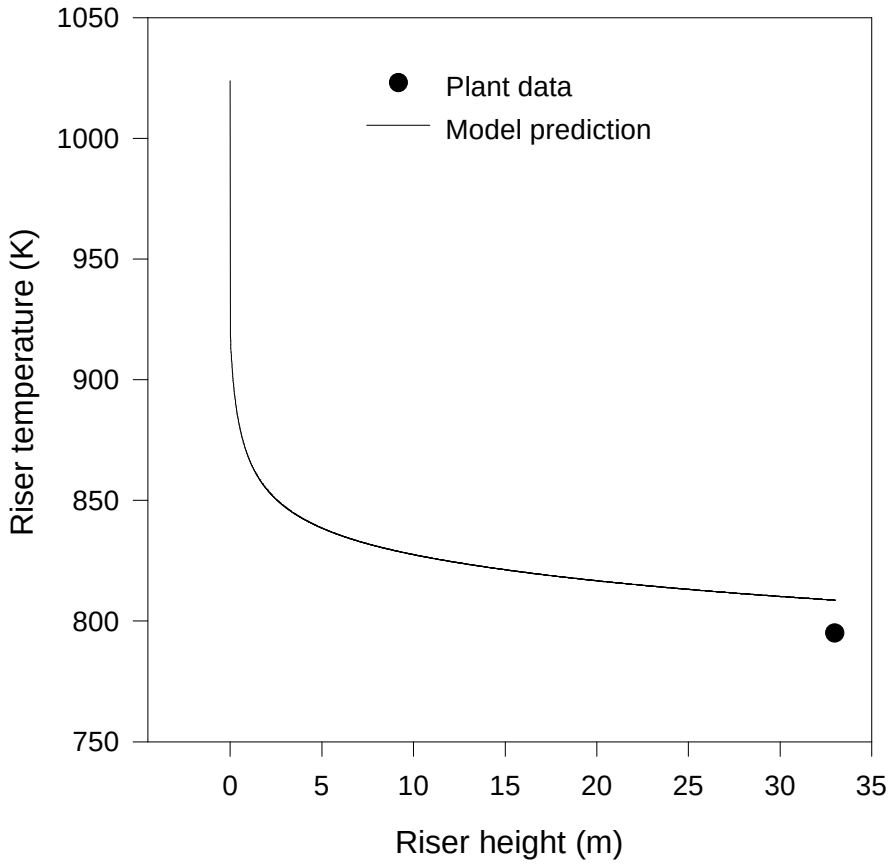

Fig. 4.16: Steady state temperature profile along the riser height, comparison with plant data reported by Ali et al. (1997)

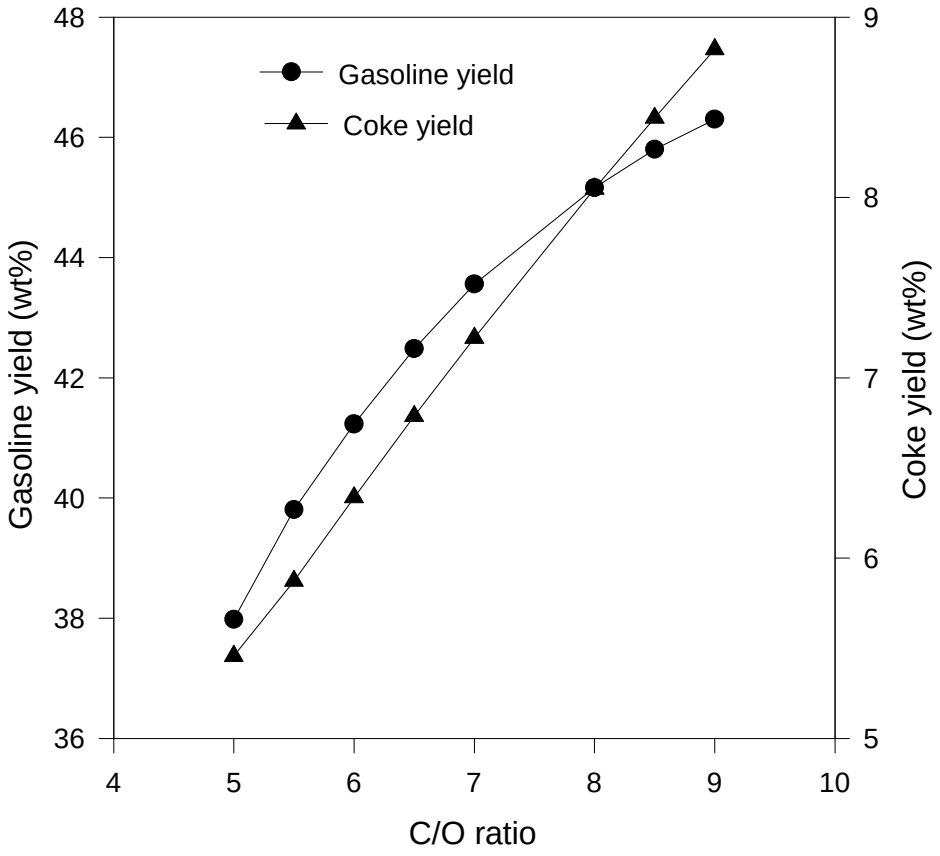

Fig. 4.17: Effect of changing C/O ratio on gasoline and coke yields

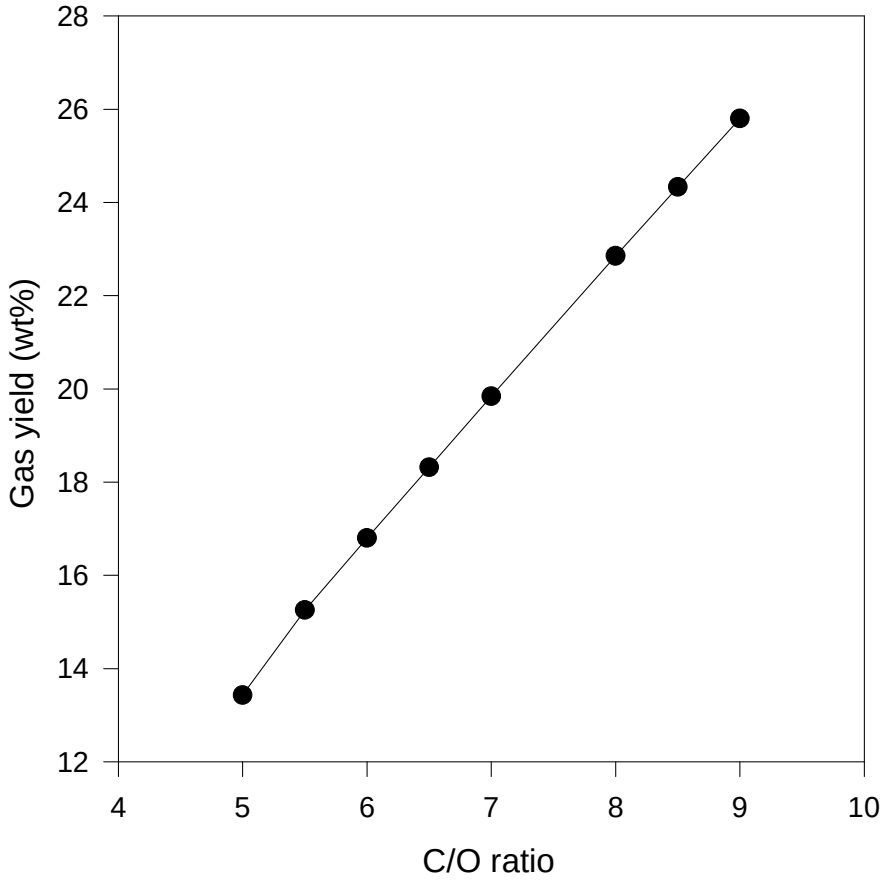

Fig. 4.18: Effect of changing C/O ratio on gas yield

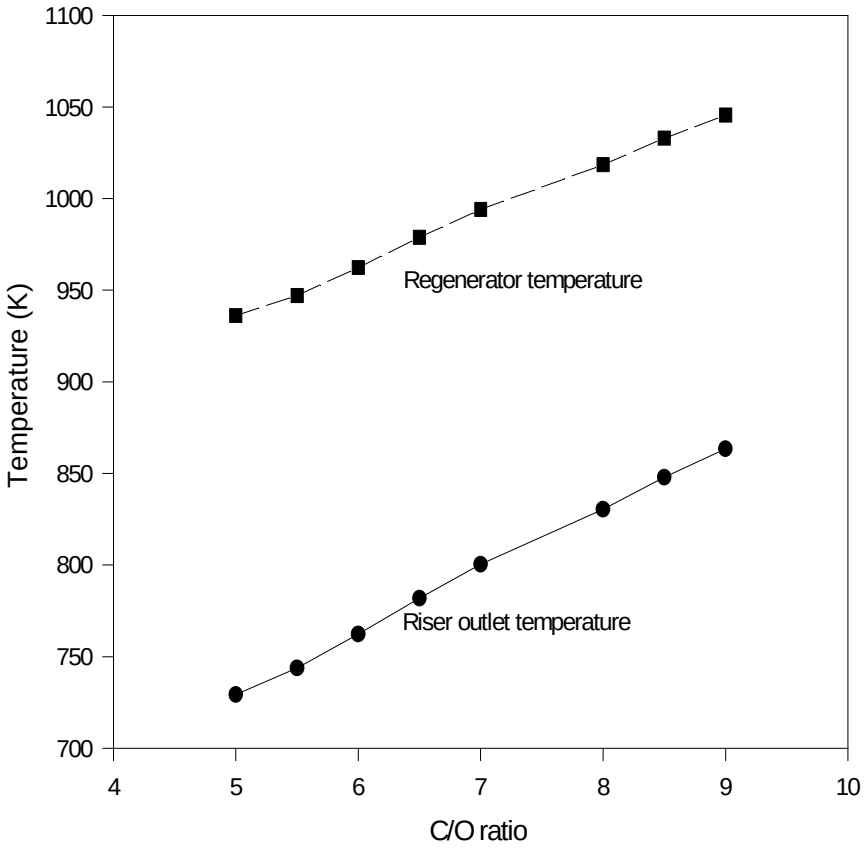

Fig. 4.19: Effect of changing C/O ratio on riser and regenerator temperatures

Despite the fact that the higher riser temperature promotes secondary cracking reactions, the net gasoline yield from the riser continue to increase with the increasing C/O ratio (Fig. 4.17). The coke on spent catalyst keeps on decreasing with the increasing C/O ratio as the mass flow rate of the catalyst keeps on increasing with the increasing C/O ratio (Fig. 4.20). The gas yield is increasing with the increasing C/O ratio due to the overcracking (Fig. 4.18).

After setting the base case for the FCC simulation, the plant data reported by Ali and Rohani (1997) for the simulation of FCC unit was compared with the model results for all the four cases reported by them. Table 4.6 shows the plant data's comparison with the simulator's predictions. The simulation results obtained for these cases are quite satisfactory.

Effect of air flow rate on the FCC unit performance was also investigated (Fig. 4.21 & 4.22). These figures show that at low air flow rates the coke on regenerated catalyst will be more as less air is available for combustion of coke in the regenerator. This will give lower temperature of the regenerator and the temperature at the riser outlet will also be less. With increasing air flow rate, the regenerator temperature and riser outlet temperature will keep on increasing till a maximum in these values is attained when there will be just sufficient air to burn all the coke produced in the riser and to convert all CO to CO_2 in the regenerator. After this maximum of regenerator temperature and riser outlet temperature, any further increase in the air flow rate will decrease the regenerator temperature by taking out heat with the exhaust gases without actually producing any heat through combustion. Decrease in the regenerator temperature will also cause a decline in the riser outlet temperature. The simulation predictions are in agreement with that of Han et al. (2000) for the steady state response to changes in air flow rate.

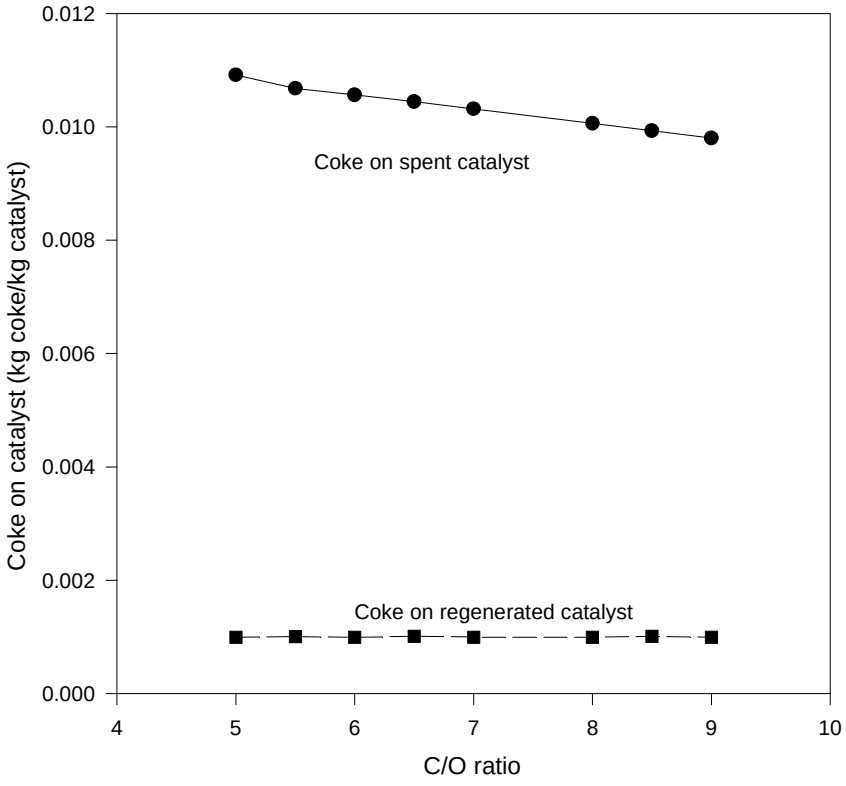

Fig. 4.20: Effect of changing C/O ratio on the coke on spent catalyst

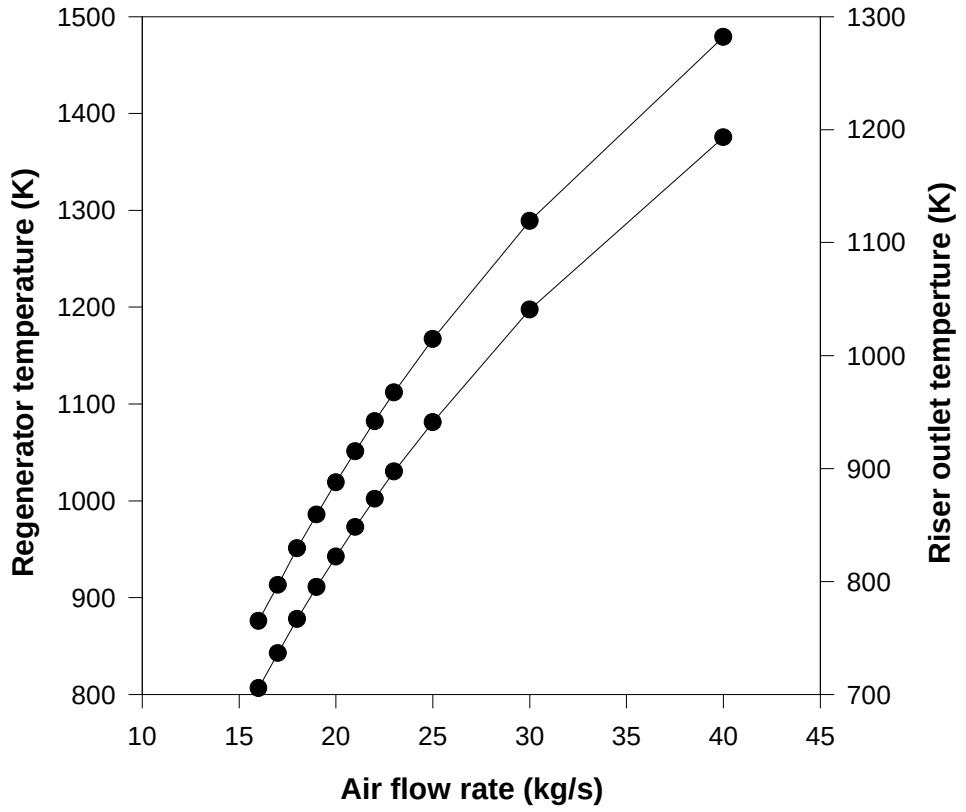

Fig. 4.21: Effect of changing air flow rate on riser and regenerator temperatures

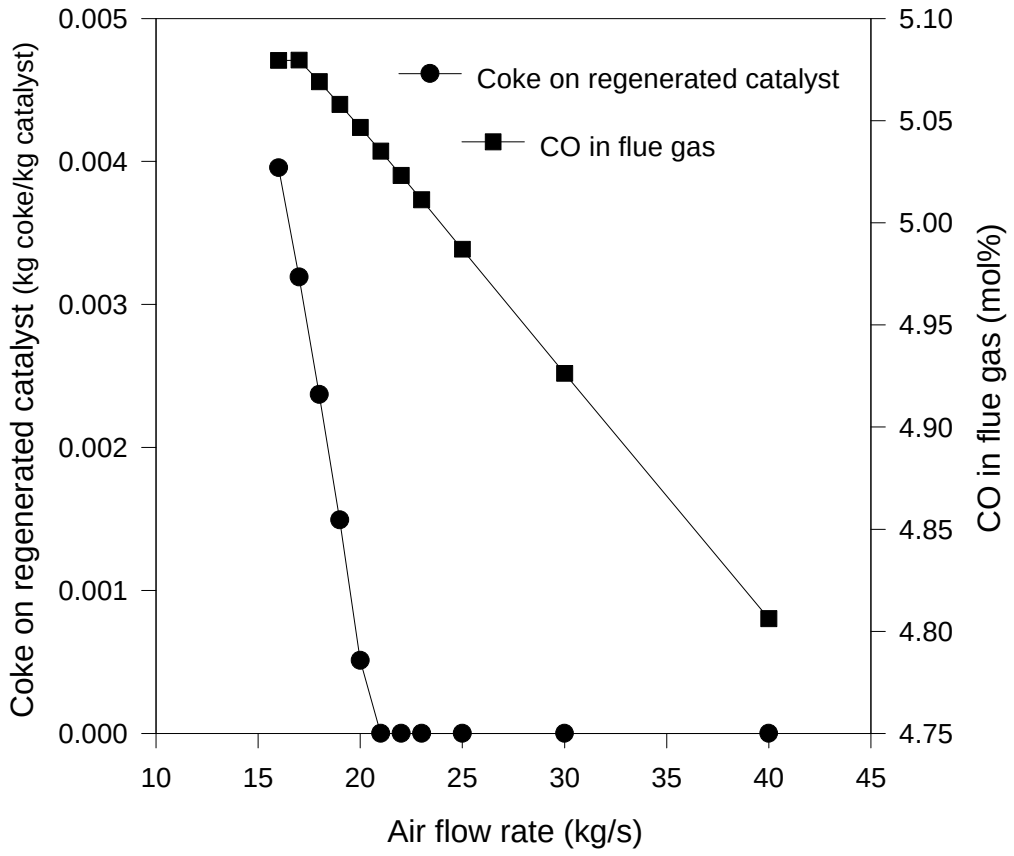

Fig. 4.22: Effect of changing air flow rate on coke on regenerated catalyst and on CO concentration in flue gas

Table 4.6: Steady state simulation results comparison with plant data reported by Ali and Rohani (1997)

	Case 1		Case 2		Case 3		Case 4	
Feed rate (kg/s)	25.70		26.93		23.61		19.95	
Feed quality (API)	21.76		22.98		22.73		22.28	
Cat/Oil ratio	6.33		5.43		6.07		7.24	
Riser reactor:								
	model result	Plant data	model result	Plant data	model result	Plant data	model result	Plant data
Gasoline yield (wt%)	41.32 (12%)	46.90	38.4(10.47)	42.79	40.76(2.44)	41.78	44.05(0.39)	43.88
Coke yield (wt%)	6.42	5.34	5.60	5.43	6.26	5.69	7.41	5.83
Outlet temperature (K)	792	808	770	805	789	806	819	795
Regenerator:								
Temperature (K)	1008	1033	991	1004	1008	1006	1034	960

Chapter - 5

CONCLUSIONS AND RECOMMENDATIONS

In the present research work a new technique for modeling the FCC riser has been developed. The model incorporated a more realistic kinetic scheme for the cracking reactions and a new correlation to evaluate Arrhenius type reaction rate constants.

5.1 Conclusions

- The proposed model is unique as it considers cracking reaction in true sense. Earlier models were based on conversion reaction and not on cracking reaction mechanism. Also, the proposed model is 'generic model' and need not to be tuned by finding rate constants by regression analysis.

- Many researchers who have used the kinetic constants reported in literature have also advocated the use of tuning parameters for closely matching the model results with the plant data. In the proposed modeling approach, however, the introduced tuning parameters have not only done away the need of using the kinetic constants from the literature (which themselves are not valid for different feedstocks, catalysts, and FCC operating conditions) but also have given freedom for matching the model results with the plant data.

- Originally six tuning parameters were introduced in the model. However, two of them approached to zero indicating that the frequency factor is independent of the molecular weight of cracking component and that the cracking of a component is independent of molecular weights of the product components.

- The four tunable parameters obtained for calculating rate constants seems to be stable. The stability of these parameters is also proved by the product yield pattern, yield profiles along the riser, and the simulation results of the entire FCC unit for variable air flow rates and C/O ratio.

- Significant variation in numerical values of a few tuning parameters (particularly τ_2 and τ_3) for different case studies may be due to different characteristics of the feedstock and operating conditions.

- The proposed model is capable of predicting overall conversion, products yields, riser temperature, catalyst activity, catalyst velocity, and gas velocity along the riser height. The model predictions are in good agreement with the industrial data reported in the literature and the data predicted by other researchers.

5.2 Recommendations

- The proposed kinetic scheme can be used for more advanced studies of the FCC riser modeling as this scheme facilitates the use of more detailed kinetic scheme (any no. of pseudocomponents) for the study of heat and mass transfer effects, adsorption effects, and detailed hydrodynamics.

- The proposed scheme can be perfected in future work after performing more and more experiment (may be in different laboratories) to establish a relation between the proposed tunable parameters and characterization factor, catalyst activity, etc. A study to correlate feedstock characteristics and other product properties and selectivity is also required.

- The present study incorporates a one dimensional riser hydrodynamics model. There is evidence in the literature that conversion can vary quite substantially along the riser radius due to the wall effect on the catalyst distribution along the riser radius. Therefore, the proposed new kinetic model can be used with a two dimensional hydrodynamic model to predict the effect of radial catalyst distribution on the conversion and yields.

Appendix 1

Petroleum fractions are mixtures of innumerable components which are difficult to be identified individually. However, Watson characterization factor can be treated as an approximate indicator of the various groups of compounds (such as paraffin, olefin, naphthene, aromatic, etc) present in the petroleum fraction. Watson and Nelson (1933) made a remarkable observation that the factor K_W ($=T_b^{1/3}/sg$), known as Watson characterization factor, is closer to 12 for paraffins and olefins, approximately 10 for aromatics, and between 11 and 12 for naphthenes when the normal boiling point of the component T_b is in Rankin and sg is the specific gravity at 60°/60°F. The characterization factor of the mixture of hydrocarbons is given by K_W=MeABP$^{1/3}$/sg, where MeABP is the mean average boiling point of the mixture (API Data Book, Chapter 2, Characterization of Hydrocarbons, 1976). Using this, Miquel and Castells (1993) proposed a method along with a computer program (Miquel and Castells, 1994) that can represent an oil fraction by an equivalent mixture of small number of hypothetical components or pseudocomponents. To use this approach atmospheric true boiling point (TBP) distillation curve and the entire fraction density is required. This method assumes that if the difference in final boiling point (FBP) and initial boiling point (IBP) of a petroleum fraction is not too high (i.e., <300 K) then the Watson characterization factor of any narrow-boiling fraction of this mixture (boiling range between 15 to 25 K) remains equal to that of original fraction.

In the present case, due to unavailability of TBP curve for the FCC feed, simulated distillation (SD) curve reported by Pekediz et al. (1997) was used. The SD curve was first converted to ASTM-D86 curve and then to TBP curve by the correlation proposed by Daubert (1994). The two-step conversion of SD data to TBP data is given in Table A1-1. To generate pseudocomponents, the TBP curve of the feed was divided into twelve parts, out of which four were of 5 volume% each and eight of 10 volume% each (shown as vertical bars in Fig.A1-1). These vertical bars represent twelve pseudocomponents of the feed. The boiling point of each individual pseudocomponent was determined by area-averaging of the TBP curve (clearly visible in Fig.A1-1).

Considering constant Watson characterization factor, specific gravity of each pseudocomponent was determined by the equation

$$sg = 1.21644 \frac{T_b^{1/3}}{K_W} \qquad \text{(Where } T_b \text{ is in K)} \tag{A1-1}$$

Table A1-1: Distillation data of hydrocarbon feed (Pekediz et al., 1997)

Vol.% Distilled	SD (K)	ASTM-D86* (K)	TBP* (K)
IBP	532	585.5	558.9
10 wt %	587	615.5	604.3
30 wt %	621	632.8	636.4
50 wt %	650	652.3	665.3
70 wt %	683	680.5	700.6
90 wt %	730	721.4	743.9
FBP	800	756.6	808.1

Density of feed (at 15^0C) = 929.20 kg/m^3
*Estimated using correlation proposed by Daubert (1994)

Molecular weights of these pseudocomponents were then calculated by the following equation proposed by Edmister and Lee (1984) which requires knowledge of boiling point and the specific gravity of a hydrocarbon fraction.

$$MW = 204.38 \cdot e^{(0.00218 \cdot T_b)} \cdot e^{(-3.07 \cdot sg)} \cdot T_b^{\,0.118} \cdot sg^{1.88} \tag{A1-2}$$

Having known values of the volume fraction, boiling point, specific gravity, and molecular weight, each individual bars of Fig.A1-1 can be treated as a pure component (of course, hypothetical pure component or pseudocomponent). To make use of the equations (A1-1) and (A1-2), an iterative method has to be adopted as the value of Watson characterization factor is not known beforehand. Miquel and Castells (1993; 1994) have explained this iterative approach in detail.

After breaking the FCCU feed into twelve pseudocomponents, and determining the exact value of Watson characterization factor, properties of other 31

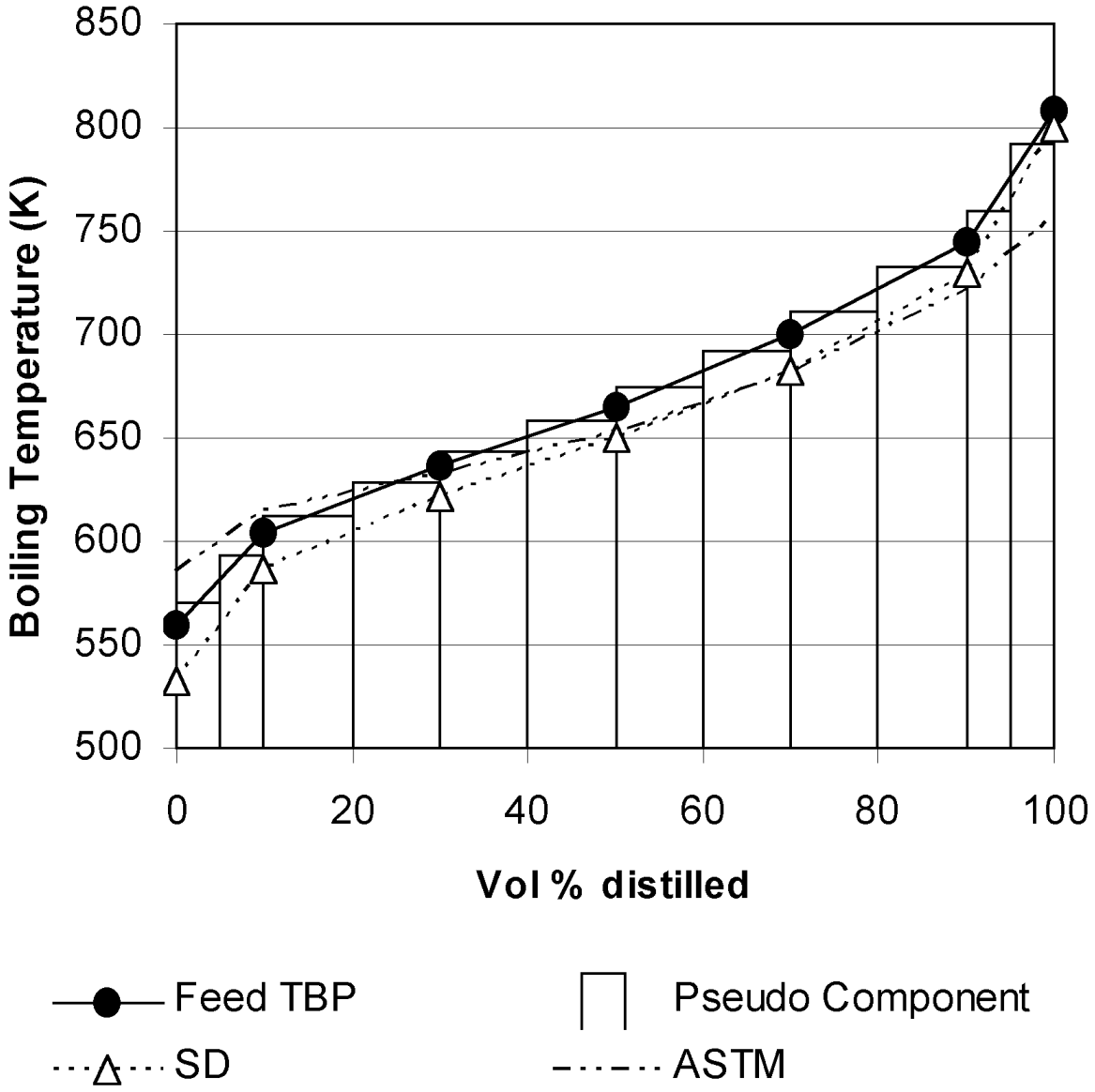

Fig. A1-1: Pseudocomponents generated from feed TBP

pseudocomponents were also determined by using equations (A1-1) and (A1-2). Boiling points of these 31 pseudocomponents were taken at equal interval between the boiling point of n-pentane and the boiling point of first pseudocomponent of FCCU feed (570 K in the present case). The lightest seven components were taken as pure paraffin which are the major constituent of gases. Initially, volume fraction of all these seven pure components and 31 pseudocomponents, which are not present in feed, were taken zero. Thus total fifty components (seven pure components and forty three pseudocomponents) were considered in the present approach for the simulation of FCC riser reactor.

After determining normal boiling point, specific gravity, and molecular weight of all pseudocomponents, heat capacities were determined using the correlations of Kesler and Lee (1976) and heat of combustion by equation (3.22 to 3.24) (Table A1-2).

Predicted concentrations of pseudocomponents in the product stream are given in Fig.A1-2. Also, various product streams, viz., Gas, Gasoline, LCO, and Residue are marked on the basis of boiling points.

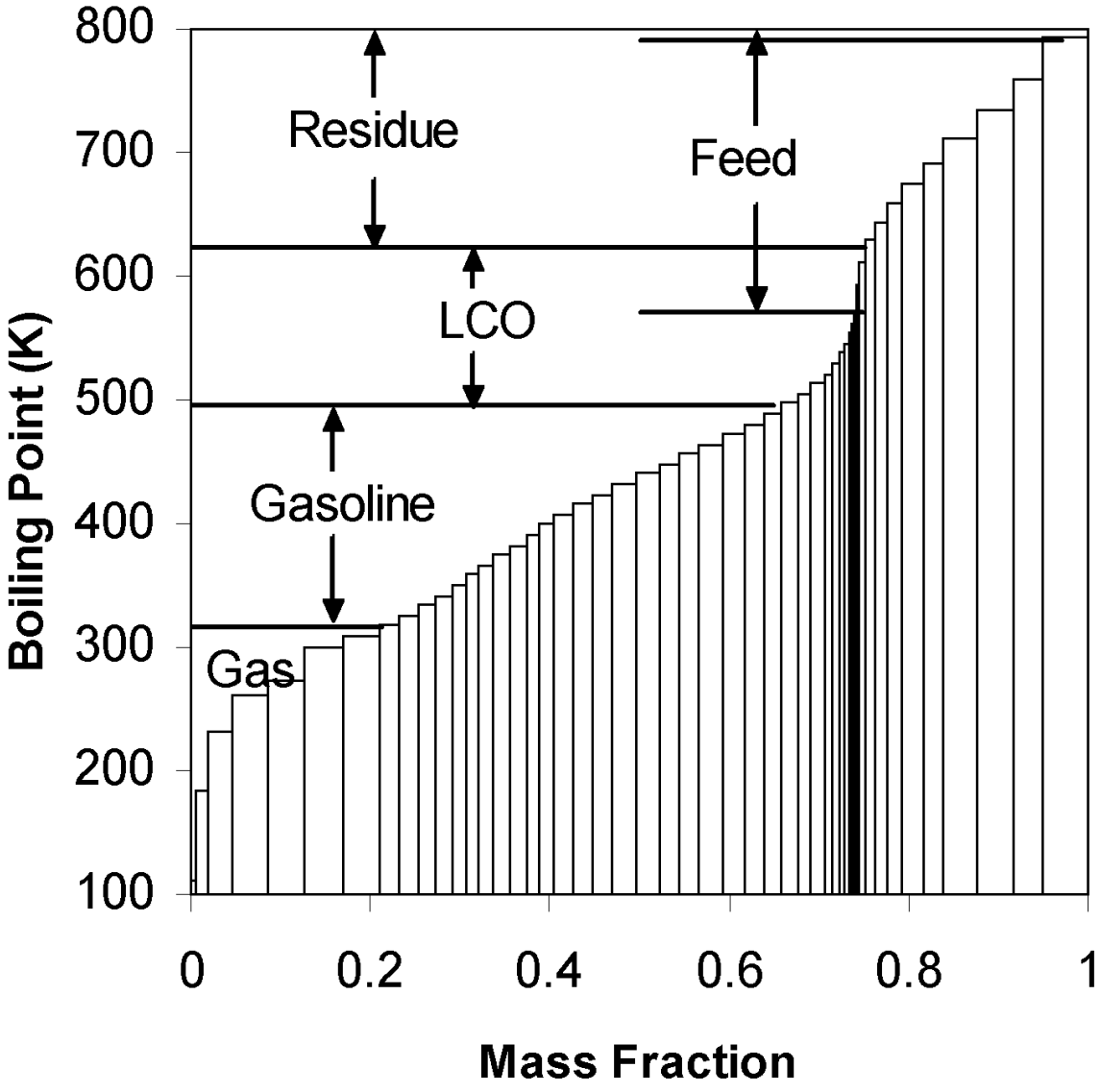

Fig. A1-2: Mass fractions of pseudocomponents in the product

Table A1-2: Properties of pseudocomponents

(PC_1 to PC_7 are pure components; PC_8 to PC_{29} constitute gasoline fraction; PC_{30} to PC_{41} constitute light cycle oil fraction; PC_{42} to PC_{50} constitute residual fraction whereas feed contains PC_{39} to PC_{50})

Component ID	Component name	Boiling point (^{0} K)	Molecular weight	ΔH_{comb} (kJ/kmol)*
PC_1	Methane	111.65	16.043	62764.79
PC_2	Ethane	184.50	30.070	58622.94
PC_3	Propane	231.09	44.097	51983.86
PC_4	i-Butane	261.43	58.124	50464.83
PC_5	n-Butane	272.65	58.124	49960.31
PC_6	i-Pentane	300.98	72.150	49073.02
PC_7	n-Pentane	309.21	72.150	48952.84
PC_8	Pseudocomponent	317.37	88.563	47318.37
PC_9	Pseudocomponent	325.54	91.443	47226.62
PC_{10}	Pseudocomponent	333.70	94.402	47137.89
PC_{11}	Pseudocomponent	341.86	97.443	47052.01
PC_{12}	Pseudocomponent	350.03	100.569	46968.81
PC_{13}	Pseudocomponent	358.19	103.781	46888.17
PC_{14}	Pseudocomponent	366.35	107.083	46809.94
PC_{15}	Pseudocomponent	374.52	110.478	46734.00
PC_{16}	Pseudocomponent	382.68	113.969	46660.24
PC_{17}	Pseudocomponent	390.84	117.558	46588.54
PC_{18}	Pseudocomponent	399.01	121.249	46517.73
PC_{19}	Pseudocomponent	407.17	125.045	46445.89
PC_{20}	Pseudocomponent	415.33	128.948	46373.59
PC_{21}	Pseudocomponent	423.50	132.964	46300.89
PC_{22}	Pseudocomponent	431.66	137.094	46227.80
PC_{23}	Pseudocomponent	439.83	141.343	46154.34
PC_{24}	Pseudocomponent	447.99	145.713	46080.57
PC_{25}	Pseudocomponent	456.15	150.210	46006.47
PC_{26}	Pseudocomponent	464.32	154.835	45932.07
PC_{27}	Pseudocomponent	472.48	159.595	45857.39
PC_{28}	Pseudocomponent	480.64	164.491	45782.42
PC_{29}	Pseudocomponent	488.81	169.530	45707.18
PC_{30}	Pseudocomponent	496.97	174.714	45631.67
PC_{31}	Pseudocomponent	505.13	180.049	45555.89
PC_{32}	Pseudocomponent	513.30	185.538	45479.85
PC_{33}	Pseudocomponent	521.46	191.187	45403.53
PC_{34}	Pseudocomponent	529.62	197.000	45326.93
PC_{35}	Pseudocomponent	537.79	202.982	45250.05
PC_{36}	Pseudocomponent	545.95	209.138	45172.88
PC_{37}	Pseudocomponent	554.11	215.474	45095.39
PC_{38}	Pseudocomponent	562.28	221.995	45017.59
PC_{39}	Pseudocomponent	570.44	228.706	44939.46
PC_{40}	Pseudocomponent	593.12	248.399	44720.49
PC_{41}	Pseudocomponent	612.48	266.496	44531.20
PC_{42}	Pseudocomponent	628.50	282.446	44353.16
PC_{43}	Pseudocomponent	643.76	298.497	44187.51
PC_{44}	Pseudocomponent	658.25	314.565	44034.96
PC_{45}	Pseudocomponent	674.30	333.352	43871.15
PC_{46}	Pseudocomponent	691.91	355.231	43697.31
PC_{47}	Pseudocomponent	711.55	381.318	43510.14
PC_{48}	Pseudocomponent	733.25	412.311	43311.36
PC_{49}	Pseudocomponent	760.13	454.185	43075.64
PC_{50}	Pseudocomponent	792.20	509.673	42808.56

* Heat of combustion values are calculated by using equations (3.22), (3.23), and (3.24)

REFERENCES

Ali, H., and Rohani, S. (1997). Dynamic modeling and simulation of a riser-type fluid catalytic cracking unit. Chem. Eng. Technol., 20, 118-130.

Ali, H., Rohani, S., and Corriou, J.P. (1997). Modeling and control of a riser-type fluid catalytic cracking (FCC) unit. Transactions of the Institution of Chemical Engineers, 75, 401-412.

Ancheyta, J.J., Lopez, I.H., Aguilar, R.E., and Moreno, M.J. (1997). A strategy for kinetic parameter estimation in the fluid catalytic cracking process. Ind. Eng. Chem. Res., 36, 5170-5174.

Arbel, A. Huang, Z., Rinard, I.H., Shinnar, R. and Sapre, A.V. (1995). Dynamics and control of fluidized catalytic crackers. Modeling of the current generation FCC's. Ind. Eng. Chem. Res., 34, 1228-1243.

Aris, R. (1989). Reactions in continuous mixtures. AIChE J., 35, 539-548.

Austin, G.T. (1984). Shreve's chemical process industries (5^{th} ed.). Singapore: McGraw-Hill.

Avidan, A.A., and Shinnar, R. (1990). Development of catalytic cracking technology. A lesson in chemical reactor design. Ind. Eng. Chem. Res., 29, 931-942.

Bader, R., Findley, J., and Knowlton, T.M. (1988). Gas-solid flow patterns in a 30.5-cm diameter circulating fluidized bed. In circulating fluidized bed Technology II (Edited by P. Basu and J.F. Large). Pergamon Press, Oxford, 123-137. *(cf. Miller and Gidaspow, 1992)*

Behie, L.A., and Kehoe, P. (1973). The grid region in a fluidized bed reactor. AIChE J., 19, 1070-1072.

Bernard, J.R., Satos-Cottin, H., and Margrita, R. (1989). Use of radioactive tracers for studies on fluidized cracking catalytic plants. Isotopenpraxis, 25(4), 161. *(cf. Viitanen, 1993)*

Berry, T.A., McKeen, T.R., Pugsley, T.S., and Dalai, A.K. (2004). Two-dimensional reaction engineering model of the riser section of a fluid catalytic cracking unit. Ind. Eng. Chem. Res., 43, 5571-5581.

Bidabehere, C.M., and Sedran, U. (2001). Simultaneous diffusion, adsorption, and reaction in fluid catalytic cracking catalysts. Ind. Eng. Chem. Res., 40, 530-535.

Blasetti, A., and de Lasa, H. (1997). FCC riser unit operated in the heat-transfer mode: Kinetic modeling. Ind. Eng. Chem. Res., 36, 3223-3229.

Brereton, C.M.H., and Stomberg, L. (1986). Some aspects of the fluid behavior of fast fluidized beds. In circulating fluid bed technology (edited by P. Basu), 133-143, Permagon Press, Toronto. *(cf. Zhou et al., 1994)*

Capes, C., and Nakamura, K. (1973). Vertical pneumatic conveying: an experimental study with particles in the intermediate and turbulent flow regimes. Can. J. Chem. Eng., 51, 31. *(cf. Tsuo and Gidaspow, 1990)*

Cerqueira, H.S. (1996). Modelageme simulacao do craqueamento catalitico de gasoleo em leito fixo: Formacao do coque. M.SC. Thesis (in Portuguese), Universidade Federal do Rio de Janeiro, Brazil. *(cf. Peixoto and de Medeiros, 2001)*

Chen, L., and Weinstein, H. (1993). Shape and extent of the void formed by a horizontal jet in a fluidized bed. AICHE J., 39, 1901-1909.

Contractor, R.M., Patience, G.S., Garnett, D.I., Horowitz, H.S., Sisler, G.M., Bergna, H.E. (1994). A new process for n-butane oxidation to maleic anhydride using a circulating fluidized bed reactor. In Circulating Fluidized Bed Technology IV (edited by Avidan, A.A.), AIChE: New York, 387. *(cf. Godfroy et al., 1999)*

Corella, J. (2004). On the modeling of the kinetics of the selective deactivation of catalysts. Application to the fluid catalytic cracking process. Ind. Eng. Chem. Res., 43, 4080-4086.

Corella, J., Bilbao, R., Molina, J.A., and Artigas, A. (1985). Variation with time of the mechanism, observable order, and activation energy of the catalyst deactivation by coke in the FCC process. Ind. Eng. Chem. Process Des. Dev., 24, 625-636.

Corella, J., Fernández, A., and Vidal, J.M. (1986). Pilot plant for the fluid catalytic cracking process: Determination of the kinetic parameters of deactivation of the catalyst. Ind. Eng. Chem. Process Des. Dev., 25, 554-562.

Corella, J., and Frances, E. (1991). Analysis of the riser reactor of a fluid catalytic cracking unit. Model based on kinetics of cracking and deactivation from laboratory tests. In fluid catalytic cracking-II: Concepts in catalyst design (edited

by Occelli, M.L.), ACS Symposium Series, Vol. 452, 165-182. Washington: American Chemical Society. *(cf. Gupta and Subba Rao, 2001)*

Corella, J., and Menedez, M. (1986). The modelling of the kinetics of deactivation of monofunctional catalysts with and acid strength distribution in their non-homogeneous surface. Application of the deactivation of commercial catalysts in the FCC process. Chem. Eng. Sci., 41, 1817-1826.

Coxon, P.G., Bischoff, K.B. (1987). Lumping Strategy, 1. Introduction techniques and application of cluster analysis. Ind. Eng. Chem. Res., 26, 1239-1248.

Das, A.K., Martin, G.B., Heynderickx, G.J. (2003). Three-dimensional simulation of a fluid catalytic cracking riser reactor. Ind. Eng. Chem. Res., 42, 2602-2617.

Daubert, T.E. (1998). Evaluated Equation Forms for Correlating Thermodynamic and Transport Properties with Temperature. Ind. Eng. Chem. Res., 37(8), 3260-3267.

Dave, D.J., and Saraf, D.N. (2003). Model for rating and optimization of industrial FCC units. Indian Chem. Engr., 45(1), 7-19.

Davidson, J.F., and Harrison, D. (1963). Fluidized particles. London: Cambridge Press.

de Lasa, H.I., and Grace J.R. (1979). The influence of the freeboard region in a fluidized bed catalytic cracking regenerator. AIChE J., 25, 984-991.

de Lasa, H.I., Errazu, A., Barreio, E., and Solioz, S. (1981). Analysis of fluidized bed catalytic cracking regenerator models in an industrial scale unit. Can. J. Chem. Eng., 59, 549-553.

Den Hollander, M.A., Makkee, M., and Moulijn, J.A. (2001). Prediction of the performance of coked and regenerated fluid catalytic cracking catalyst mixtures. Opportunities for process flexibility. Ind. Eng. Chem. Res., 40, 1602-1607.

Derouin, C., Nevicato, D., Forissier, M., Wild, G., and Bernard, J.R. (1997). Hydrodynamics of riser units and their impact on FCC operation. Ind. Eng. Chem. Res., 36, 4504-4515.

Dewachtere, N.V., Santaella, F., and Froment, G.F. (1999). Application of a single-event kinetic model in the simulation of an industrial riser reactor for the catalytic cracking of vacuum gas oil. Chem. Eng. Sci., 54, 3653-3660.

Edward, W.M., and Kim, H.N. (1988). Multiple steady states in FCC unit operations. Chem. Eng. Sci., 43, 1825-1830.

Ellis, R.C., Li, X., and Riggs, J.B. (1998). Modeling and optimization of a model IV fluidized catalytic cracking unit. AIChE J., 44, 2068-2079.

Elnashaie, S.S.E.H., and El-Hennawi, I.M. (1979). Multiplicity of steady state in fluidized bed reactors-IV. Chem. Eng. Sci., 34, 1113-1121.

Elnashaie, S.S.E.H., and Elshishini, S.S. (1990). Digital simulation of industrial fluid catalytic cracking units: Bifurcation and its implementations. Chem. Eng. Sci., 45, 553-559.

Elshishini, S.S., Elnashaie, S.S.E.H., and Alzahrani, S. (1992). Digital simulation of industrial fluid catalytic cracking units-III. Effect of hydrodynamics. Chem. Eng. Sci., 47, 3152-3156.

Elnashaie, S.S.E.H., and Elshishini, S.S. (1993). Digital simulation of industrial fluid catalytic cracking units-IV. Dynamic behaviour. Chem. Eng. Sci., 48, 567-583.

Errazu, A.F., de Lasa, H.I., and Sarti, F. (1979). A fluidized bed catalytic cracking regenerator model. Grid effects. Can. J. Chem. Eng., 57, 191-197.

Ewell, R.B., and Gadmer, G. (1978). Design cat crackers by computer. Hydroc. Proc., 4,125-134. (*cf. Dave and Saraf, 2003*)

Farag, H., Ng, S., and de Lasa, H. (1993). Kinetic modeling of catalytic cracking of gas oils using in situ traps (FCCT) to prevent metal contamination. Ind. Eng. Chem. Res., 32, 1071-1080.

Feng, W., Vynckier, E., and Froment, G.F. (1993). Single event kinetics of catalytic cracking. Ind. Eng. Chem. Res., 32, 2997-3005.

Fligner, M., Schipper, P.H., Sapre, A.V., and Krambeck, F.J. (1994). Two phase cluster model in riser reactors: Impact of radial density distribution on yields. Chem. Eng. Sci., 49, 5813-5818.

Fogler, H.S. (1992). Elements of Chemical Reaction Engineering (2^{nd} edition, pp.62). New Delhi: Prentice-Hall of India.

Froment, G.F., and Bischoff, K.B. (1979). Chemical reactor analysis and design. New York: John Wiley.

Gao, J., Xu, C., Lin, S., Yang, G., and Guo, Y. (1999). Advanced model for turbulent gas-solid flow and reaction in FCC riser reactor. AIChE J., 45, 1095-1113.

Gao, J., Xu, C., Lin, S., Yang, G., and Guo, Y. (2001). Simulation of gas-liquid-solid 3-phase flow and reaction in FCC riser reactors. AIChE J., 47, 677-692.

Gates, B.C., Katzer, J.R., and Schuit, G.C.A. (1979). Chemistry of catalytic process. New York: McGraw-Hill.

Geldart, D. (1973). Types of gas fluidization. Powder Technology, 7, 677-692.

Gianetto, A., Faraq, H., Blasetti, A., and de Lasa, H. (1994). FCC catalyst for reformulated gasolines. Kinetic modeling. Ind. Eng. Chem. Res., 33, 3053-3062.

Gidaspow, D., and Hulin, L. (1998). Equation of state and radial distribution functions of FCC particles in a CFB. AIChE J., 44, 279-293.

Godfroy, L., Patience, G.S., and Chauki, J. (1999). Radial hydrodynamics in risers. Ind. Eng. Chem. Res., 38, 81-89.

Goelzer, A. (1986). Asphalt molecule shattering in S & W's FCC feed distributor, question and answer sessions with short communications. Ketjen catalyst symposium, Scheveningen, The Netherlands, pp. 18-23. *(cf. Gupta and Subba Roa, 2001)*

Gross, B., Jacob, S.M., Nace, D.M., and Voltz, S.E. (1976). Simulation of catalytic cracking process. US Patent 3960707. *(cf. Arbel et al., 1995)*

Gross, B., Nace, D.M., and Voltz, S.E. (1974). Application of a kinetic model for comparison of catalytic cracking in fixed bed microrecator and a fluidized dense bed. Ind. Eng. Chem. Process Des. Dev., 13, 199-203.

Gupta, A., and Subba Rao, D. (2001). Model for the performance of a fluid catalytic cracking (FCC) riser reactor: Effect of feed atomization. Chem. Eng. Sci., 56, 4489-4503.

Gupta, A., and Subba Rao, D. (2003). Effect of feed atomization on FCC performance: simulation of entire unit. Chem. Eng. Sci., 58, 4567-4579.

Gupta, R., Kumar, V., and Srivastava, V.K. (2005). Modeling and simulation of fluid catalytic cracking unit. Reviews in Chemical Engineering, 21(2), 95-131.

Han, I.S., Chung, C.B., and Riggs, J.B. (2000). Modeling of fluidized catalytic cracking process. Comput. Chem. Eng., 24, 1681-1687.

Hartge, E., Li, Y., and Werther, J. (1986). Analysis of the local structure of two phase flow in a fast fluidized bed. In Circulating Fluidized Bed Technology (edited by Basu, P.), Pergamon , Oxford. *(cf. Tsuo and Gidaspow, 1990)*

Iscol, L. (1970). The dynamics and stability of a fluid catalytic cracker. In proceedings of Joint Automatic Control Conference, Atlanta, Georgia, 602-607. *(cf. Ali and Rohani, 1997)*

Jacob, S.M., Gross, B., Voltz, S.E., and Weekman, V.W., jr. (1976). A lumping and reaction scheme for catalytic cracking. AIChE J., 22, 701-713.

Jin, Y., Yu, Z., Qi, C. and Bai, D. (1988). The influence of exit structures on the axial distribution of voidage in fast fluidized bed. In Fluidization 88: Science and Technology (edited by Kwauk, M., and Kunii, D.), 165-173. Beijing: Science Press. *(cf. van der Meer et al., 1999)*

Khandalekar, P.D., and Riggs, J. B. (1995). Nonlinear process model based control and optimization of model IV FCC unit. Comput. Chem. Eng., 19, 1153-1168.

Kimm, N.K., Berruti, F., and Pugsley, T.S. (1996). Modeling the hydrodynamics of down flow gas-solids reactors. Chem. Eng. Sci., 51, 2661-2666.

King, D.F. (1989). Estimation of dense bed voidage in fast and slow fluidized beds of FCC catalyst. In Fluidization VI: Proceedings of the international conference on fluidization (Edited by Grace, R., Shemilt, L.M., and Bergougnou, M.A.), 1-9, Alberta, Canada, New York: Engineering Foundation. *(cf. Gupta and Subba Roa, 2003)*

Knowlton, T.M. (1995). Modelling benchmark exercise. Workshop at the eighth engineering foundation conference on fluidization. Tours, France. *(cf. Godfroy et al., 1999)*

Kraemer, D., Larocca, M., and de Lasa, H.I. (1991). Deactivation of cracking catalyst in short contact time reactors: Alternative models. Can. J. Chem. Eng., 69, 355-360.

Krishna, A.S., and Parkin, E.S. (1985). Modeling the regenerator in commercial fluid catalytic crcking units. Chem. Eng. Prog., 31(4), 57-62.

Kumar, S., Chadha A., Gupta, R., and Sharma, R. (1995). CATCRACK: A process simulator for an integrated FCC-regenerator system. Ind. Eng. Chem. Res., 34, 3737-3748.

Kumar, V., and Upadhyay, S.N. (2000). Computer simulation of membrane processes: ultrafiltration and dialysis units. Comput. Chem. Eng., 23, 1713-1724.

Kunii, D. and Levenspiel, O. (1969). Fluidization Engineering, Wiley, New York.

Larocca, M., Ng, S., and de Lasa, H. (1990). Ctalytic cracking of heavy gas oils: Modelling coke deactivation. Ind. Eng. Chem. Res., 29(2), 171-180.

Lee, L., Chen, Y., Huang, T. and Pan, W. (1989a). Four lump kinetic model for fluid catalytic cracking process. Can. J. Chem. Eng., 67, 615-619.

Lee, L., Yu, S., Cheng, C., and Pan, W. (1989b). Fluidized bed catalytic cracking regenerator modeling and analysis. Chem. Eng. J., 40, 71-82.

Mao, X., Weng, H., Zhu, Z., Wang, S., and Zhu, K. (1985). Investigation of the lumped kinetic model for catalytic cracking: III. Analyzing ligh oil feed and products and measurement of kinetic constants. Acta Pet. Sin. (Pet. Process Sect.), 1, 11, *(cf. Gao et al., 1999)*

Martin, M.P., Derouin, P.T., Forissier, M., Wild, G., and Bernard, J.R. (1992). Catalytic cracking in riser reactors. Core-annulus and elbow effects. Chem. Eng. Sci., 47, 2319-2324.

Mathews, J.H. (1998). Numerical methods for mathematics, science and engineering, (2^{nd} ed, 3^{rd} Indian reprint), Delhi: Prentice-Hall of India.

Maxwell, J.B. (1968). Data book on hydrocarbons. New York: Robert E. Krieger Publishing Co., Inc.

Mauleon, J. L., and Courelle, J.C. (1985). FCC heat balance critical for heavy fuels. Oil Gas J., 83, 64-70.

McFarlane, R.C., Reineman, R.C., Bartee, J.F., and Georgakis, C. (1993). Dynamic simulator for a model IV fluid catalytic cracking unit. Comput. Chem. Eng., 17, 275-300.

McKeen, T., and Pugsley, T.S. (2003). Simulation of cold flow FCC stripper hydrodynamics at small scale using computational fluid dynamics. International Journal of Chemical Reactor Engineering, 1, A18.

McKetta, J.J. (1981). Encyclopedia of chemical processing and design, cracking catalytic, vol. 13, Marcel Dekker, New York, 1-132.

Merry, J.M.D. (1971). Penetration of a horizontal gas jet into fluidization bed. Trans. Inst. Chem. Eng., 49, 189-195.

Miller, A., and Gidaspow, D. (1992). Dense, vertical gas-solid flow in a pipe. AIChE J., 38, 1801-1815.

Mirgain, C., Briens, C., Pozo, M.D. Loutaty, R., and Bergougnou M. (2000). Modeling feed vaporization in fluid catalytic cracking. Ind. Eng. Chem. Res., 39, 4392-4399.

Morley, K., and de Lasa, H. (1987). On the determination of kinetic parameters for the regeneration of cracking catalyst. Can. J. Chem. Eng., 65, 773-783.

Murphy, J.R. (1992). Evolutionary design changes mark FCC process. Oil Gas J., 90(20), 49-58.

Nace, D.M. (1970). Catalytic cracking over crystalline aluminosilicates. Micro-recator study of gas oil cracking. Ind. Eng. Chem. Process Des. Dev., 9(2), 203-209.

Nace, D.M., Voltz, S.E., and Weekman, V.W., Jr. (1971). Application of a kinetic model for catalytic cracking. Effects of charge stocks. Ind. Eng. Chem. Process Des. Dev., 10, 530-537.

Ocone, R., Goodwin, J.A.S., and Delebarre, A. (2000). Flow structures of Geldart A solids in circulating fluidized beds. Chem. Eng. Res. Des., Transactions of the Institute of Chemical Engineers, Part A, 78, 860-865.

Oliveira, L.L. (1987). "Estimação de Parâmetros e Avaliação de Modelos de Craqueamento Catalítico", M.Sc. Thesis (in Portuguese), University Federal do Rio de Janeiro, Brazil. *(cf. Peixoto and de Medeiros, 2001)*

Pachovsky, R.A., and Wojciechowski, B.W. (1971). Theoretical interpretation of gas oil conversion data on an X-sieve catalyst. The Canadian Journal of Chemical Engineering, 49, 365-369.

Paraskos, J.A., Shah, Y.T., Mckinney, J.D., and Carr, N.L. (1976). A kinetic model for catalytic cracking in a transfer line reactor. Ind. Eng. Chem. Process des. Dev., 15(1), 165-169.

Pareek, V.K., Adesina, A.A., Srivastava, A., and Sharma, R. (2002). Sensitivity analysis of rate constants of Weekman's riser kinetics and evaluation of heat of cracking using CATCRACK. Journal of Molecular Catalysis A, 181, 263-274.

Pareek, V.K., Adesina, A.A., Srivastava, A., and Sharma, R. (2003). Modeling of a non-isothermal FCC riser. Chem. Eng. J., 92, 101-109.

Pitault, I., Forissier, M., Bernard, J.R. (1995). Determination de constantes cinetiques du craquage catalytique par la modelisation du test de microactivite (MAT). The Canadian Journal of Chemical Engineering, 73, 498-503.

Pitault, I., Nevicato, D., Forissier, M., and Bernard, J.R. (1994). Kinetic model on a molecular description for catalytic cracking of vacuum gas oil. Chem. Eng. Sci., 49, 4249-4262.

Peixoto, F.C., and de Medeiros, J.L. (2001). Reactions in multiindexed continuous mixtures: Catalytic cracking of petroleum fractions. AIChE J., 47, 935-947.

Pekediz, A., Kraemer, D., Blasetti, A., de Lasa, H. (1997). Heats of catalytic cracking. Determination in a riser simulator reactor. Ind. Eng. Chem. Res., 36, 4516-4522.

Pugsley, T.S., Berruti, F. A. (1996). Predictive hydrodynamic model for circulating fluidized bed risers. Powder Technology, 89, 57-69.

Sa, Y., Chen, X., Liu, J., Weng, H., Zhu, Z., and Mao, X. (1985). Investigation of the lumped kinetic model for catalytic cracking and establishment of the physical model. Acta Pet. Sin. (Pet. Process Sect.), 1, 3. *(cf. Gao et al., 1999)*

Sa, Y., Liang, X., Chen, X., and Liu, J. (1995). Study of 13-lump kinetic model for residual catalytic cracking. Selective papers in memorial of 30th anniversary of fluid catalytic cracking process in China, Luoyan, Petrochemical Engineering Corporation, Luoyang, China, p. 145. *(cf. Gao et al., 1999)*

Saltelli, A. (2000). Sensitivity Analysis (edited by Chan, K., and Scott, E.M.). New York: John Wiley & Sons, Inc.

Samuelsberg, A., and Hjertager, B.H. (1996). Computational modeling of gas/particle flow in a riser. AIChE J., 42, 1536-1546.

Schnitzlein, M.G., and Weinstein, H. (1988). Flow characterization in high-velocity fluidized beds using pressure fluctuations. Chem. Eng. Sci., 43, 2605-2614.

Seko, H., Tone, S., and Otake, T. (1978). Operation and control of a fluid catalytic cracker. J. Chem. Eng. Jpn., 11 (2), 130-135.

Senior, R.C., and Brereton, C. (1992). Modelling of circulating fluidized-bed solids flow and distribution. Chem. Eng. Sci., 47, 281-296.

Shah, Y.T.,Huling, G.T., Paraskos, J.A., and Mckinney, J.D. (1977). A kinematic model for an adiabatic transfer line catalytic cracking reactor. Ind. Eng. Chem. Process Des. Dev., 16(1), 89-94.

Sun, B., and Gidaspow, D. (1999). Computation of circulating fluidized-bed riser flow for the fluidization VIII benchmark test. Ind. Eng. Chem. Res., 38, 787-792.

Sundaresan, S. (2000). Modeling the hydrodynamics of multiphase flow reactors: Current status and challenges. AIChE J., 46, 1102-1105.

Takatsuka, T., Sato, S., Morimoto, Y., and Hashimoto, H. (1987). A reaction model for fluidized-bed catalytic cracking of residual oil. Int. Chem. Eng., 27(1), 107-116.

Theologos, K.N., Lygeros, A.I., Markatos, N.C. (1999). Feedstock atomization effects on FCC riser reactors selectivity. Chem. Eng. Sci., 54, 5617-5625.

Theologos, K.N., and Markatos, N.C. (1993). Advanced modeling of fluid catalytic cracking riser-type reactors. AIChE J., 39, 1007-1017.

Theologos, K.N., Nikou, I.D., Lygeros, A.I., and Markatos, N.C. (1997). Simulation and design of fluid catalytic cracking riser-type reactors", AIChE J., 43, 486-493.

Tsuo, Y.P., and Gidaspow, D. (1990). Computation of flow patterns in circulating fluidized beds. AIChE J., 36, 885-896.

van der Meer, E.H., Thrope, R.B., and Davidson, J.F. (1999). Dimensionless groups for predicting the similarity of circulating fluidized beds. Chem. Eng. Sci., 54, 5369-5376.

van der Meer, E.H., Thrope, R.B., and Davidson, J.F. (2000). Flow patterns in the square cross-section riser of a circulating fluidized bed and effect of riser exit design. Chem. Eng. Sci., 55, 4079-4099.

van Swaaij, W.P.M., Buurman, C., van Berugel, J.W. (1970). Shear stresses on the wall of a dense gas-solid riser. Chem. Eng. Sci., 25, 1818. *(cf. Miller and Gidaspow, 1992)*

Viitanen, P.I. (1993). Tracer studies on a riser reactor of a fluid catalytic cracking plant. Ind. Eng. Chem. Res., 32, 577-583.

Voories, A. (1945). Carbon formation on catalytic cracking. Ind. Eng. Chem., 37, 318-322.

Wang, I. (1974). High temperature catalytic cracking. Ph.D. Dissertation, Fuels Eng. Department, University of Utah, Salt Lake City, Utah. *(cf. Lee et al., 1989b)*

Wang, L., Yang, B., and Wang, Z. (2005). Lumps and kinetics for the secondary reactions in catalytically cracked gasoline. Chemical engineering Journal, 109, 1-9.

Weekman, V.W., Jr. (1968). A model of catalytic cracking conversion in fixed, moving, and fluid-bed reactors. Ind. Eng. Chem. Process Des. Dev., 7, 90-95.

Weekman, V.W., Jr. (1979). Lumps, models, and kinetics in practice. AIChE Monograph Series 11, 75, 3-29.

Weekman, V.W., Jr., and Nace, D.M. (1970). Kinetics of catalytic cracking selectivity in fixed, moving, and fluid bed reactors. AIChE J., 16, 397-405.

Wei, J., and Prater, C.D. (1963). A new approach to first-order chemical reaction system. AIChE J., 9, 77-81.

Weinstein, H., Shao, M., Schnitzlein, M., and Graff, R.A. (1986). Radial variation in void fraction in a fast fluidized bed. Fluidization V, proc. 5th Eng. Found. Conf. Fluidization, Elsinore, Denmark. (Edited by K. ostergaard, A. Sqrensen), pp. 329. *(cf. Miller and Gidaspow, 1992)*

Weisz, P.B. (1966). Combustion of carbonaceous deposits within porous catalyst particles, III. The CO_2/CO product ratio. J. Catal., 6, 425-430.

Wilson, J.W. (1997). Fluid catalytic cracking technology and operations. Oklahoma: PennWell Publishing Company.

Wojciechowski, B.W. (1968). A theoretical treatment of catalyst decay. Can. J. Chem. Eng. 46, 48-52.

Wojciechowski, B.W. (1974). The kinetic foundation and practical application of the time on stream theory of catalyst decay. Cat. Rev. Sci. Eng., 9, 79-113.

Xu, B.H., and Yu, A.B. (1997). Numerical simulation of the gas-solid flow in a fluidized bed by combining discrete particle method with computational fluid mechanics. Chem. Eng. Sci., 52, 2785-2809.

Yen, L.C., Wrench, R.E., and Kuo, C.M. (1985). FCCU regenerator temperature effects evaluated. Oil Gas J., 83, 87-92.

Yen, L.C., Wrench, R.E., and Ong, A.S. (1988). Reaction kinetic correlation equation predicts fluid catalytic cracking coke yields. Oil Gas J., 86, 67-70.

Zheng, Y. Y. (1994). Dynamic modeling and simulation of a catalytic cracking unit. Comput. Chem. Eng., 18, 39-44.

Zhou J., Grace, J.R., Qin, S., Brereton, C.M.H., Lim, C.J., and Zhu, J. (1994). Voidage profiles in a circulating fluidized bed of square cross-section. Chem. Eng. Sci., 49, 3217-3226.

Zhou J., Grace, J.R., Lim, C.J., and Brereton, C.M.H. (1995). Voidage profiles in a circulating fluidized bed of square cross-section. Chem. Eng. Sci., 50, 237-244.

Zhu, K., Mao, X., Weng, H., Zhu, Z., and Liu, F. (1985). Investigation of the lumped kinetic model for catalytic cracking: II. A prior simulation for experimental planning. Acta Pet. Sin. (Pet. Process Sect.), 1, 47. *(cf. Gao et al., 1999)*

LIST OF PUBLICATIONS

1. **Rajkumar Gupta**, Vineet Kumar, and V.K. Srivastava. Modeling and simulation of fluid catalytic cracking unit. Reviews in Chemical Engineering, Vol. 21, No. 2, 95-131, 2005.
2. **Rajkumar Gupta**, Vineet Kumar, and V.K. Srivastava. A new generic approach for the modeling of fluid catalytic cracking (FCC) riser reactor. Chemical Engineering Science, 2006 (Communicated).
3. **Rajkumar Gupta**, Vineet Kumar, and V.K. Srivastava. Non isothermal modeling of fluid catalytic cracking (FCC) riser reactor. Canadian Journal of Chemical Engineering, 2006 (Communicated).